UCRL-10607

University of California

Ernest O. Lawrence Radiation Laboratory

CONTROLLED THERMONUCLEAR RESEARCH SEMIANNUAL REPORT

July through December 1962

BERKELEY AND LIVERMORE, CALIFORNIA

TWO-WEEK LOAN COPY

This is a Library Circulating Copy which may be borrowed for two weeks. For a personal retention copy, call Tech. Info. Division, Ext. 5545

DISCLAIMER

This document was prepared as an account of work sponsored by the United States Government. While this document is believed to contain correct information, neither the United States Government nor any agency thereof, nor the Regents of the University of California, nor any of their employees, makes any warranty, express or implied, or assumes any legal responsibility for the accuracy, completeness, or usefulness of any information, apparatus, product, or process disclosed, or represents that its use would not infringe privately owned rights. Reference herein to any specific commercial product, process, or service by its trade name, trademark, manufacturer, or otherwise, does not necessarily constitute or imply its endorsement, recommendation, or favoring by the United States Government or any agency thereof, or the Regents of the University of California. The views and opinions of authors expressed herein do not necessarily state or reflect those of the United States Government or any agency thereof or the Regents of the University of California.

Research and Development

UCRL-10607
UC-20 Controlled Thermonuclear Processes
TID-4500 (18th Ed.)

UNIVERSITY OF CALIFORNIA
Lawrence Radiation Laboratory
Berkeley and Livermore, California

Contract No. W-7405-eng-48

CONTROLLED THERMONUCLEAR RESEARCH SEMIANNUAL REPORT

July through December 1962

January 16, 1963

Printed in USA. Price $2.25. Available from the
Office of Technical Services
U. S. Department of Commerce
Washington 25, D.C.

CONTROLLED THERMONUCLEAR RESEARCH SEMIANNUAL REPORT

July through December 1962

Contents

INTRODUCTION 1

I. PYROTRON (MAGNETIC MIRROR) PROGRAM

1. Introduction and Summary (Post). 4
2. Multistage High-Compression Experiments (Coensgen, Cummins, Nexsen, Sherman, and Ellis) . . 5
3. Table Top III (Perkins and Post) 10
4. Alice (Energetic Neutral-Atom Injection) (Barr, Damm, Foote, Futch, Gordon, Hunt, Oleson, Post and Steinhaus) . 15
5. P-4 (Steady-State Plasma) System (Barr and Gardner). . . 36

II. ASTRON PROGRAM

1. Introduction (Christofilos). 41
2. Astron Electron Accelerator (Comella, Hester, Lamb, Reagan, Sherwood, and Wright) 42

III. LIVERMORE PINCH PROGRAM (Colgate, Birdsall, Furth, Hartman, Kuivinen, and Spoerlein)

1. Summary 44
2. Levitron Operation. 44
3. Levitron Development 49
4. Linear Hard-Core Experiments 50
5. Resistive-Sheet Pinch Experiment 50
6. Collisionless Plasma Shock (Experimental) 51
7. Collisionless Plasma Shock (Theoretical). 51
8. Turbulence Theory. 51
9. Instability Theory 52

*Preceding reports: UCRL-10294, UCRL-9969.

IV. BERKELEY PLASMA RESEARCH

1. Rotating-Plasma Research (Ehlers, Halbach, Layman, and Paxson) 53
2. Boundary Effects and Instabilities in Rotating-Plasma Experiments (Kunkel) 55
3. Hydromagnetic Waves and Cyclotron Heating (Boley, Cooper, Hamilton, and Wilcox) 60
4. Hydromagnetic Ionizing Fronts (Sherwood and Kunkel) 68
5. Sheet Pinch Studies (Anderson) 69
6. Experiment on Lorentz Dissociation and Partially Ionized Plasma (Pyle and Co-Workers) 70
7. On the MHD Helmholtz Instability (Macmahon) 71

V. THEORETICAL AND BASIC EXPERIMENTAL PLASMA PHYSICS

1. A Self-Consistent Distribution of Electrons in the Astron E Layer (Heckrotte and Neil) 72
2. The Effect of Finite Larmor Radius on the Interchange Instability (Newcomb) 73
3. Plasma Potential and Electron Energy Distributions in the Alice Experiment (Killeen, Futch, and Wagoner) 74
4. Longitudinal Oscillations in Multicomponent Plasma with Anisotropic Velocity Distributions (Kammash and Heckrotte) 75
5. Ion Density Versus Time in Neutral Injection Systems (Hiskes and Tarter) 77
6. Low-β Plasma Stability in the Astron (Woods) 77
7. Bumpy Torus (Gibson, Jordan, and Lauer) 78
8. Atomic Scattering and Cross Section Measurements (Baker, Brink, Chambers, McFarland and Soltysik) 79

VI. ENGINEERING AND TECHNOLOGICAL DEVELOPMENT

1. Ultrahigh-Vacuum Development (Milleron) 83
2. Mechanical Engineering Development (Batzer) 84
3. Electrical Engineering Development (Van Ness) 88

VII. TALKS AND PUBLICATIONS 94

CONTROLLED THERMONUCLEAR RESEARCH SEMIANNUAL REPORT

July through December 1962

Lawrence Radiation Laboratory
University of California
Berkeley and Livermore, California

January 16, 1963

INTRODUCTION

C. M. Van Atta

The most striking feature of the controlled thermonuclear research program during the period July to December, 1962, was the increasing realism of plasma-stability theory and the improvement in understanding of plasma experiments in terms of recently developed theory. Some of the highlights of events during the past six months are briefly described below.

Alice. The Alice energetic neutral-atom injection mirror machine has been in intermittent operation during all the report period. Results of interest include observations on ion cyclotron radiation, low-frequency oscillations($\approx$ 16 kc/sec) close to the ion precessional frequency, and the plasma potential. The frequency of the "low-frequency" oscillations increases about linearly with the plasma density (up to about 10^8 ions/cm^3), consistent with the concept that a stable mode of oscillation predicted from the finite-orbit theory is responsible. The amplitude of the low-frequency oscillation increases about linearly with the plasma potential, values of which range up to 5 kV and are generally about 20 times the expected value. Ion cyclotron radiation is observed only when the plasma density is large enough that the plasma frequency exceeds the ion cyclotron frequency. When the injected beam is turned off, two modes of decay are observed: (a) one in which the frequency of the low-frequency oscillations remains constant for as long as 1 or 2 seconds as the plasma decays, and (b) one in which this frequency decreases approximately exponentially with the time over a period of about a second. Although there is no explanation for the two modes of decay, the plasma-decay times of the order of 1 or 2 seconds are impressive.

Finite-Orbit Theory. The effect of finite Larmor orbits in stabilizing the interchange instability in a mirror machine has been calculated explicitly. The result is a specific sufficient condition for stabilization against the flute instablity, which can always be satisfied in principle by making the distance between the mirrors greater than some critical length. In another extension of the finite-orbit theory, a dispersion formula for stable oscillations and modes of instability has been derived. The low-frequency oscillations observed in Alice seem to correspond to certain modes of stable oscillation predicted by the theory, although the possibility that they are due to an $\overline{E} \times \overline{B}$ rotation resulting from the high plasma potential cannot as yet be ruled out.

Toy Top. As a result of improvement of the symmetry of the field by alignment of the field coils and elimination of field bumps where the radius of curvature of the field lines was small, the catastrophic loss of the plasma to the wall in the Toy Top machine has been eliminated. Thermonuclear neutron output now persists over a period of 250 to 300 μsec, reaching a maximum at about the time of field maximum and then falling off smoothly with a 1/e period of about 50 μsec. Efforts to decrease the loss rate have thus far had no effect. More detailed diagnostics are now in progress to determine whether the decay of the plasma is due to an instability or to atomic processes such as charge-exchange loss or plasma cooling due to neutral or charged contaminants.

Levitron. The Levitron (toroidal hard-core pinch) was put into operation in August with greatly improved base pressure. In the sequence of operation, first establish the azimuthal (B_θ) field by inducing current in the hard-core ring, and then compress the B_θ field together with plasma with a rising axial (B_z) field. Long confinement periods (up to about 2 msec) are observed, particularly for low initial deuterium pressure (≈ 0.1 μ). For the first 200 μsec or so the confinement is apparently completely stable, but at a critical time in the cycle, a fluctuating B_r signal appears. At the same time, hot electrons (≈ 100 eV) are observed near the wall, and the plasma potential is observed to change sign from negative to positive, indicating loss of electrons. These indications are all consistent with the conclusion that at the critical time an instability develops. Since most of the known infinite and finite conductivity modes seem to be excluded by the field configuration and plasma properties, the character of the observed instability is not yet determined.

Astron. During the past six months the construction of the Astron accelerator was completed, and the routine of adjusting the pulse timing and wave form of the input primary circuits was about half completed. The electron gun and the first two (of six) accelerator units were operated with approximately design current. On the basis of present progress, full operation of the accelerator by February 1963 is expected.

Homopolar V. A switch has been added to the discharge circuit of the Homopolar V so that the voltage can be held off until the optimum time for full ionization at all values of the voltage and gas density. This improvement removes an obstacle against increasing the electric and magnetic fields; this increase could not be made with full ionization in the absence of the switch. The intention is to increase the fields, keeping E/B^2 (and therefore the Larmor orbit) constant in an effort to increase neutron output for easier diagnosis of neutron yield as a function of time during the pulse. Meanwhile, a stilbene detector circuit with pulse-shape discrimination is being developed to distinguish between neutrons and x rays, to facilitate unambiguous measurement of the neutron output.

Hothouse II. Plasma heating by ion cyclotron absorption of torsional Alfvén waves in Hothouse II has apparently been limited by impurity radiation. The Hothouse II vacuum chamber and system are being modified to provide much cleaner conditions, which will include a hot liner to reduce plasma contamination from the wall and Vac-Ion pumps to eliminate hydrocarbons. At

present the amplitude of the diamagnetic signal of the heated portion of the plasma is about 2 gauss, corresponding to an ion average energy of about 200 eV. The ion density in the region of wave-energy absorption has been observed to decrease significantly. Although at one time it was believed that the factor by which the density decreased was much larger, microwave transmission measurements indicate that this factor is not more than about 10.

I. PYROTRON (MAGNETIC MIRROR) PROGRAM

1. INTRODUCTION AND SUMMARY

Richard F. Post

During the report period, significant new data on plasma confinement were obtained, both in the Alice and in the Multistage experiments. In addition, detailed information was obtained on the nature of the triggered instability that leads to a rotating plasma form in Table Top. The P-4 experiment was terminated, after a long and useful career, with a fast-compression mirror experiment in a plasma regime somewhat different from the usual. The most intriguing aspect of all the experiments, however, is the possibility, not yet proved, that the behavior in all our experiments shares a particular common theoretical denominator; i.e., the theory of finite-orbit stabilization effects as applied to the mirror machine.

In the Multistage experiment (Toy Top III S) an important conclusion was reached: In the device as it now exists, with greatly improved field symmetry and smoothed field gradients, gross transport of the hot plasma across the magnetic field has been reduced below the limit of detectability. It may not be a coincidence that this reduction was accomplished only after the field was reshaped so that the finite-orbit stability criterion can be satisfied. The fusion-neutron time history, however, now shows a decay-time constant of some 50 to 70 μsec. This time constant is insensitive to operating parameters. We hope the observed neutron decay rate can be explained by appeal to purely "classical" effects, such as excessive cooling of the plasma ions by collisional damping with cold electrons. Such effects could presumably be alleviated. Alternatively, although there is at present no direct evidence indicating this, it is possible that the neutron decay could arise from the presence of other kinds of instabilities, types not leading to rapid transport across the field, but to excessive cooling or to rapid losses out the mirrors.

In the Alice experiment, much data relevant to plasma confinement was obtained. Although the vacuum required, theoretically, for exponential buildup was not achieved, a hot plasma with a density in excess of 10^8 cm^{-3} was produced and confined. Evidence was obtained for cooperative behavior, including the existence of a new stable low-frequency mode of oscillation and the emission of radiation at the ion cyclotron frequency. By cutting off the injected beam, it was shown that long-time confinement (≈ 1 second) was possible, with no evidence of gross transport across the field and apparently limited only by charge-exchange losses.

One of the most interesting aspects of the low-frequency oscillations observed was that they apparently agree closely with the oscillation modes that were theoretically predicted on the basis of an extension of finite-orbit theory to the low-density regime. This theory, discussed briefly in Sec. I.4.b, predicts that as plasma density is varied, there may exist two stable regimes of confinement lying respectively above and below an intermediate-density regime which is unstable. Alice now appears to be operating in the lower of the two regimes. The apparently stable plasmas in Table Top lie in the upper regime, becoming unstable as the intermediate regime is entered, and again

stable at low densities. If these correlations with theory are valid, they indicate that, if no precautions are taken, grossly unstable plasma behavior may be encountered in Alice as the density is increased. The same theory shows, however, how to avoid this eventually, by modifying the machine and operating parameters.

In summary, we are now beginning to see the fruits of an intensive programmatic emphasis on the problem of confinement and plasma instability, where a serious attempt is being made to correlate the plasma conditions with theory. We hope we are entering a phase in which the old original nemesis of the mirror machine, the interchange instability, will be understood and controlled. What remains beyond is the forest of the microinstabilities and the "universal" instabilities that may occur. Only time will tell whether these are of serious concern or only of secondary importance.

2. MULTISTAGE HIGH-COMPRESSION EXPERIMENTS

Frederic H. Coensgen, William F. Cummins, William E. Nexsen, Jr., Arthur E. Sherman, and Robert E. Ellis

A. Toy Top III S

Introduction

Investigations in Toy Top III S during the past 6 months have been primarily concerned with the transverse transport of plasma from the interior of the confining field across the magnetic field to the vacuum chamber walls. Measurements have been limited to the determination of (a) the reaction history through the observation of prompt neutrons, (b) the time dependence of the visible light from the reaction chamber, and (c) the transverse plasma transport by means of electrostatic probes located at the walls in the midplane of the compression chamber. From this work we have obtained two important results. First, the gross cross-field transport of the plasma column to the walls has been eliminated, and second, the reaction rate now decays with an apparently invariant time constant of 50 to 70 μsec. Although we have made considerable effort to correlate experimental results with the theoretically derived conditions for stabilization by finite ion orbits, it is not possible at this time to state with certainty that the predicted effects have or have not been verified.

Transverse Plasma Transport

As reported at Salzburg,[1] the plasma in the second stage of Toy Top III (operated from September 1960 to September 1961) was found to reach the vacuum chamber wall about 90 μsec after injection. It was shown that the entire plasma column moved across the field in a preferred direction which was correlated with asymmetries of the pulsed magnetic field. At that time

[1] F. H. Coensgen, W. F. Cummins, W. E. Nexsen, Jr., and A. E. Sherman, in Nuclear Fusion, 1962 Supplement, Part 1, p. 125.

it was an open question whether the plasma behavior was a true example of the m = 1 mode flute instability (hydromagnetic) or whether it was driven by magnetic-field gradients.

As reported in an earlier progress report,[2] a 6-in. system was built of five multiturn magnets and was operated from October 1961 to January 1962. Although the 6-in. fields were not measured precisely, it was expected on the basis of the ratio of the number of turns in the magnet windings to the number of current feeds that the symmetry of this system should have been improved by an order of magnitude over that of Toy Top III. As reported earlier[2], the plasma behavior was for the most part the same as that observed in Toy Top III. That is, the reaction rate terminated very sharply coincident with intense light signals from the containment chamber and with large plasma signals received by electrostatic probes at the walls. At this time it then appeared that the only effect of improved symmetry was randomizing the direction of the drift of the plasma, and that indeed there was an m = 1 instability. Fortunately, owing to increased counter sensitivity and a greater rate of neutron production, it was possible to follow the reaction history for each cycle of the experiment rather than obtain a histogram from a large number of observations. This made it possible to distinguish (in the 6-in. system) two modes of decay of the reaction rate: first and predominant, the catastrophic termination as described above; second and seldom, a less rapid smooth decay of the reaction rate without attendant light signals or large probe signals.

The III S system is a 9-in. system of approximately the same volume as the second stage of Toy Top III. Not only are the fields of the individual pulsed magnets quite symmetric, but also considerable care was taken to align the individual magnetic axes when assembling the system. In an effort to obtain stabilization of higher-order modes (m > 1) of the flute instability, all sharp bends in the magnetic field lines were eliminated. The condition for stabilization by finite orbits as presented by Rosenbluth, Krall, and Rostaker has been used as a guide. They derive the following condition for stability (m > 1):

$$Q = \frac{\bar{a}_i R^{1/2}}{r_0^{3/2}} \quad \frac{(m - 1)}{m^{1/2}} > 1.$$

In this experiment, the size of the average ion orbit $\bar{a}_i$ is determined by the injectors and cannot be appreciably changed. The radius of the plasma, r_0, can be varied somewhat by changing the injector array and through the use of baffles. R, the radius of curvature of the confining magnetic-field lines, is determined by the geometry of the pulsed magnet system, the operating level of the individual magnets, and the time sequence of their actuation.

---

[2] Frederic H. Coensgen, William F. Cummins, William E. Nexsen, Jr., Arthur E. Sherman, and Robert E. Ellis, in Controlled Thermonuclear Research Quarterly Report, UCRL-9969, January 19, 1961, p. 5.

The striking difference between this system and previous systems is the apparent absence, for any available operating condition, of gross movement of the plasma column across the field. This observation is limited to the first 250 to 300 μsec, as both the neutron detector and end-loss signal indicate that the high-energy plasma is lost by 300 μsec. As the suppression of the gross movement is not, and is not theoretically expected to be, dependent upon R, it appears that the rapid drift of the plasma to the walls in Toy Top III is associated with a field asymmetry and that drift, in the 6-in. system, is associated with misalignment of the magnetic axes of the five pulsed magnets. Such misalignments would be expected to be random, and could produce random drifts resulting from slight variations in the position of the injected plasma and from slight jitter in the pulsed-magnet firing sequence.

Although gross plasma transport is not found, there is still some plasma transport to the walls during the compression cycle of Toy Top III S. Only occasionally are large signals detected that can be correlated with lower-than-average neutron production. There does appear to be a correlation between the value of R and the size and frequency of the plasma signals at the wall. For example, as the contribution of the center magnet is decreased to zero the wall probes detect larger plasma signals. However, in this experiment, R cannot be varied without changing dB/dt over an appreciable part of the compression chamber, so it is not clear whether the observed variation in transverse plasma transport is due to a change in R or a change of dB/dt.

Decay of Reaction Rate

Upon elimination of the gross plasma drift the decay of the reaction rate changed from an abrupt decline within 15 to 20 μsec to a smoother decay with a $\frac{1}{e}$ time constant of 50 to 70 μsec. The principal object of the research now is to understand this decay and to increase the time constant. So far the decay constant appears to be an invariant. Within the range for which the neutron production is large enough for the determination of the reaction history, the decay constant is insensitive to changes in the compression ratio, density, wall conditions, end conductors or multipolar fields (eight-element longitudinal conductors). Many of these observations are preliminary, and do not rule out effects of the order of 30%. However, it is apparent that an improvement of the decay rate by a factor of two or more cannot be readily achieved by any of the simple procedure mentioned.

As neither multipolar windings nor the fulfillment of the Rosenbluth criterion $Q > 1$ has an effect on the decay constant, it can be speculated that the plasma loss is not due to hydromagnetic instabilities. However, in view of the prevalent discussions of cooperative effects it is hardly necessary to mention that other instabilities or oscillations may easily account for either a plasma loss or energy loss of sufficient magnitude to account for the observed decay of the reaction rate. It should be pointed out that there are also a number of effects resulting from atomic processes that can account for the decay. Among these are (a) charge-exchange effects due to neutrals, (b) charge-exchange with ionized heavy-ion contaminants, (c) excess Coulomb scattering from trapped multiple-ionized impurities, and (d) large energy transport from the ions to the electrons due to a suppression of electron temperature.

Future Toy Top III S Program

During the next period the existing observations will be augmented by (a) μW determinations of density and electron temperature, (b) neutral detectors at the midplane, (c) spectrographic determination of impurity content, (d) mass and energy analysis of the ions lost out of the mirror, (e) electromagnetic radiation determinations, (f) probe arrays outside of one mirror to determine the pattern of the end-loss flux, and (g) the time history of electron temperature.

To allow better comparison of the experiment and the stability condition, improved determinations of ion energy and r_0 are in progress.

Plasma Injector Development

The objectives of this development are (a) higher initial ion energies, (b) cleaner plasmas, (c) greater output, and (d) simplification of injector arrays and maintenance. This work is proceeding slowly, since in the past four months there has been only a two-man effort.

If no other injectors are developed, 50 to 100 of the 0.5-in. Toy Top injectors will be used in the 2X experiments. Therefore, several simplifications in both material and fabrication have been investigated. It was found that the tantalum rings could be replaced by copper rings and that rings sprayed with AlO_3 by means of a plasma-jet technique could replace the present assembly of alternate metal and ceramic rings. A larger injector (1.75-in. i. d.) has been tested and found to emit larger quantities of plasma. The larger injector was also used in the Toy Top III S experiment and found to perform satisfactorily. This development will decrease the number of injectors needed for 2X.

A gas-fed gun similar to that used by J. Osher at LASL has been built and operated. Within reasonable limits the reported energy distribution has been verified. However, the energy distribution is very broad and the number of high-energy ions is quite low. This gun is being converted to operate in a manner described by J. Marshall (LASL). In the latter operating mode, the average ion energy is reported to be of the order of 10 keV, the density and total output are reported to be much higher than that for the "high-energy mode" reported by Osher, and the impurity content is said to be "very low." If this gun can be used to inject into our field, it offers the possibility of higher initial ion energies, fewer impurities, and a simplification of the injector array.

A 4-in. gas-fed version of the Toy Top injector has been constructed. The Toy Top injector geometry has the advantage of known performance in a magnetic field. Gas injection may reduce the impurity content of the plasma. The investigation of this gun has just been initiated and little is known about it other than that it fires and does produce a large burst of plasma.

2X Construction

Twelve of the 25 large dc magnets have been received and tested. The vacuum-chamber parts have been received and are being leak tested.

Construction of the vacuum foreline is nearly completed.

Construction of the North Bay banks is nearly completed. There remains a large part of the control wiring and installation and power reruns, as well as all the installation of the first section of Bank 6 (1/4 of Squash bank).

At the present manpower level, we estimate the first operation of the 2X facility will be in August 1963.

B. Magnetic-Field Calculations

An IBM 7090 program (called M-Pulse) for the calculation of the time-varying currents in each loop (coil) of a system of inductively coupled R-L-C and R-L loops has been completed and tested. In conjunction with an IBM 7090 program developed for Oak Ridge National Laboratory for the calculation of magnetic-field quantities,[3] this code is being used in an attempt to calculate magnetic-field components and constant flux surfaces (or field lines) for the system of coaxial, sequentially pulsed, and dc coils of the Toy Top machine. Mutual inductances may be calculated with the Oak Ridge code. Self-inductances are hand calculated or measured. Computer runs are now in progress, the results of which will be compared with detailed measurements of the magnetic field in Toy Top made earlier this year. In the event that the magnetic-field code in its present state does not produce satisfactory results for some of the pulsed coil designs now in use, the M-pulse code may be used to determine the correct input currents for a code previously used to calculate the time-varying field for a system in which coupling was ignored. In this case, the measured field distribution for each individual, isolated coil energized by a known current is properly added to the field produced by all the other coils in the system, with the current in each coil being determined by the M-pulse code. A cathode-ray tube display of the magnetic-field components as a function of axial position at a given radius and for a given time is available and has proved useful for analyses of field configurations derived by the variation of such machine parameters as capacitor bank voltages and firing sequences.

[3] W. F. Gauster and Carl E. Parker (Oak Ridge National Laboratory), private communication.

3. TABLE TOP III

A. Experimental Studies of Rotating Plasma Form

Walton A. Perkins and Richard F. Post

To aid in the interpretation of the electrical signals detected by electrostatic (capacity) probes placed near the unstable rotating plasma, a mechanical model was constructed. The mechanical analog with one or two charged rotating disks simulated the rotating-plasma form. Only one charged disk proved to be necessary to produce signals similar to those detected with the rotating plasma. A diagram of the mechanical analog and an electrostatic probe is shown in Fig. I-1. The metal disk of the electrostatic probe and the rotating charged disk together form a variable capacitor. Solution of the electric circuit of Fig. I-1 (with the probe and rotating disk replaced by a variable capacitor), showed that shape of the signals will vary with ratio of the rotation period to the product of the termination resistance and capacity to ground (cable capacity). By adjusting the electrical time constants in proportion to the ratio between the rotation periods of the plasma and of the mechanical rotor, direct comparison between the two cases is possible.

Figure I-2 shows signals obtained by using various ratios of τ/RC. The corresponding signals obtained with the mechanical analog in which the plasma is replaced by a charged disk are shown in the middle set. The bottom set is the calculated signals for the equivalent electrical circuit. The τ/RC values listed at the top were used for the other sets with the one exception marked. The value $\tau/RC = 0.01$ was cut off the accuracy range of the analog computer that was used to obtain the calculated signals. However, the shape does not change much as τ/RC is decreased below 0.3. For $\tau/RC \ll 1$, we obtain the true capacity function shown on the right side. For $\tau/RC \gg 1$, we obtain the derivative of the capacity function shown on the left side. For $\tau/RC \approx 1$, we get partial differentiation as shown in the central column. The excellent agreement over the large range of τ/RC values strongly supports our model. From these signals, information can thus be obtained about the rotating plasma's potential and shape. The differentiated and integrated signals clearly show a negative potential. By comparison with the mechanical analog, we see that the plasma form could be a disk of radius $r_0 \leq 3.5$ cm. For the calculated signal, the best fit was obtained with r_0 from 2 to 3 cm.

A study of the inner plasma shape and motion during an instability was made with a multiple-channel end scintillator probe composed of eight or ten 1.9-cm-diam scintillators placed outside the magnetic mirror to intercept the end-scattered electron flux. The configuration of the eight-channel probe is shown in Fig. I-3.

An instability was triggered by pulsing a nearby axial magnetic coil. In event (a) the scope traces were initiated just before the triggering mechanism that caused the sharp increase in the central end scintillators (1, 3, 6) at 8 μsec. The plasma leaves the axial region as shown by the decrease of scintillator 6. The pulses on the end scintillators indicate the location of the rotating plasma form as it spirals outward. Finally, it is detected by

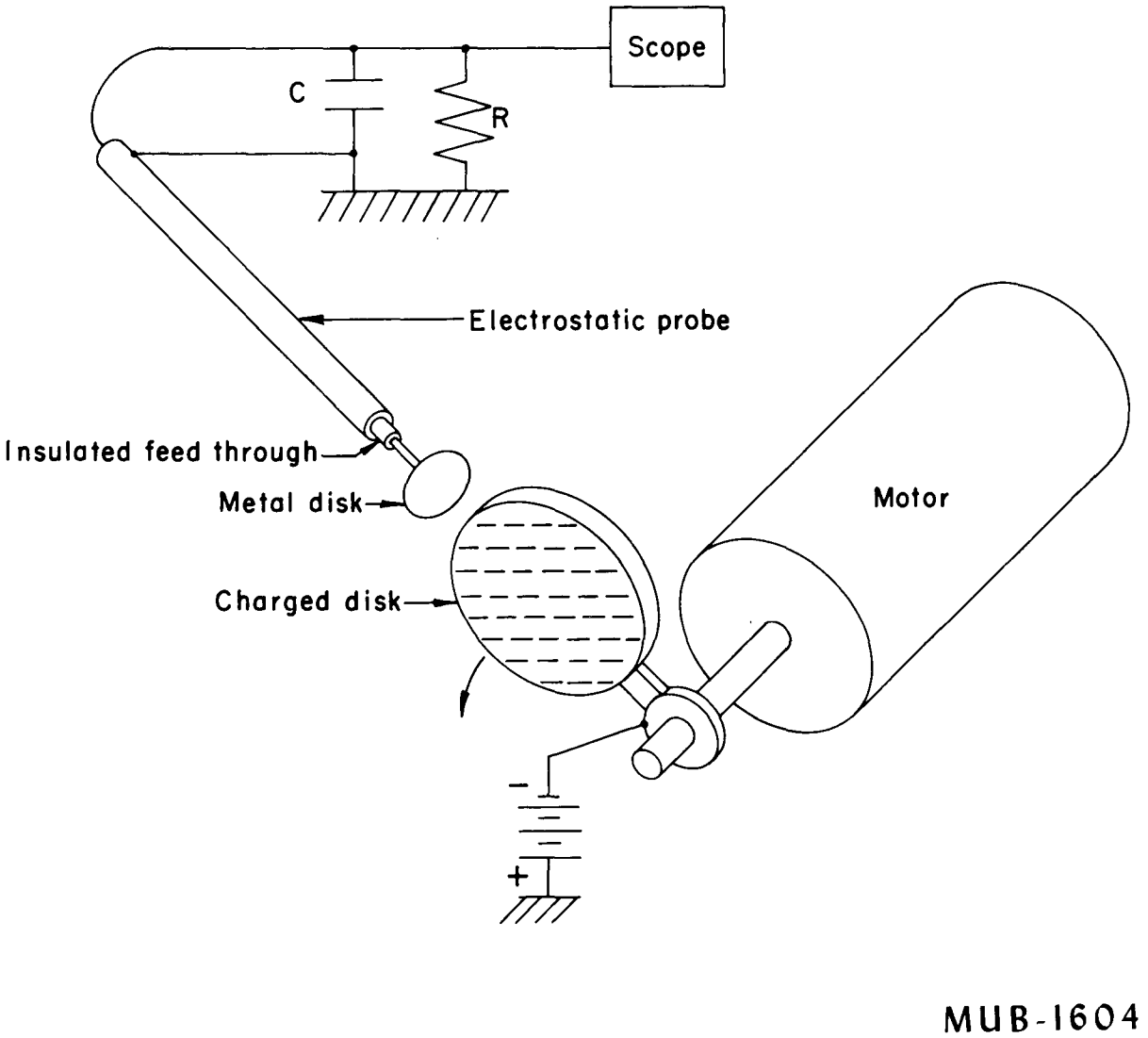

Fig. I-1. Diagram of mechanical-analog-simulating rotating-plasma column with electrostatic-probe detection system.

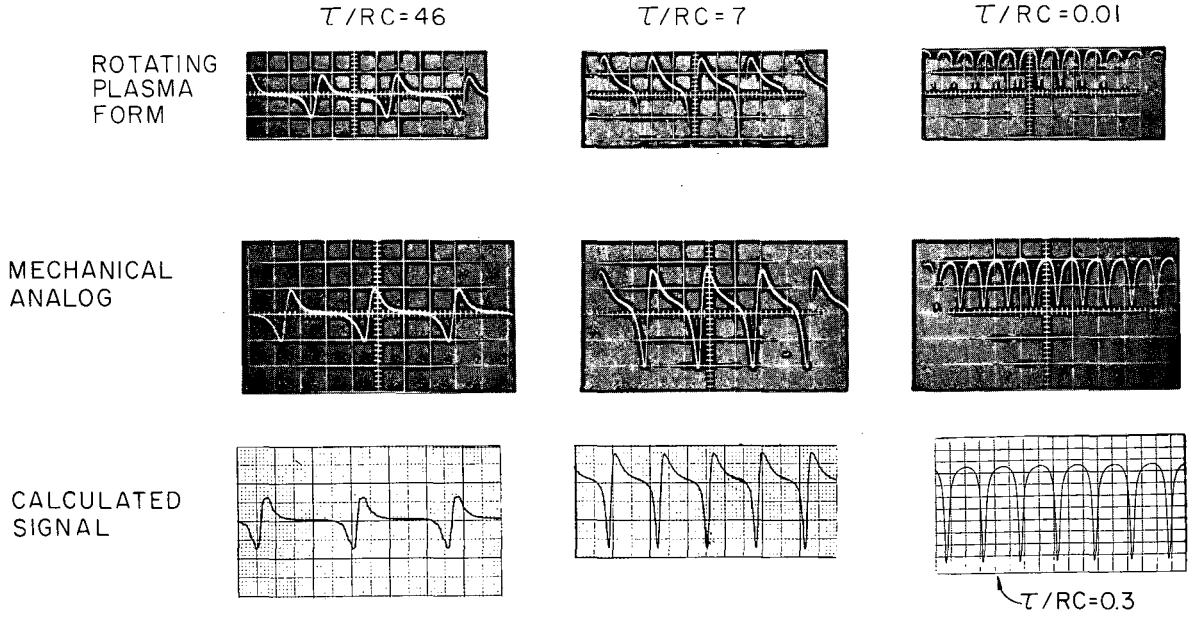

ZN-3565

Fig. I-2. Electrostatic-probe signals for different ratios of τ/RC where τ is the rotation period, R is the termination resistor and C is the termination capacitor (see Fig. I-1). The traces in the top set were taken with the probe in the vicinity of the plasma. In the middle set, the plasma was replaced by a rotating charged metal disk (see Fig. I-1). The traces in the bottom set were calculated.

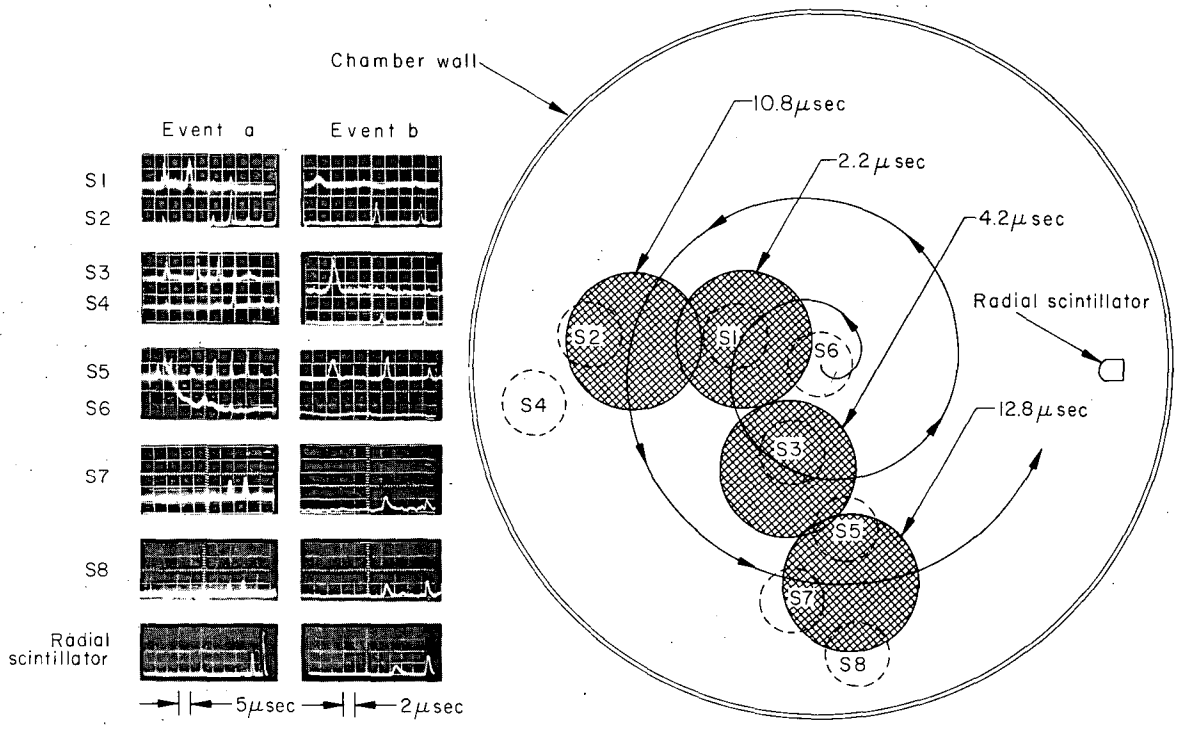

ZN-3564

Fig. I-3. Traces from eight-channel end scintillator probe and radial scintillator during the time the plasma column leaves the central region and spirals outward. Dashed circles indicate the radial and azimuthal position of end probes which were placed just outside one of the mirrors.

the radial scintillator. For event (b) the initiation of the scope traces was preceded by the triggering mechanism. These signals clearly indicate a body motion of the plasma, which has the shape of a column of roughly circular cross section. The average column radius (half width at half maximum) is about 2 cm. The estimated locations of the plasma column for event (b) are shown in Fig. I-3 as cross hatched circles with the time of its presence marked outside each.

A radial instability velocity was determined by analysis of 20 events such as those of Fig. I-3. The velocities ranged from 2 to 9×10^5 cm/sec.

B. Instability Studies With a Mirror Machine Using Different Compression Times

Walton A. Perkins

As discussed in the preceding Report,[1] experiments were initiated to see if the unstable plasma behavior that occurred in slow-compression mirror machines would persist at faster compression times. Mirror coils with rise times of 16 μsec and 4 μsec were used. The main diagnostic tools were radial scintillator probes and electrostatic probes. The main points are:

(a) Turbulent behavior was indicated in the early radial scintillator and electrostatic probe signals.

(b) Later, the radial scintillator signal attained the typical periodic line structure indicating the rotation. The electrostatic-probe signals also took on their periodic shape for differentiated or integrated signals, depending on the choice of τ/RC.

(c) The typical rotation period was 0.5 μsec, compared with the usual 2.0-μsec period for Table Top III.

(d) Electron heating seemed to be roughly as effective with the 16-μsec-rise-time coils as with the slower compression coils, but electron heating was much less effective with the 4-μsec-rise-time coils.

(e) No triggering is necessary or very effective, as the fast compression time is in itself enough. These one-turn coils (unlike the 240-turn coils of Table Top III) are very asymmetrical, and this may influence the instability.[2]

(f) The instability signals (1) increase with increasing final compression field, (2) decrease with increasing base pressure, and (3) decrease with increasing source voltage for reasonable high source voltage.

---

[1] Walton A. Perkins and Norris W. Carlson, in Controlled Thermonuclear Research Semiannual Report, UCRL-10294, July 1962, p. 15.

[2] F. H. Coensgen, W. F. Cummins, W. E. Nexsen, Jr., and A. E. Sherman, in Nuclear Fusion, 1962 Supplement, Part I, p. 125.

4. ALICE (ENERGETIC NEUTRAL ATOM INJECTION)

A. Alice Plasma Experiments

Charles C. Damm, James H. Foote, Archer H. Futch, Frank J. Gordon, Angus L. Hunt, and James F. Steinhaus

Observations of plasma behavior in Alice have been carried on with essentially the same operating conditions described previously.[1] The beam intensity has been increased to 60 mA (power equivalent) of 20-keV H^0 atoms, with a beam cross-sectional area of about 20 cm^2. The gas density in the trapping region is equivalent to 1×10^{-8}-mm Hg, at the highest beam levels, due largely to scattered beam particles. This pressure is from 6 to 10 times higher than that required for exponentiation of the plasma density, and improved beam control together with some additional fast pumping is planned to bring the gas density down. The magnetic-field intensity was adjusted to various values between 5 kG and 25 kG for these experiments, and beam injection was accomplished for a period of 3 to 5 sec during the magnetic-field pulse. Field variation during injection was less than 10% and was monitored. One coil failure was experienced early in this report period, caused by an improperly brazed joint.

Plasma Density

The average plasma density was measured from the flux of fast atoms observed at the periphery of the trapping region, these atoms being the result of charge-exchange collisions of plasma protons with background gas molecules. While this flux is proportional to the product of fast-ion density and gas density, the integrated flux arriving after turn off of the injected beam is independent of gas density and is proportional to the number of ions in the plasma at the time of beam termination. The solid-angle efficiency of the fast-atom detector used was estimated to be 4% and the volume of plasma was estimated to be 750 cm^3. The secondary-electron emission coefficient for the detector plate was assumed to be two.[1] We assign an uncertainty of a factor of two to the densities quoted, although relative densities may be more accurate.

On this basis, the maximum average density measured in Alice is 2×10^8 ions/cm^3. This is to be compared to an average density of less than 2×10^7 ions/cm^3 expected on the basis of trapping by residual gas only. We attribute the additional trapping to Lorentz-force ionization of excited atoms, thus reversing an earlier tentative conclusion based on a lower and less refined estimate of trapped density. John Hiskes of this laboratory has kindly made available his estimate of the Stark lifetimes for the $n = 12$ level of the hydrogen atom. This is probably the level responsible for the trapping contribution in our case. Based on these lifetimes, and our own measurements of the effective excited-state populations (see Sec. I, 4), the trapped density in Alice is estimated to be between 1.4 and 6.8×10^{-8} ions/cm^3, thus overlapping the experimental result. This agreement is also evidence that there are no large plasma losses other than those caused by charge-exchange collisions, an assumption tacitly employed in making the density estimate above.

[1] Charles C. Damm, James H. Foote, Archer H. Futch, Frank J. Gordon, Angus L. Hunt, and James F. Steinhaus, in Controlled Thermonuclear Research Semiannual Report, January through June 1962, UCRL-10294, July 1962, p. 15 (unpublished).

Occasional discontinuous jumps in plasma density by about a factor of two are observed via the fast-atom detector, especially at high beam levels, high magnetic fields, and at the best vacuum conditions. These variations are presently unexplained and could be associated with a true loss mechanism, or with an axial volume expansion of the plasma. Additional instrumentation will be required to clarify this behavior.

Characteristic Decay Times

The characteristic density decay times have been measured as a function of chamber pressure by admitting helium to the trapping region. Pressures were measured with a nude ionization gauge located just outside of the plasma. The results are shown in Fig. I-4. The lower points contain strong contributions from the residual gas, of unknown composition. To convert the ionization gauge readings to an equivalent helium pressure, it was assumed that the residual gases in question had a gauge factor of unity, and had a charge-exchange cross-section for protons equal to that of hydrogen. While these are plausible assumptions, verification awaits mass spectrometric data. The linear 45° slope of Fig. I-4 again indicates no loss other than charge-exchange, and the slight displacement from the theoretical curve probably represents a gauge-calibration factor. We note that the longest decay time observed (with beam off and beam-admission-valve closed) was 0.61 sec, corresponding to the chamber-base pressure of about 4×10^{-10}-mm Hg.

Radio-Frequency Activity

A single-turn loop antenna, located radially just outside of the plasma volume, was used to detect coherent radiation at the ion cyclotron frequency. Strong emission was observed for magnetic-field levels up to about 12.7 kG. The detector used was a spectrum analyzer which scanned a frequency interval of about 4 mc at a repetition rate of up to 30 times per second. Above 14.2 kG, no emission at the ion cyclotron frequency was detected, as shown in Fig. I-5, while between 12.7 kG and 14.2 kG, the emission was intermittent. At lower beam levels, the cutoff of the detected radiation occurred at lower magnetic fields. The present instrumentation cannot reveal the presence of short, intermittent bursts of radio-frequency activity, so that no conclusion can be reached yet concerning the presence or absence of emission bursts at the high fields. It is certain, however, that there is a decided change in the activity as a function of plasma density and magnetic field.

If the beam values of Fig. I-5, are converted to plasma densities it is interesting to note that the transition region occurs along a curve where $\sqrt{n}/B$ is approximately constant, and where the plasma frequency is approximately equal to the ion cyclotron frequency. This is the kind of behavior expected from a Harris-type instability,[2] but further measurements, both qualitative and quantitative, will be required to clarify the interpretation.

[2] E. G. Harris, Phys. Rev. Letters 2, 34 (1959).

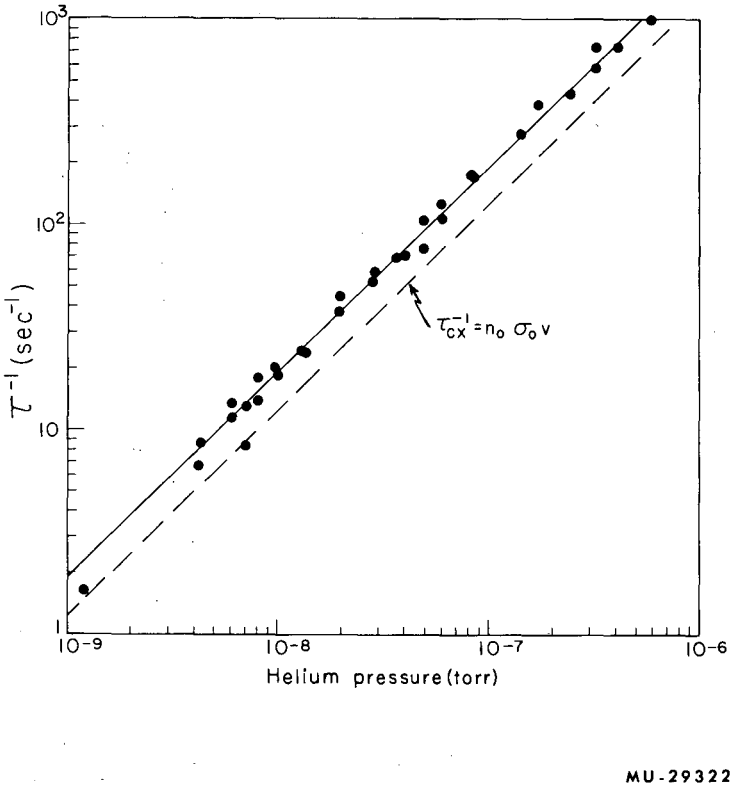

Fig. I-4. Variation of reciprocal characteristic decay time with the equivalent helium pressure in the trapping region. The theoretical relation (dashed line) is based on the helium-proton charge-exchange cross section, σ_0.

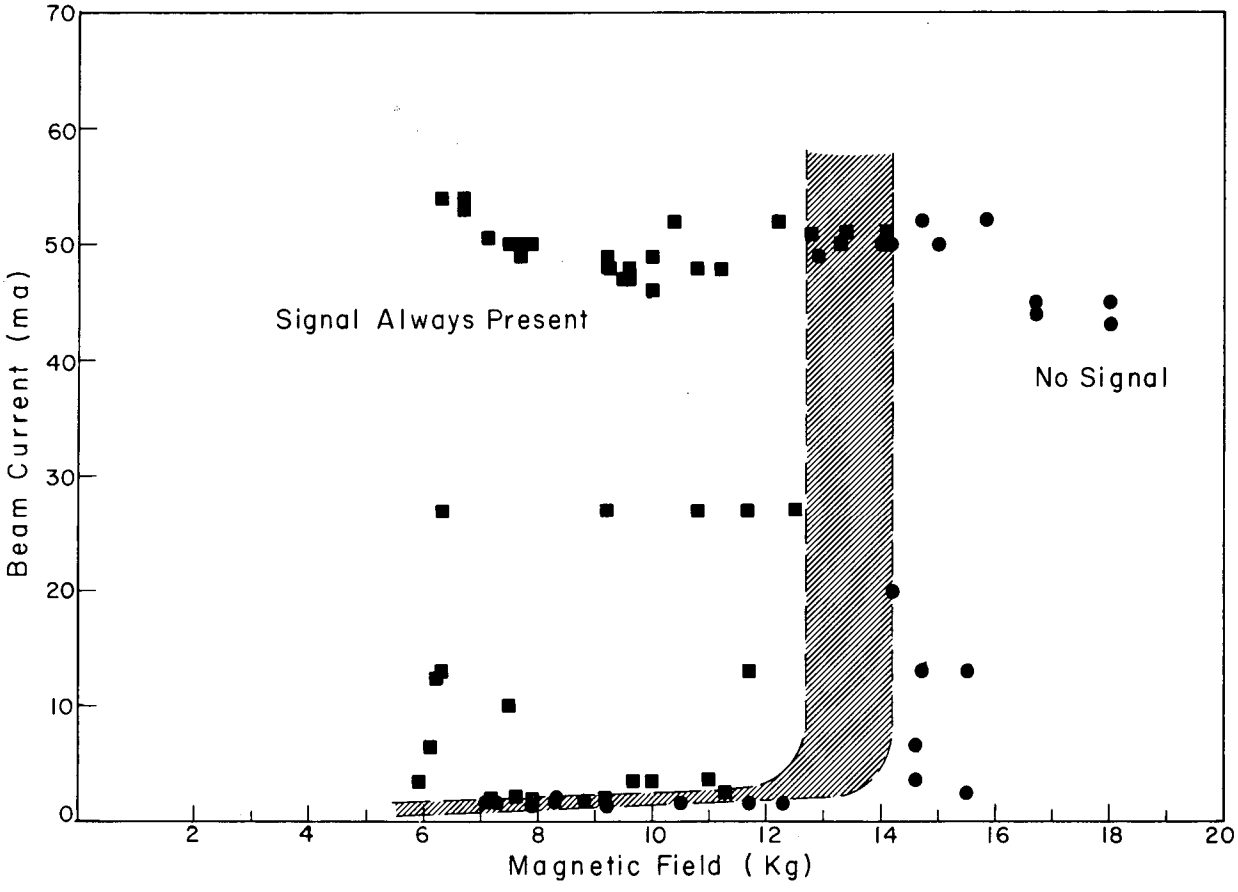

MUB-1605

Fig. I-5. Regions of rf activity at the ion-cyclotron frequency. The shaded area represents a region of intermittent activity.

It should be noted that the strong rf emission is often observed during plasma decay, persisting for seconds after beam turnoff. It does not appear that any large ion losses are incurred by this activity.

Plasma Oscillations

Plasma oscillations have been observed by means of an electrically isolated copper plate which also acts as a radial limiter for the plasma. The amplitude of the signal observed corresponds to about 10^{-4} A, with a dc level of 1% of this value. The amplitude is related directly to the injected-beam intensity. These oscillations are also observed on the molybdenum filaments located at the edge of the plasma region. The phasing of the signals on these various probes corresponds to a rotation of the signal in the direction of positive-ion precession in the nonuniform magnetic field.

The period of the oscillations is related to plasma density and magnetic field, as shown in Fig. I-6. The curve "splitting" at 12.5 kG is only suggested by the data, and later analysis indicates that there is no splitting within experimental uncertainty. At both fields, the curves are seen to approach the precessional period calculated for a 20-KeV proton in the nonuniform magnetic field. (To the first order, this period is independent of the radial location of the orbit.) After beam turnoff, with the magnetic field nearly constant, the oscillations are observed to decay in intensity approximately as the plasma density decays, although there is some irregular or discontinuous behavior in both signals at the initial (higher) levels. The oscillation frequency, monitored on a frequency meter, is observed at high magnetic fields to stay constant during the plasma decay. This constancy is maintained out to the sensitivity limit of the frequency meter for times like 1 sec, and during plasma-density changes by at least two orders of magnitude. At magnetic fields of 12.5 kG and lower, when strong radiation at the ion cyclotron frequency is observed, the frequency decays as the plasma density decays. In both high- and low-field cases, the plasma potential, as measured with a Li^+ ion beam (see Plasma Potential Measurements, in this section) is observed to decay as the plasma density decays.

From the persistence of the oscillations after beam turnoff, it does not appear that any large plasma losses are associated with the oscillations; within experimental uncertainty, the decay is by charge-exchange loss alone. Also, since the frequency is constant in the high-field case, the oscillation cannot be attributed to a simple $E \times B$ rotation of the plasma. The most plausible interpretation of the data presently is in terms of a stable, normal-mode oscillation of the plasma. An extension of the theory of finite-orbit stabilization[3] to the low density regime which has been made by R. F. Post (see Sec. I-4. b.) predicts stable oscillatory modes for the plasma in terms of the density and a parameter A related to the plasma density gradient. For the case that the oscillation period reaches the precessional period, A = 4 and the theoretical curve is determined. The data at 12.5 kG have been analyzed in this way, with the preliminary result shown in Fig. I-7. While the agreement looks exceedingly good, further work is underway to establish experimental errors, and to extend the analysis to other magnetic fields.

[3] M. N. Rosenbluth, N. A. Krall, and N. Rostoker, in Nuclear Fusion, 1962 Supplement, Part I, p. 143 (1962).

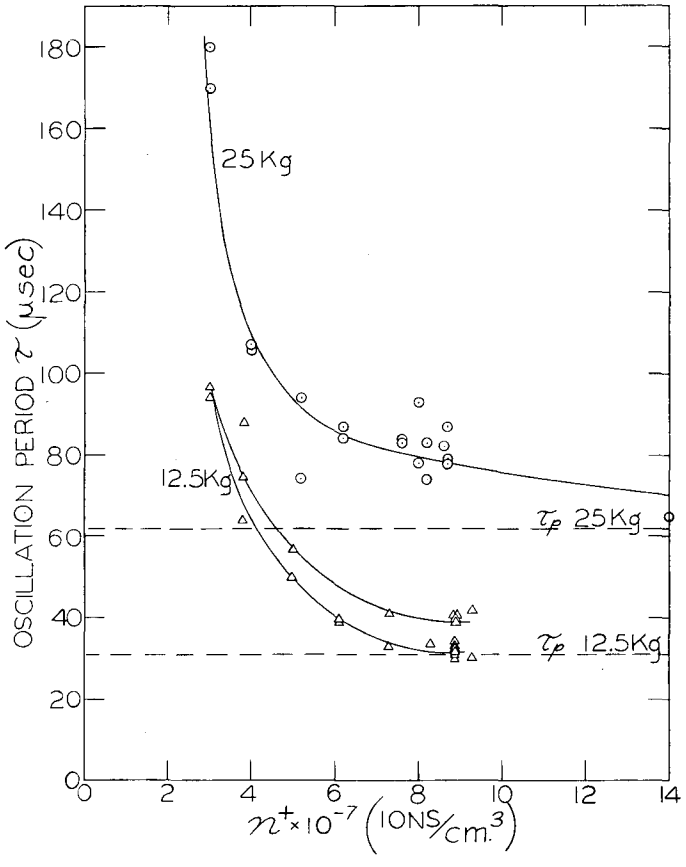

MU-29320

Fig. I-6. Plasma oscillation period as a function of plasma ion density for two values of magnetic field.

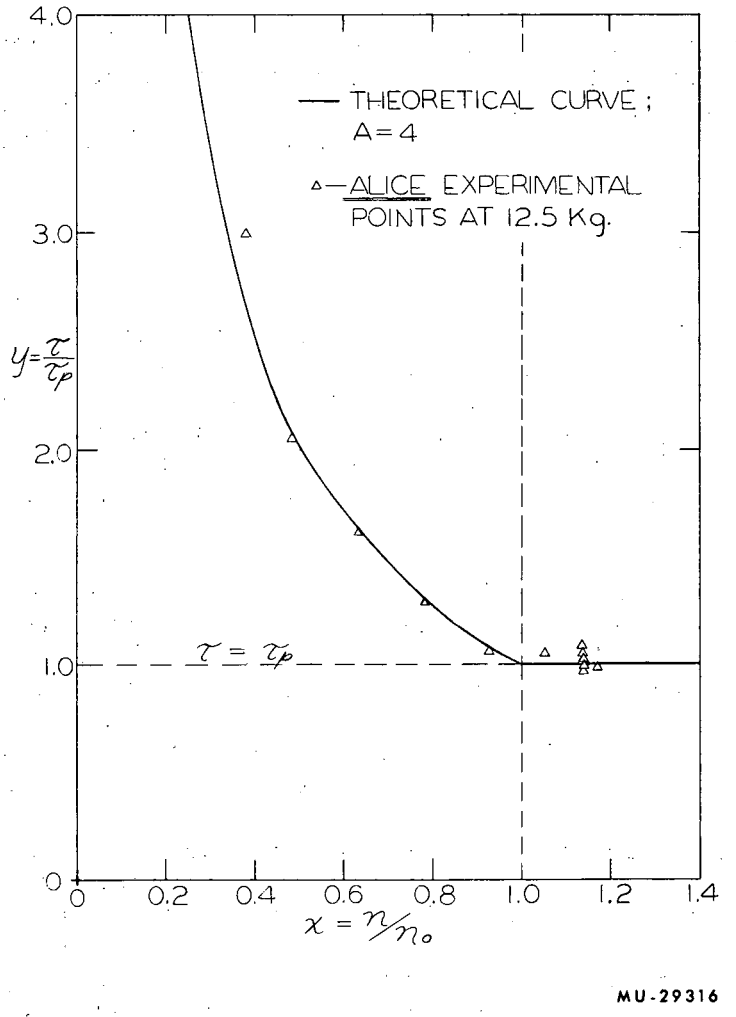

Fig. I-7. Preliminary comparison of oscillation-period data with the finite-orbit normal-mode analysis of Post.

The constant frequency observed during plasma density decay is interpreted as a change to another branch of the theoretical curve, where frequency independent of density is predicted. Which branch is selected by the system, and what relation this bears to the presence of radio-frequency activity is presently unexplained.

The positive dc level of the oscillatory signal is tentatively attributed to ions trapped within an orbit diameter of the edge of the probe. These ions are captured on their first precessional drift to the probe, but the associated electrons quickly drain along magnetic-field lines, leaving a net positive charge collected.

Plasma-Potential Measurements†

The potential of a plasma of constant density in a magnetic-mirror field is determined by an equilibrium between the rates at which charged particles are produced and lost. If the plasma is formed by injection and trapping of neutral atoms, the ion energy is greater than the electron energy. Initially, therefore, the electrons will have a higher mirror-loss rate than the trapped ions and a positive electrostatic potential will be generated. An understanding and knowledge of this potential is essential in understanding the plasma behavior.

Measurements of the plasma potential have been made using a technique described by Haste and Barnett.[4] A beam of positive lithium ions are accelerated from outside one of the mirrors along the magnetic-field lines. If the ion energy is greater than the plasma potential, a current is collected by a Faraday cup outside the opposite mirror from the lithium source, the plasma potential is defined as the accelerating potential of the lithium ions at which the transmission through the plasma became significant.

The measured values of the plasma potentials are considerably greater than theoretical values derived from equations which assume collisional heating of the electrons. An approximate treatment of the plasma potential, in which we assume collisional heating, has been discussed previously.[5] Recently, these calculations have been refined by using a Folker-Planck equation to calculate the electron-energy distribution. The present calculations are discussed in Sec. V.3.

---

†We wish to acknowledge the help of Lt. Cmdr. Carol Smith, Naval Postgraduate School, Monterey, California, who participated in the development of the Lithium ion source used in these experiments.

[4]G. R. Haste and C. F. Barnett, Bull. Am. Phys. Soc. 2, 152 (1961).

[5]A. H. Futch, Jr., W. Heckrotte, C. C. Damm, J. Killeen, and L. E. Mish, Phys. Fluids 10, 1277 (1962).

The disagreement between the experimental measurements and present theory implies that at least some of the electrons are gaining energy by an additional process. The additional process could be a fluctuating electric field resulting from a cooperative motion or oscillation of the plasma. This conclusion is shown to be justified by the experimental results shown in Fig. I-8. The plasma potential was found to be a function of the amplitude of the plasma oscillations as measured and described in the section on Plasma Oscillations just preceding.

Cold Plasma Trapping

A beginning has been made on formation of hot plasma by trapping on a burst of cold plasma. Using a cold plasma source as described previously[1], trapping of 15% of the beam for 200 μsec has been observed. This agrees approximately with the prediction based on the measured cold plasma density in excess of $10^{14}/cm^3$. The hot-plasma density achieved could not be measured, and improved timing of the cold-plasma burst in relation to beam turnoff will be required for an estimate of the hot-ion density. In any event, decay times are short because of high gas pressure during the burst, and ways of improving this are being explored.

Conclusions

In summary, we have observed the plasma density build up to about the predicted levels, and we have observed decay times in agreement with the interpretation that charge exchange is the dominant loss mechanism. Intermittent density variations by about a factor of two are presently unexplained, but could represent an axial expansion of the plasma. Cooperative behavior of the plasma is observed even at low densities and attempts are being made to interpret the observations in terms of theoretical models. The anomalously high values obtained for the plasma potential, and the detailed relation of plasma potential to plasma oscillation amplitude, remain to be explained.

Modifications to the beam control and vacuum systems are underway in order to improve pressures in the trapping chamber. Lower gas density should yield higher plasma density in direct proportion until the exponentiation condition is reached.

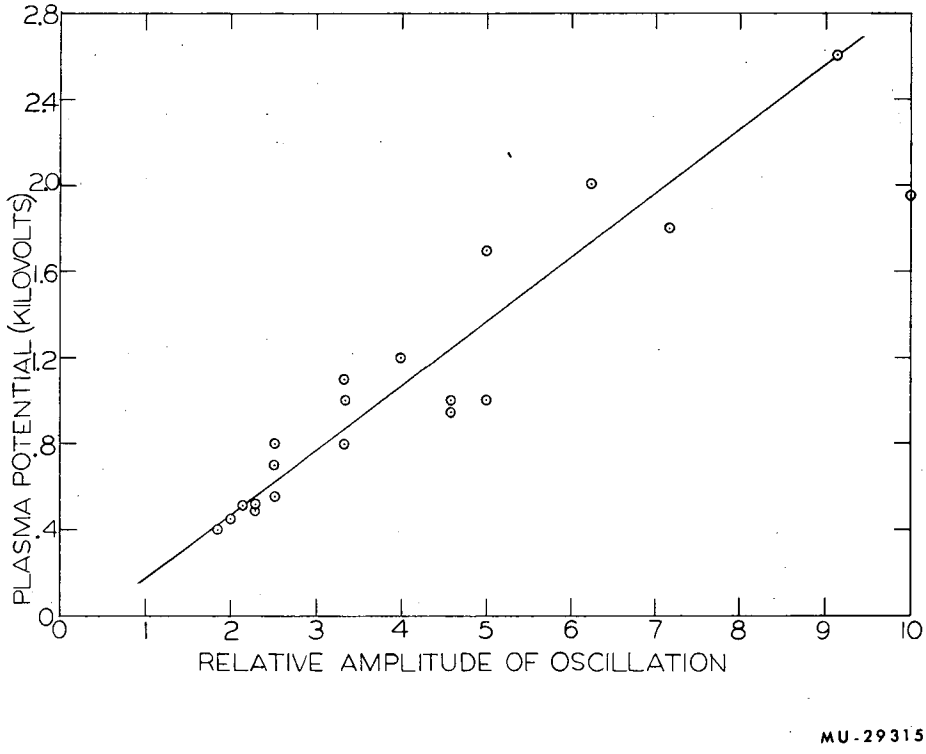

Fig. I-8. Plasma potential as related to plasma oscillation amplitude, measured by a Li^+ beam transmission technique.

B. The Effect of Plasma Density and Composition On Finite Orbit Stabilization

Richard F. Post

As mentioned in other sections of this report, there seems to be reason to believe that the so-called "finite-orbit" effects play an important role in the behavior of plasmas confined in all of our mirror-machine experiments. In this progress report, Newcomb reports an extension, by a different method, of the theory of Rosenbluth, et al.[1] to cases more directly applicable to the mirror machine. In order to cover plasma-particle density regimes spanning the range between Alice (10^7 to 10^8 cm^{-3}) to Table Top and Toy Top III (10^8 to 10^{14} cm^{-3}) an independent calculation by yet a third method has been made and is here summarized. This case reduces to one treated by Rosenbluth, et al.[1] (valid at "high" densities) and is in agreement with Newcomb's results (valid at "intermediate" densities). In addition, it predicts new effects, occurring at densities lower than those considered by Newcomb. Stable low-frequency modes of oscillation are found, the frequencies of which appear to agree with oscillations which have been observed in the Alice experiment.

The starting point for the calculation is a guiding-center Boltzmann-Vlasov equation in which finite-orbit effects are taken into account by calculating the effect on the guiding-center drifts of the actual electric field at the particles.

The problem is solved in plane geometry and converted, approximately, to an equivalent cylindrical problem by introducing periodic boundary conditions. Upon Fourier analysis in space and time an eigenvalue equation for the characteristic frequency, ω, is found. Real ω's correspond to stability, complex ones to unstable cases. The result applies to a plasma of arbitrary density, composition and temperature of the components. When evaluated for the interesting special case where $T_e \ll$ the ion energy, and for a delta function ion-energy distribution (of interest in the Alice experiment), the result found for ω is

$$\omega = \frac{k_x g}{2\omega_c}\left[\frac{b^2}{1+b^2}\right]\left\{\left[1+\frac{\omega_c^2 k_0 a^2}{2gb^2}\right] \pm \sqrt{\left[1+\frac{\omega_c^2 k_0 a^2}{2gb^2}\right]^2 - \frac{4(1+b^2)k_0\omega_c^2}{b^4 k_x^2 g}}\right\} . \quad (1)$$

Stable cases correspond to those in which the radicand is positive. Here k_x is the instability wave number $2\pi/\lambda$, g is the acceleration, ω_c is the ion gyro frequency, $k_0 = (1/n)(dn/dy)$ the "scale height" parameter, a^2 is the mean-square ion gyroradius, and b^2 is a mean value of the quantity $B^2/4\pi\rho c^2$ which is twice the ratio of magnetic-energy density to mass-energy density in the plasma.

---

[1] M. N. Rosenbluth, N. A. Krall, N. Rostoker, in Nuclear Fusion, 1962 Supplement, Part I, 143 (1961).

To convert this expression to an approximate dispersion equation for a cylindrical plasma in a mirror machine such as Alice, we introduce periodic boundary conditions, relate the scale-height parameter to plasma radius and replace g by $(\frac{1}{2}v^2)/P$, the acceleration associated with the gradient B precession (P = mean radius of curvature of the magnetic lines). If we normalize the expression to the precession angular frequency, $\omega_B = \frac{1}{2} a^2 \omega_c / rP$, we find for the mth azimuthal mode that

$$\frac{\omega}{\omega_B} = \frac{m}{2}\left[\frac{1+x}{1+\frac{x}{k_0 P}}\right]\left\{1 \pm \sqrt{1 - 8\left(\frac{r}{a}\right)^2\left[\frac{1+\frac{x}{k_0 P}}{1+x}\right]\left[\frac{x}{1+x}\right]}\right\}, \tag{2}$$

where $x = k_0 P/b^2 = n/n_0$, a parameter proportional to plasma density. A new stability criterion can be deduced from this relation. Introducing the result $L^2 \approx Pr$ (L = length between the mirrors, r = effective plasma radius) we can write that for stability

$$\left[\frac{La}{r^2}\right]^2 > \left(\frac{16}{3\pi}\right)\left\{\frac{(1+b^2)}{(1+b^2/k_0 P)^2}\right\}, \quad \text{stable.} \tag{3}$$

In the limit $b^2 \ll 1$, this reduces to the result found by Rosenbluth, et al., apart from a small numerical factor arising from the geometry. Also, apart from numerical factors of order unity, it agrees with Newcomb in the intermediate density regime, $b^2 < k_0 P$. (Note that $k_0 P \approx P/r \gg 1$, in general.)

Examination of this expression shows that it predicts the following sequence of behavior as plasma density is reduced below that considered by Rosenbluth: At high densities ($b^2 \ll 1$) the plasma may be stable provided Rosenbluth's original criterion is satisfied. As the density is decreased, b^2 increases and the plasma tends toward instability. If the density is still further decreased (but still within the plasma regime, i.e., Debye length < r) a stable state will again be achieved, when the denominator becomes important.

Comparison with the measured parameters in Alice shows that in the present experiments the plasma apparently is in the lower stable regime for all m. Here Eq. (2) shows that for m = 1, the two-eigen frequencies lie below ω_B, one decreasing to zero with decreasing density, the other approaching ω_B from below. In the section on the Alice experiment a comparison between some experimental data and the lower branch of Eq. (2) (for m = 1) is shown. The indicated agreement is striking and does not seem to be explainable by coincidence.

In the Table Top experiments, the sequence stable at low density, unstable at intermediate densities, stable at high densities, which we have previously reported, seems also to be consistent with the above picture. Other effects may also be operating in this case, however.

In Toy Top III S, the new results in which at "high" densities no plasma transport is seen across the field, also may agree with the finite orbit-theory predictions, as discussed by Coensgen. Certainly the satisfaction of the finite-orbit criterion was accompanied by a marked change in the plasma transport.

In summary, it appears that finite-orbit effects may play an important role over the whole range of densities presently of interest in the mirror program. We seem to have been able to establish quantitative contact between theory and experiment. If the theory is to be believed, a clear prescription for avoiding the interchange instability can be made, and some puzzling features of past experiments with mirror machines may be explained.

C. Ion-Source Development

Frank J. Gordon and Charles C. Damm

Two of the ion-source parameters varied during this period were found to have better values than those previously used. The source should probably be positioned in the magnetic field to ± 1/16 in. for maximum beam. More data is necessary to determine this setting accurately. Enlarging the arc defining slot by 50% in the anode farthest from the filament has resulted in smaller arc currents and longer operation at peak output. This slot has tended to constrict excessively during operation because of a buildup of material on the carbon slot edges.

With these two changes, the atomic-hydrogen beam to the trapping chamber is now 50 to 63 mA (power equivalent).

It is planned to add a neutral beam of possibly mixed species at energies up to 40 keV. This will enter the trapping chamber from the present beam tube after being neutralized and traversing the present ion-source chamber. A compact version of the Lofgren-Lamb[1] ion source modified in a manner suggested by Demirkhanov, et al.,[2] in nearing the testing stage.

---

[1] W. A. S. Lamb and E. J. Lofgren, Rev. Sci. Instr. 27, 907 (1956).

[2] R. A. Demirkhanov, O. F. Poroshin, P. E. Belensov, and G. P. McKeidze, High Current Injector of Hydrogen Ions, International Conference on High Energy Accelerators, (to be published).

D. Analysis of a Cold Plasma for Beam Trapping

James F. Steinhaus, Norman L. Oleson,† and William L. Barr

Previous progress reports covered pressure measurements[1] and an analysis of the plasma[2, 3] associated with the occluded-gas cold-plasma source. In this report we mention some additional results of the plasma analysis and plans for the immediate future. A complete summary of the cold-plasma investigation to date, from the occluded-gas source, will be published in UCRL-7097.[4]

Ion velocities obtained from Doppler-shift measurements on the spectral lines ranged from 0.5 to 3.0×10^6 cm/sec for all observable species in the plasma. Spectrographic data was taken with the pulse line charged to 15 kV, with 200 μsec pulses. The velocities were fairly constant and somewhat independent of charge. Also, since the neutral atoms of the different species have approximately the same velocities, a gas-expansion mechanism of acceleration is suggested. Time-of-flight measurements are in good agreement with these results.

The electron temperature was measured with a floating double probe. The general values of the kinetic temperature ranged from 12 to 3 eV, decreasing during the 200 μsec pulse. Plasma density calculations from these measurements can only be approximate, but happen to agree very well with the more accurate microwave cutoff data ($\approx 10^{14}$/cc).

The density output is definitely affected by the number of shots on the source washer. We have found that the duration of cutoff for any given density drops an average of 46% or about half during the first 1000 shots, and decreases negligibly thereafter. Since Ti is always present in the washer, it would appear that the decrease in density is due to decreased output of hydrogen from the washer.

Current effort is being directed toward lengthening the duration of the square-wave pulse line on the source to 600 μsec. This should greatly increase the duration of the high plasma densities. Consideration is also being given toward modifications which would reduce the effective neutral-particle output of the source.

---

†U. S. Naval Postgraduate School, Monterey, California.

[1] James F. Steinhaus and Charles C. Damm, in Controlled Thermonuclear Research Semiannual Report, July through December 1961, UCRL-9969, January 1961, p. 25 (unpublished).

[2] James F. Steinhaus, in Controlled Thermonuclear Research Semiannual Report, January through June 1962, UCRL-10294, July 1962, p. 19 (unpublished).

[3] William L. Barr, Controlled Thermonuclear Research Semiannual Report, January through June 1962, UCRL-10294, July 1962, p. 27 (unpublished).

[4] James F. Steinhaus, Norman L. Oleson, and William L. Barr, Investigation of a Plasma from an Occluded-Gas Cold Plasma Source, UCRL-7097, in preparation.

E. Alice Diagnostics

James H. Foote

For proper observation of the signals from the detectors in Alice, amplification is usually required. Amplifier characteristics of particular importance are gain, response time, and noise level. An amplifier that has proved useful to the Alice experiment, especially in the investigation of the plasma frequency in the kilocycle range, is the new Tektronix Type-O Operational Amplifier Plug-In Unit. In initial testing of one of the sections of this amplifier, used as a current-to-voltage converter, we obtained the following approximate results:

R_f (ohms)	C_f (pF)	Voltage out / Current in (V/A)	Response time (μs)	Peak-to-peak noise plus ripple (equivalent input current) (A)
1×10^9	0	-10^9	2500	2.6×10^{-10}
1×10^8	0	-10^8	250	1.0×10^{-9}
1×10^7	0	-10^7	40	3.5×10^{-9}
1×10^6	5	-10^6	8	1.5×10^{-8}
1×10^5	20	-10^5	2	5.0×10^{-8}
1×10^4	55	-10^4	0.6	2.0×10^{-7}

The response time as used here was the time for the output voltage to fall to 0.37 of its original value (or rise to 0.63 of its final value) when the input was a square-wave current signal. The quantities R_f and C_f are the feedback resistance and capacitance (added between the output and input points of the amplifier). We choose the value of C_f, when possible, just large enough to avoid overshooting or oscillating of the output-voltage signal. The capacity between the input and ground was 2000 pF (our input-cable capacitance).

When the current levels from our detectors are low, and when slower response times can be tolerated, we have found useful the Philbrick P2 Solid-State Operational Amplifier. Typical numbers of interest are:

Voltage out / Current in (V/A)	Response time (ms)	Peak-to-peak noise plus ripple (equivalent input current) (A)
-10^8	4	4×10^{-11}
-10^7	0.2	4×10^{-10}

Once again, the input capacitance was 2000 pF. The low noise level of this amplifier improves its utility.

F. Lorentz Ionization Experiment

Archer H. Futch and Charles C. Damm

Measurements of the Lorentz ionization of neutral hydrogen atoms produced by charge-exchange collisions are continuing. Typical results obtained using water vapor as the charge-exchange vapor are shown in Figs. I-9 through I-11. Figure I-9 shows the fraction of an ionized 44-keV neutral beam versus the electric field. The points plotted are the average of a number of runs; the standard deviations are indicated by the brackets. The distance from the center of the neutralizer to the ionizing field is approximately 100 cm. Increasing this distance from 100 cm to 217 cm results in only a small loss (approximately 20%) in the fraction of the beam ionized by an electric field of 100 kV/cm.

The integral curves, such as shown in Fig. I-9, are not sufficiently accurate to show structure corresponding to the different ionization levels of the hydrogen atom. Differential curves obtained by an electronic method are sufficiently accurate for this purpose. Figure I-10 is a differential curve for a 37-keV neutral-hydrogen beam. The labeling of the peaks corresponding to the principal quantum number, n, is based on theoretical calculations of the threshold field for ionization of the $n = 10$ level made by John Hiskes.[1] For comparison with Sweetman's results at 200 keV, arrows are drawn indicating the peaks of his curves labeled 10, 11, and 12, respectively.[2]

The fraction of the neutral beam which is ionized as a function of energy is given in Fig. I-11. The first two points were obtained using deuterium instead of hydrogen. These points were plotted at an energy a hydrogen atom would have if it had the same velocity as the deuterium atoms.

Tentative data using lithium as the neutralizing vapor is presented in Fig. I-12. We have been particularly interested in lithium, since theoretical considerations lead one to expect an increase in the population of the excited levels of about a factor of 10 if alkali vapors are used as the charge-exchange gas instead of hydrogen. The surprising thing about the result shown here is the strong dependence on the vapor pressure in the neutralizer. Attempts to make measurements at higher pressures were unsuccessful as the vapor condensed on a collimating hole blocking the path of the beam. We expect to continue these measurements on both water vapor and lithium, and to improve the techniques and accuracy of the experiment.

---

[1] John R. Hiskes, Electric and Magnetic Dissociation of Molecular Ions and Neutral Atoms, UCRL-6372, May 1961.

[2] D. R. Sweetman, in Nuclear Fusion, 1962 Supplement, Part I, p. 279.

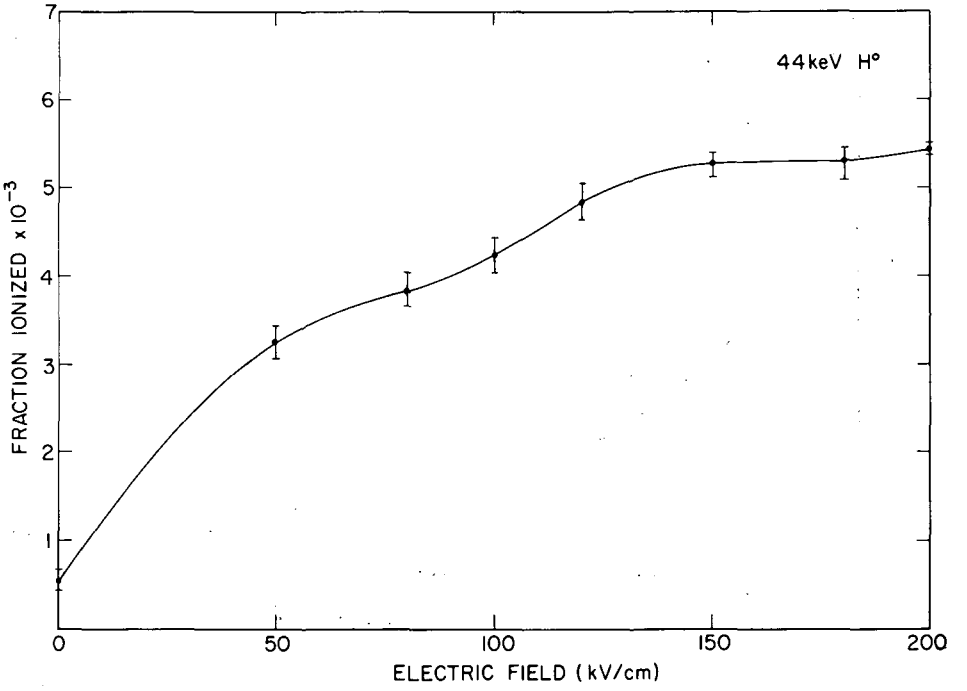

MU-29321

Fig. I-9. Fraction ionized versus electric field.

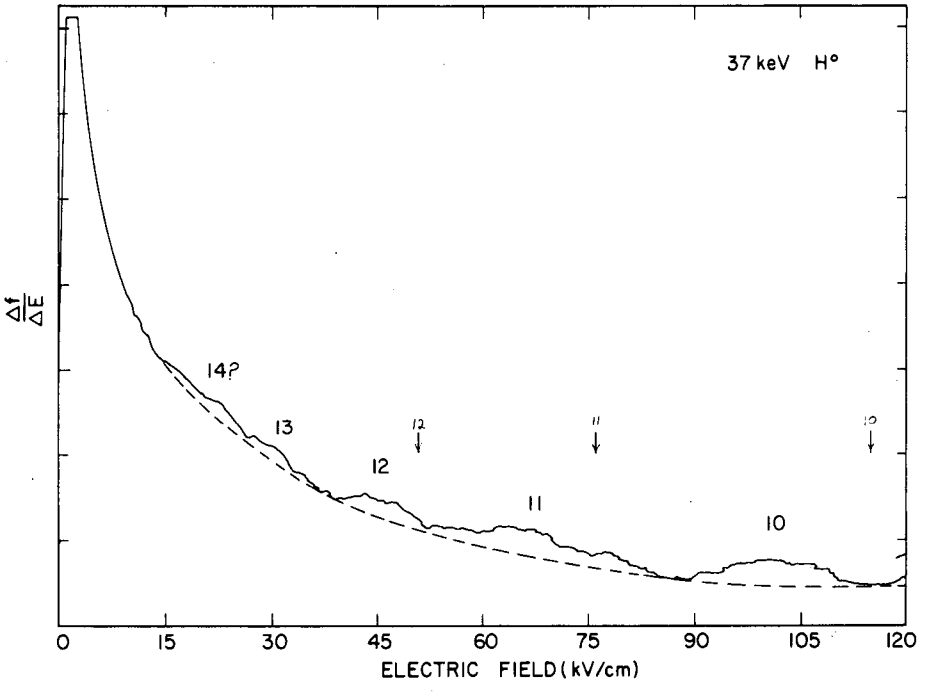

MU-29319

Fig. I-10. The ratio of change in the ionization rate to the change in the electric field versus the electric field.

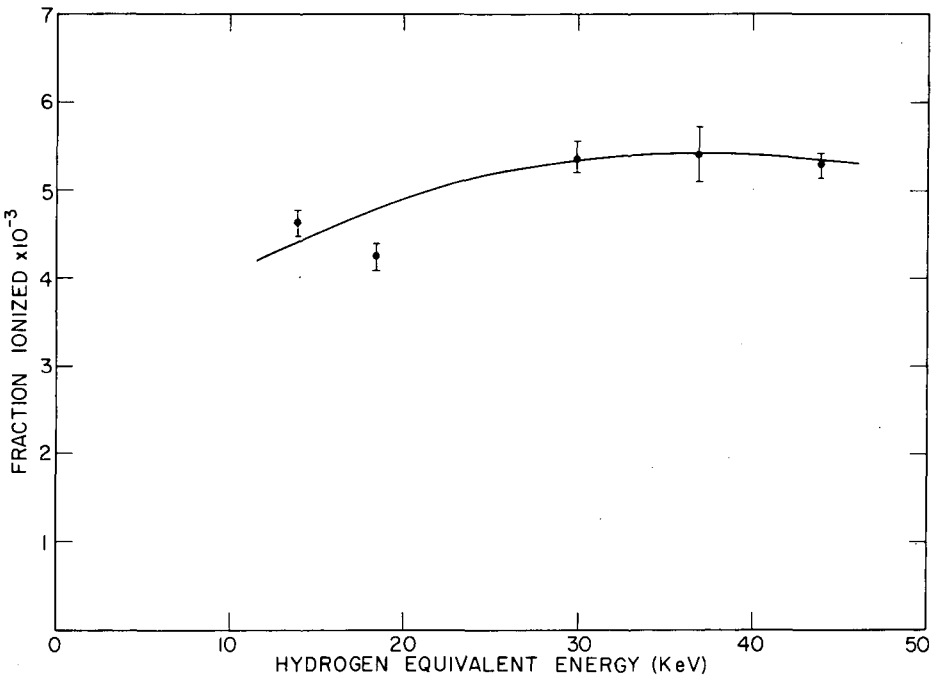

MU-29318

Fig. I-11. Fraction ionized versus beam energy.

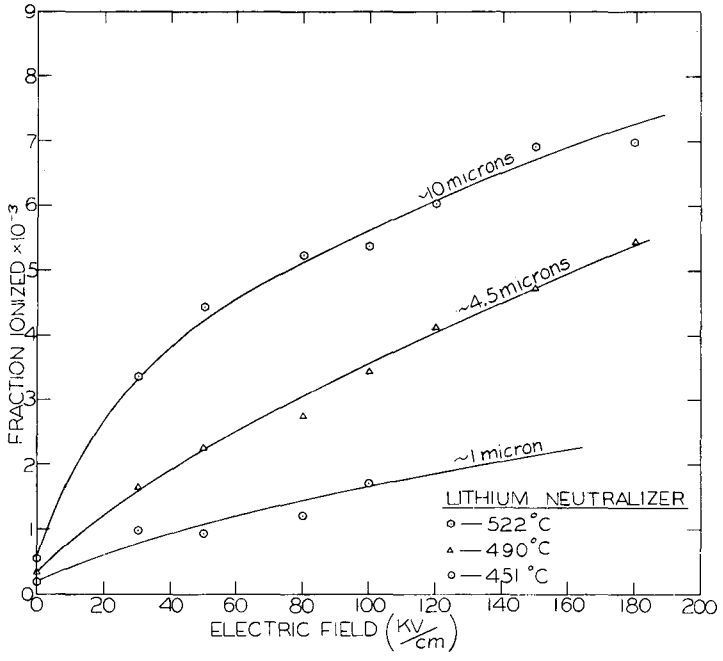

MU-29317

Fig. I-12. Fraction ionized as a function of the electric field.

G. Vacuum and Surface Studies

Angus L. Hunt and Charles C. Damm

Surface Bombardment Studies

The apparatus and the results of bombarding 305 stainless steel targets with 7.5- to 16-keV protons and deuterons have been previously described. The previous work suggested that normally incident protons or deuterons were not reflected from the surface but were buried within the surface. The increase in buried-particle concentration results in diffusion to the surface and molecular desorption. It also was suggested that loosely bound surface contamination was sputtered from the surface or desorbed by thermal spikes.

The previous work from room temperature to 200°C showed the composition of the gas evolved by bombardment was dependent on target temperature, so a new target assembly was constructed that would allow cooling the target to 80°K as well as heating to 300°C. Provision for evaporating molybdenum films on the target was included. Targets of 304 stainless steel, copper, tungsten, and molybdenum films on these targets at temperatures from 80°K to 485°K were bombarded with 10- to 15-keV deuteron beams and the composition of the evolved gas monitored with a mass spectrometer.

For all targets at temperatures near 80°K, the deuterium evolution during bombardment was almost undetectable for incident fluxes of approximately 5 $\mu A/cm^2$. In conformity with the model, the beam appeared to be buried within the target and diffusion to the target surface was extremely slow during bombardment periods as long as 30 minutes. It also was found that the rate of increase of the deuterium partial pressure within the target chamber increased with the temperature of the target.

For targets of about the same temperature but differing in mass number, the highest-mass target produced the lowest rate of rise of deuterium in the gas phase during the deuteron bombardment. It is uncertain from these experiments whether the reduced diffusion current to the surface of the tungsten target was due to a small diffusion coefficient for deuterium in tungsten or a smaller gradient of deuteron concentration in the high-mass target. It was experimentally apparent that trapping the high-energy neutral deuterium atom after it escapes from magnetic confinement would be very efficient if a low-temperature high-mass wall were to be used.

In addition to the direct beam interaction with the target, the second consideration is the desorption or sputtering of surface contamination. As previously reported, this problem can be most serious from the viewpoint of plasma contamination, as it was found that ordinary well-baked stainless steel, after cooling, had sufficient desorbable gas on the surface to produce gross plasma contamination if bombarded.

In recent work, each mass component from mass-to-charge ratios of 2 through 44 was monitored during bombardment of the various targets at temperatures from 80°K to 485°K. As expected, it was found that the magnitude and type of surface-contamination component appearing in the gas

phase were dependent on the history of the vacuum system and target. It was concluded that cooling the target resulted in larger bombardment-induced desorption because the cold targets had more adsorbed gas on their surfaces.

At all temperatures, fresh molybdenum films, which were evaporated on stainless steel, copper, or tungsten targets, greatly reduced the bombardment-induced desorption. Although the fresh molybdenum films were not atomically clean surfaces, surface contamination was sufficiently low that bombardment-induced desorption was much less than that for the original metallic substrates.

These collective results indicate that atomically clean high-mass metallic surfaces below 110°K will provide satisfactory walls for some high-purity plasma experiments. The evaporated molybdenum film on a liquid-nitrogen-cooled substrate is the best approximation to such a surface found to date.

5. P-4 (STEADY-STATE PLASMA) SYSTEM

William L. Barr and Andrew L. Gardner

In July, the decision was made to phase out the operation of the P-4 system in order to permit greater effort in other portions of the program. Consequently, the studies of electron-beam interaction with the plasma were discontinued to permit the remaining brief activity to be devoted to compression and confinement measurements on a portion of the plasma column.

A. Plasma Compression

A quartz tube 8-5/8 in. long by 2-1/2 in. i.d. was installed with viton gaskets and ceramic flanges to encircle a segment of the plasma at a position of low neutral density and relatively high ion temperature near the downstream end of the system. A pulsed four-turn compression coil surrounded the quartz tube. The coil-support structure had windows at the midplane (between the magnetic mirrors) to permit microwave and optical viewing of the plasma.

Both helium and hydrogen plasmas were used. From previous measurements, the helium-ion temperature was known to reach 8 eV or so at this location but hydrogen-ion temperatures had not been measured. By using helium as a tracer in a predominantly hydrogen plasma, and by assuming that the He^+ ions and the protons are in thermal equilibrium, an approximate determination of the proton temperature was obtained.

With an input mixture of 75% H_2 and 25% He, the temperature of the He^+ ions inside the quartz pipe was approx 50% higher than when 100% He was used. When the fine structure of the spectral line is ignored the observed He II 4686 line width corresponds to a temperature of 12.4 eV with H_2 and to 8.3 eV in He. The higher ion temperature in hydrogen exists presumably because the electrons can share their energy more easily with the light protons

than with the heavier ions. These measurements were made by modifying a Jarrell-Asch monochromator so that nine adjacent 0.5-Å-wide segments of the visible spectrum could be monitored simultaneously. The fraction of the observed line width that is due to fine structure in the line is determined by the relative populations of the various fine-structure levels. If the populations are maintained by electron excitation directly from the ground level, then the fine structure contribute only a negligible amount to the line width at these temperatures. This is assumed to be the situation in P-4.

The approximate plasma conditions prior to the pulse were as follows:

	Helium	Hydrogen
Ion density on axis (cm^{-3})	$1\text{-}2\times10^{13}$	$\approx 1\times10^{13}$
Neutral density (cm^{-3}) (measured 20 in. upstream)	4×10^{11}	1.5×10^{11}
Ion temperature (eV)	8	10 to 15
Ion self-collision time (μsec)	4 (He^+)	4-7
Diam of plasma column (cm)	2	2
Magnetic field (kG) (homogeneous)	0.9 - 1.3	0.9 to 1.3
Ion cyclotron period (μsec)	2-3	0.5 to 0.7

Two pulse-coil configurations were used. These had the following pulsed-field characteristics:

	Coil A	Coil B
Mirror ratio	1.15	3.8
Maximum central field used(kG)	27	5.9
Distance between mirror peaks(cm)	8.2	10.7
Rise time (μsec)	7.5	5.6
Decay time (μsec)	200	~150

B. Probe Measurements

A stainless steel tube 3/16-in. in diam × 2 in. long, with a shielded lead, was located in the bottom of the quartz tube and between the mirror peaks, to serve as an electric probe for indications of radial escape of the plasma. During the pulse the probe potential was held at the floating potential it naturally sought prior to compression.

Coil A Results

No significant probe signals were observed.

Coil B Results

Definite probe signals were observed from 5 to 15 μsec after the start of the compression with both helium and hydrogen plasmas. Net positive charges of the order of 10^{12} were collected per pulse. High-speed resolution of the probe signal did not reveal any definite periodicity.

C. Microwave Measurements

Transmission cutoff measurements were made at 64 Gc with Coil A and at 64, 38, and 30 Gc with Coil B.

Although the high-frequency cutoff was readily achieved and maintained up to 10 μsec after the start of the compression, by 15 or 20 μsec essentially complete transmission was observed, even at the lower frequencies which were partially or completely cut off prior to the compression.

D. Optical Measurements

When the compression coil is pulsed the light from He^+ rises (by as much as a factor of ten for the highest compression) from the steady-state level, peaks at about 3 μsec, and then falls below the noise level by 10 μsec. Light from neutral He changes little for about 0.5 μsec and then falls to a low but measurable level in about 5 μsec. Because the quartz was delivered with a ground surface instead of the polished surface as specified, optical observations of the size and position of the plasma were not feasible. It had been planned to use the nine-channel detector from the polychromator to observe any gross motion of the plasma.

E. Conclusions

The rapid decay of the He^+ light, after its initial rise upon compression and heating, no doubt results from complete stripping of the helium ions, which rapidly depletes the available number of emitters. The neutral helium emitters are similarly reduced but a continuing influx from the region around the plasma maintains an observable signal.

The lack of confinement with Coil A is attributed to its high mirror losses. If the lower-frequency microwaves had been used with this coil, perhaps some confinement of H^+ could have been seen, but the short self-collision time for He^{++} ions makes appreciable He confinement impossible.

The measurements with the hydrogen plasma and Coil B are of the most interest. Here radial loss of plasma was apparent in a case for which finite-orbit stabilization calculations may indicate a marginally stable situation. This cannot be considered, however, as a result necessarily at variance with the theory, because of quantitative uncertainties, and the absence of a conducting wall.

As discussed in the sections by Newcomb (Sec. V. 2) and by Post (Sec. I. 4) the stability criterion can be written in the form

$$\left[\frac{La}{r^2}\right]^2 > C,$$

where

L = distance between mirrors,

a = rms ion Larmor radius,

r = plasma radius at the median plane, and

C depends on the mirror ratio.

The following tables compare rough evaluations of $[La/r^2]^2$ and the calculated value of "C" from Newcomb's expression. This is done for a range of assumed values of plasma radius which may be expected to bracket the most appropriate value.

Hydrogen (Coil B, L = 10.7 cm)

Initial central field	1.3 kG
Peak central field	5.9 kG
Mirror ratio (peak field)	3.19
Ion-orbit radius (rms) (assuming only 2/3 power heating)	≈0.12 cm

Assumed plasma radius before compression (cm)	r (cm) (compressed)	$[La/r^2]^2$	C	"Predicted Behavior" (for m > 1 modes)
3.18 (quartz radius)	1.49	0.335	≤ 6.7	unstable
2.0	0.94	2.13	≤ 6.7	unstable
1.0	0.47	34.2	≤ 6.7	stable
0.75	0.352	107.5	≤ 6.7	stable

75% H_2, 25% He (Coil B, L = 10.7 cm)

Initial central field	0.9 kG
Peak central field	6.8 kG
Mirror ratio (peak field)	3.43
Proton orbit radius (rms) (assuming only 2/3 power heating)	≈0.12 cm

Assumed plasma radius before compression (cm)	r (cm) (compressed)	$[La/r^2]^2$	C	"Predicted Behavior" (for m > 1 modes)
3.18(quartz radius)	1.15	0.93	≤ 7.2	unstable
2.0	0.728	5.9	≤ 7.2	marginal
1.0	0.364	94.0	≤ 7.2	stable
0.75	0.273	297	≤ 7.2	stable

II. ASTRON PROGRAM

1. INTRODUCTION

Nicholas C. Christofilos

The construction of the 5-MeV electron accelerator was practically completed in September 1962. Therefore it was possible to operate the first of seven units, namely, the electron gun (620 keV, 200 A) on September 28. Progressively more units will be tested until all seven units are operating reliably. At this time, three units are in preliminary operation. The results observed thus far are described in more detail in Sec. II. 2.

The mechanical assembly of the Astron tanks and coils is progressing. During this period the mirror vacuum chamber and pumping system were assembled and leak-checked. Assembly of the cantilever sections (in the electron injection tank) started. Most of the field coils have been installed.

The "debugging" of the accelerator is expected to be completed early next spring. The balance of the Astron facility, however, is expected to be ready at late summer. Consequently, this period of six months, until the complete facility will be ready for starting experiment on the generation of the E layer, will be devoted to improving the reliability of the accelerator or performing experiments on interaction of the electron beam with plasma in a variety of conditions, or both. Thus, plasma oscillations as well as hydromagnetic interaction of the relativistic electron beam with the plasma can be studied.

There have been many papers published, in the last ten years, on interaction of electron beams with plasmas. However, this is the first time that an electron beam of 10^9 W will be available for studies of interactions with a plasma. Therefore it is of extreme interest to study the interaction of the Astron accelerator electron beam with a plasma column, in the domain of both plasma oscillations and hydromagnetic oscillations. Consequently, this interim of six months will be used profitably in the research and study of generating of plasma oscillations, to determine the energy transfer from the beam to the plasma, for studies of the conditions for unstable or stable oscillations, and so on. These experiments will be performed by injecting the electron beam along the axis of a tank that is 60 ft long. The plasma column will be generated by the electron beam ionizing the neutral gas. A variety of neutral gases at different pressures will be used in these experiments.

2. ASTRON ELECTRON ACCELERATOR

Thomas M. Comella, Ross E. Hester, William A. S. Lamb,
Daryl D. Reagan, William A. Sherwood, and Robert E. Wright

Preliminary beam operation of the 700-keV electron gun was obtained on September 28, 1962. The initial try for beam was made using a 6-in. diam cathode in place of the 10-in. diam cathode. We used the 6-in. cathode to minimize the heat load on the metal-ceramic accelerating column; this heat load resulted from the failure of the spare column. This preliminary operation with the smaller cathode established the principle of the accelerator and enabled us to obtain operating experience with the electronic system.

By mid October we had installed the 10-in. diam cathode and obtained the operating conditions outlined below:

(a)	peak beam current:	180 A
(b)	pulse length:	0.3 μsec
(c)	repetition rate:	5 pps
(d)	approximate beam energy	620 keV
(e)	beam diam 96 in. from cathode:	< 3-1/2-in. diam.

The energy of the beam was estimated by magnetic analysis and the diameter was estimated by means of an adjustable iris on the collector cup. An alternative method of estimating the energy is to add up the voltage which can be monitored on each core.

Although an absolute energy measurement was difficult to obtain under these circumstances, the energy pass of the collimating and magnet system was easier to estimate; this we found to be ±5 keV. Under these conditions, no variation in the beam-current trace from pulse to pulse after magnetic analysis could be seen.

The larger cores required for the gun section made it necessary to use three pulse-forming networks per core where one pulse-forming network per core was adequate in the accelerator units. Because of this, the gun electronics' system is one-fourth that of the total system, which consists of the gun and six accelerator units. Consequently, much valuable operating experience on the system was obtained.

The gun and two of the six accelerator units were operated in mid December and the first beam was obtained on December 19, 1962. With a 3.75-in. diam collector cup at the end of the second accelerator section, the operating conditions were:

(a)	peak beam current:	120 A
(b)	pulse length:	0.25 μsec
(c)	repetition rate:	5 pps
(d)	approximate beam energy:	1.7 MeV

These results represent the first beam through the machine and are the beginning points to optimize accelerator conditions. During these two runs the system was operated, in each case, in excess of four hours without mishap.

III. LIVERMORE PINCH PROGRAM

Dale H. Birdsall, Stirling A. Colgate, Harold P. Furth, Charles W. Hartman, Charles E. Kuivinen,* and Ross L. Spoerlein

1. SUMMARY

During this period, the 12-in. levitron and the 12-in.-by-36-in. linear hard-core pinch have been put into operation. In both cases, pinch formation at unusually low particle densities was found possible. Some interesting equilibrium state and instability phenomena have been discovered. In particular, on the levitron, ultra-small-amplitude magnetic turbulence is observed, and appears to be responsible for an anomalous energy drainage by hot-electron motion across the zero-order magnetic field.

The theory of finite-resistivity hydromagnetic instabilities has been developed further in a number of areas, notably the calculation of stability criteria for the "tearing" mode in cylindrical geometry. Experiments designed to observe the "tearing" mode in a Triax (reverse-B_θ) pinch tube have yielded satisfactory qualitative agreement with theory.

2. LEVITRON OPERATION

Pinch experimentation on the levitron began in August. The previous experience with linear hard-core pinches had indicated coupling times (between B_z and B_θ field) of about 30 to 60 μsec. Accordingly, a B_z field rising to approx 5 kilogauss in 60 μsec was used to compress an initial B_θ field. No pre-ionization was used, and a D_2 pressure range from 0.7 to 15 μ gave satisfactory coupling. Maximum coupling times of approx 200 μsec were found for operation at 1.5 μ. The B_z rise time was then increased to 175 μsec, and the optimum pressure fell to 0.5 μ. At the same time, the coupling time τ_I increased to 400 μsec, and spectroscopic evidence confirmed that the electron temperature was higher than before. The B_z rise time was then extended stepwise up to 1400 μsec, with an associated drop of optimum D_2 pressure down to 0.1 μ, and an increase of τ_I up to 1700 μsec (see Fig. III-1). The reduction in mean resistivity (estimated from the field-intermixing) for the lower-density, slower-rise-time regimes is also shown in Fig. III-1. We note that the degree of coupling between B_z and B_θ diminishes. This is reflected in the ratio between the maximum toroidal plasma current I_p and the initial hard-core current I_0 (see Fig. III-1). From the degree of coupling and the initial D_2 density, one can estimate the energy input per electron ($\Delta W/N_e$); this is found to be correlated with the observed conductivity: both improve rapidly at first, but reach nearly constant values as the density and rate-of-rise are reduced.

When the ring-core support rods are not withdrawn during pinching, the coupling times are greatly diminished, particularly at low density. The

*Hughes Aircraft Corp., Microtube Division, Inglewood, California.

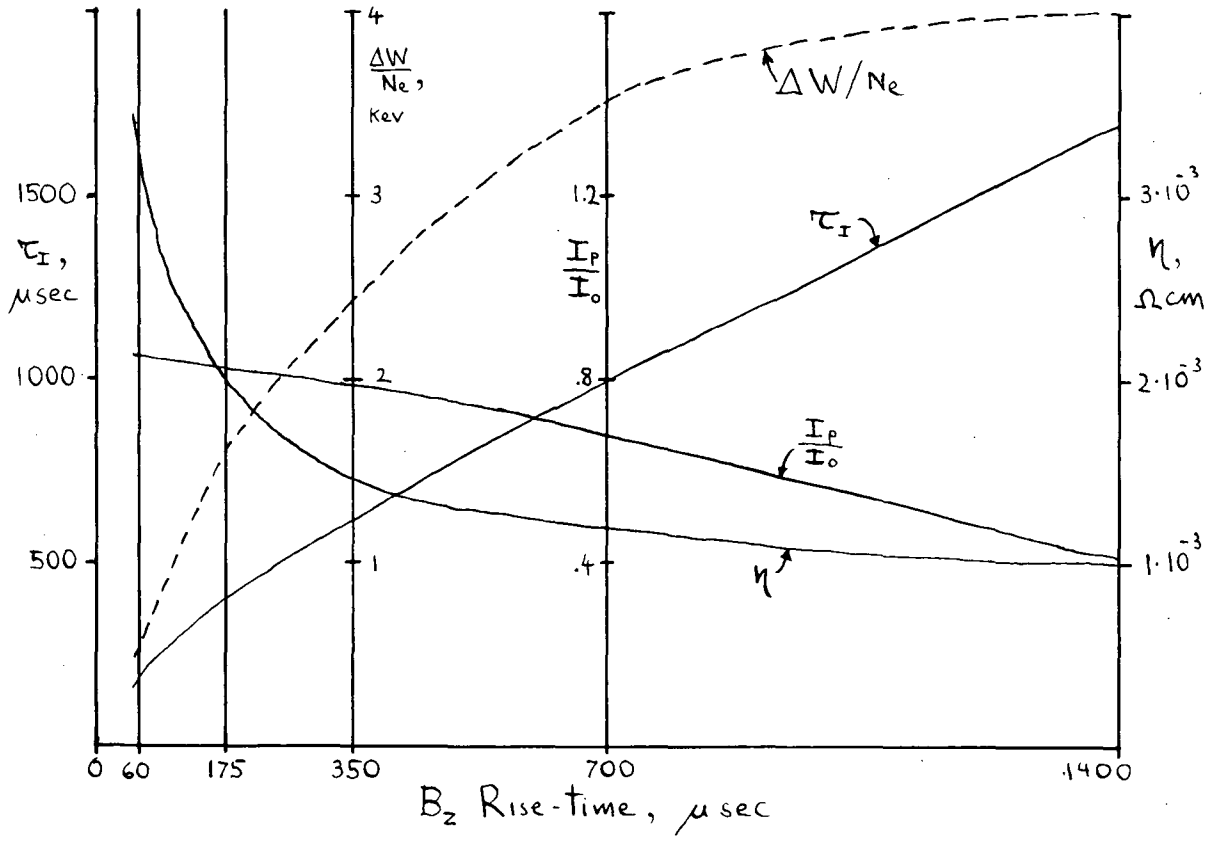

MUB-1603

Fig. III-1. Dependence of levitron-performance characteristics on B_z rise-time. The values of initial D_2 pressure giving maximum coupling time τ_I are used.

same result is achieved by contamination with 0.05-0.1 μ air, or by failure to bake out the stainless steel liner prior to operation.

Most of the diagnostic studies were done on the regime with 1400-μsec rise time, and with a D_2 pressure of 0.1 μ. The measured field configuration is shown in Fig. III-2. It should be noted that insertion of a magnetic-field probe tends to shorten the field-coupling time substantially. Field monitoring is usually done only near the thin stainless liner, or outside it.

The principal features of a 0.1-μ discharge are illustrated in Fig. III-3. The B_z and B_θ fields monitored outside the liner show B_θ entrapment starting 300 μsec after B_z firing, and lasting some 1500 μsec (under optimally clean conditions, more than 1700 μsec), or until slightly after maximum B_z. During the first 200 μsec or so of the discharge (up to $t = t_c$), the deuterium is ionized fully and the impurity light in the visible at first rises and then drops. The voltage around the outer torus shell (which measures the rate of change of B_θ flux between the hard core and the shell) drops sharply at first, showing that the B_z field is coupling increasingly well to the B_θ field. At the "critical time" t_c, there is a discontinuous change in dV_{tor}/dt, showing that the plasma conductivity suddenly starts to become worse again. At roughly the same time, an unintegrated B_r probe near the liner detects the onset of fluctuating fields in the 2 to 5 gauss, 2000-kc range. The B_r-components of smaller amplitude are also found going into the 10-Mc range. The plasma confinement, as measured with single Langmuir probes near the liner, is good up to $t = t_c$, after which hot electrons in the 100 eV, 3×10^{12} cm^{-3} temperature and density ranges are observed. The floating potential ϕ_3 relative to the liner, and measured 3 cms from the liner, is also shown in Fig. III-3. An initial negative signal results from run-away electrons, and is followed after $t = t_c$ by a persistent positive signal on the order of 200 V, corresponding to the loss of hot electrons from the plasma to the liner. The complex x-ray pattern shown in Fig. III-3 is highly reproducible. At still lower densities only the pre-breakdown x-ray burst remains. At higher densities, or with impurity contamination, the x-ray burst is greatly increased in amplitude and lasts throughout the discharge. Our preliminary results on time-resolved uv spectra confirm that high electron temperatures are present during most of the pinch cycle.

While the investigation of this pinch regime is far from complete, the following general remarks can be made. In the period up to t_c, everything seems to be proceeding according to classical rules. If this regime could maintain itself, a stable pinch in the kilovolt range with $\beta \approx 10\%$ would be achieved. The onset of instability after t_c disrupts effective containment. Due to the high electron temperature, even the very small observed magnetic-field fluctuations (less than - part in 1000) are sufficient to link the flux surfaces and permit the electrons to carry the Ohmic input energy to the wall. This energy transfer proceeds mainly by ordinary thermal conduction along the "tangled" field lines. In view of the low density and large input energy (approx 4 keV per electron) the energy losses by radiation are estimated to be relatively less important.

The nature of the basic instability mode is still undetermined. All infinite-conductivity modes and the finite-conductivity "tearing" mode are

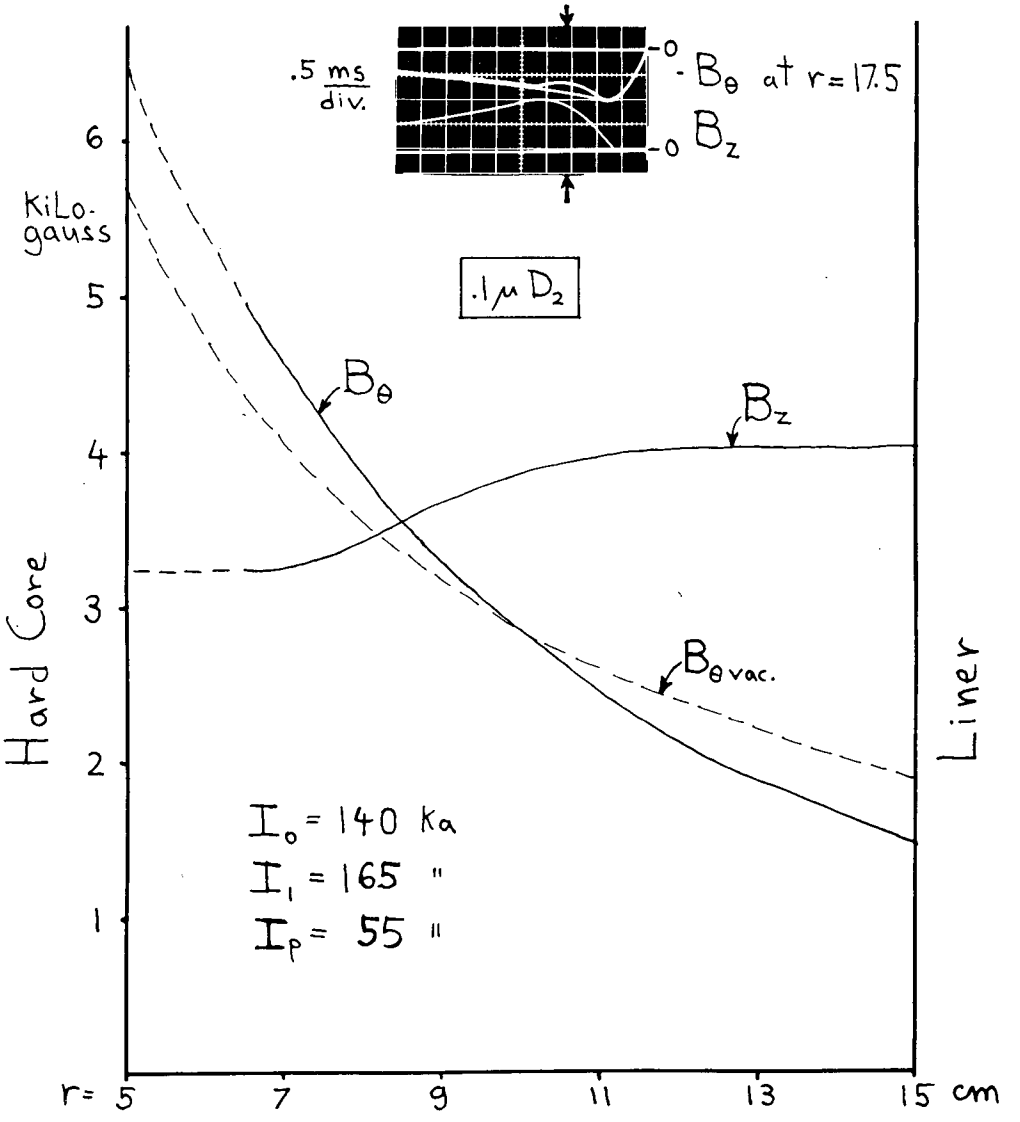

MUB-1606

Fig. III-2. Magnetic-field configuration of the "inverse stabilized pinch" type, obtained in the levitron for 1400 μsec B_z rise time at 0.1 μ D_2.

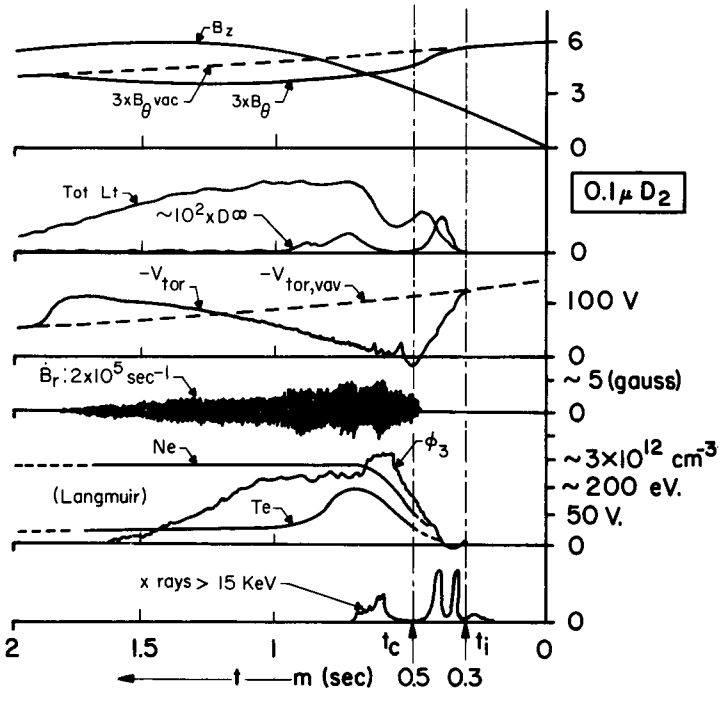

Fig. III-3. Principal diagnostic results on levitron discharges of the type illustrated in Fig. III-2.

stable by virtue of the field distribution. The "rippling" mode is stabilized by thermal conductivity.[1] Accordingly, the only hydromagnetic mode that could possibly be blamed is the finite-conductivity interchange mode resulting from the large negative B^2 gradient radially outward. The most plausible interpretation is probably that the instability is of nonhydromagnetic origin, and results from the directed energies of the current carriers (as much as 30 eV), which are certainly not very small compared with thermal energies.

Our next step will be to diagnose the observed instability more fully. Alternatively, the duration of the stable regime can be extended by lowering the plasma current. Use of a hot initial plasma (injected or preheated by radio-frequency) may even permit the instability to be avoided altogether for regimes that are of practical interest for hot-plasma-containment studies.

3. LEVITRON DEVELOPMENT

The levitron diagnostic equipment is being improved and augmented to provide more detailed information on the plasma.

A dual Langmuir probe has been constructed for obtaining more precise data on electron and ion temperature. A miniature multiple-grid electron-energy analyzer probe has been completed. Preliminary measurements with newly installed microwave gear indicate that absorption measurements can be made by reflecting a signal from the hard core. A new miniature multiple probe has been constructed which will provide fine-grained magnetic-field distributions across the plasma without substantially interfering with the coupling time. A grazing-angle vacuum spectrograph has been installed to aid in locating ultraviolet spectral lines for additional time-resolved monochromator measurements. An electron energy analyzer and an infrared bolometer are in the testing stage.

The levitron vacuum system still requires improvement. A cryogenic pump has been constructed and, once a liquid-helium transfer line is completed, pumping tests will be made. The Sherwood Mechanical Engineering Group is designing and testing this system.

Since the initial levitron experiments have proved that fast-rising magnetic fields (i.e., 50 to 500 μsec) are not necessary for spontaneous breakdown of the gas, it seems feasible to construct a discharge tube with a single, relatively thick, stainless-steel wall which would be strong enough to bear the vacuum load. Collapse studies on small models are under way in the Mechanical Engineering Department, to determine the minimum wall thickness for a torus of this type. Such construction would greatly simplify the mechanical, electrical, and vacuum problems associated with the present design.

---

[1] Harold P. Furth, John Killeen, and Marshall N. Rosenbluth, Finite-Resistivity Instabilities of a Sheet Pinch, to be published in Phys. Fluids.

For the levitron plasma-injection source, a cold-cathode mode of operation has been found, which appears to provide satisfactory output. The source has been redesigned to optimize ionization of the total pulsed-gas input.

4. LINEAR HARD-CORE EXPERIMENTS

A 12-in. hard-core pinch (36-in. long), provided with multiple probe ports and rings of spark triggers in a stainless steel cathode, is now under operation. Studies thus far have been conducted with the "inverse stabilized pinch" configuration.

Spark triggers were found to extend the range of initial gas pressure so that appreciable plasma current is observed even at the base pressure, 0.05 μ. If the initial pressure is less than several μ D_2, breakdown requires several μsec during which cylindrical tubes of low density current (1 to 10 A/cm^2 are present. The initial current emanates from spark-trigger rings and is carried primarily by "runaway" electrons of several hundred eV coupled to the inductive electric field. Also, at low pressure, the triggers define the radial position and thickness of the current layer.

Cathode sheath potential has been observed with a floating Langmuir probe located in the current layer, 0.5 cm from the cathode. A positive floating potential of several hundred volts is observed during the first quarter cycle (15 to 20 μsec) of pinch current at all pressures examined (0.05 to 100 μ D_2). Subsequently, the potential decreases rapidly to tens of volts. During the period of large sheath drop at 1 μ D_2, high-frequency (1 Mc) magnetic-field flutter is observed in the current layer midway between cathode and anode. As the sheath potential falls, high-frequency flutter disappears; however, a low-frequency (0.1 Mc) fluctuation persists.

5. RESISTIVE SHEET PINCH EXPERIMENT

The operation of the 12-in. Triax (reverse-B_θ) experiment has been greatly improved by the following measures: The peak current was raised to 500 kA. The inside and outside circuits were carefully balanced, so as to position the tubular discharge properly between the central and outer insulating tubes. Volatile impurities were removed from the tube walls by a discharge-cleaning process.

As a result, well defined tubular sheet pinches were formed, clearly separated from the inner and outer tube walls, and of a thickness considerably smaller than the space between them. Under these conditions, hydromagnetic theory[1] predicts that the "tearing" instability will grow freely.

Experiments with both D_2 and argon, at pressures of 30 to 300 μ, indeed exhibit the "tearing" mode,[2] as observed both by magnetic probes and by Kerr-cell photography. The growth rates to the non-linear phase are typically 3 to 10 μsec, with the latter figure corresponding to 300 μ of argon. These figures, and their mass dependence, agree roughly with the theoretical

prediction. Similarly, the predicted wavelength of maximum growth is roughly as observed, both in magnitude and mass dependance.

The possibility of making highly precise numerical comparisons between theory and experiment is limited by a number of factors. The hydromagnetic approximation easily breaks down for the Triax configuration, where gyro-radii become large near the null in the B_θ field. Fortunately, in the present experiment, ion mean free paths are much shorter than gyro-radii, and thus the hydromagnetic picture is probably adequate. On the other hand, viscosity effects generally play a role, and these are treated only approximately by Furth, et al.[1] A second difficulty is that the "tearing" mode produces a configuration that is unstable against infinite-conductivity "kink" and "sausage" modes, which grow much more rapidly than the "tearing" itself. Thus the structure of the mode tends to be obliterated by nonlinear effects before it is highly developed.

This experiment is now terminated, but it is hoped that further relevant data will become available from the high-power-level version of the Triax, in Berkeley.

6. COLLISIONLESS PLASMA SHOCK (EXPERIMENTAL)

Stripping rates of nitrogen have been observed during constrastreaming of plasmas at about $2 \times 10^{15} D^+/cm^3$ (1 % N_2) combined density and 1 keV kinetic energy. The N^I, N^{II}, and N^{III} states are burned out in several μsec and, from the rate of population $N^{IV} \rightarrow N^V$, the electron temperature is estimated to be 50 to 100 eV. Similar temperatures are observed when a nuetral D_2 background is present in the drift region.

7. COLLISIONLESS PLASMA SHOCK (THEORETICAL)

Mass-ratio-100 calculations have been carried through 10 ion-plasma periods. Thermalization of the ion distribution has not been attained; however, a long-wavelength potential of $\frac{1}{2} M_i v_s^2$ has formed which appears to be dominating the ion motion. The origin of the long-wavelength mode ($\frac{\lambda}{2} \approx$ length of shocked plasma) is not yet understood.

8. TURBULENCE THEORY

A turbulence power spectrum has been derived for the case where the input-energy is derived solely from a nonlinear term

$$\frac{dW}{dt} = \langle \vec{J} \rangle \cdot \langle \partial \vec{B} \times \vec{u} \rangle .$$

The power spectrum peaks at a wavelength corresponding to some modest fraction of the current layer thickness and then decays as a typical fluid turbulent power spectrum ($u^2 \approx k^{-\gamma}$) to a damping limit which may be resistive, viscous, or Landau.

9. INSTABILITY THEORY

The theory of finite-resistivity hydromagnetic instabilities is being extended in several ways. In the original paper,[1] a number of modes are exhibited, which are indicated to be the modes of maximum growth rate. Some question has been raised meanwhile concerning the possible existence of faster growing modes. Using a convenient quadratic form, derived from the two basic second-order differential equations of the problem, we have now shown rigorously that the modes exhibited by Furth et al.[1] are indeed the modes of maximum growth rate, as the resistivity goes to zero.

The major effort has gone into deriving convenient stability criteria for the long-wave "tearing" mode, particularly in cylindrical geometry. The "rippling" and gravitational interchange modes are always either stable or unstable, depending only on whether the resistivity gradient at $\overline{k} \cdot \overline{B}_o = 0$ is null or not, and whether the gravitational gradient is negative or positive. The wavelength of the instability, the magnetic-field structure, and the proximity of conducting walls have no effect. The "tearing" mode on the other hand, is just like the infinite-conductivity hydromagnetic modes, in that it has a marginal-stability condition that depend on $\overline{k}$, on the detailed zero-order field structure, and on the placement of conducting walls. Indeed, the second-order linear differential equation that must be solved is just the same as that in the infinite-conductivity case; only the behavior of the perturbation at $\overline{k} \cdot \overline{B} = 0$ is different.

To obtain stability conditions for the "tearing" mode, given a specific field configuration, is in a sense a trivial problem, since one need merely solve a second-order differential equation for each choice of $\overline{k}$. The object has been to derive a set of convenient stability condition that are either necessary or sufficient for stability, and that are applicable to a wide range of zero-order configurations.

Especially for purposes of obtaining sufficient stability conditions, it has been found useful to follow the method of Furth.[2] The results are in good agreement with the remarks made in Furth et al.[1] Namely, if $k^2 \rightarrow 0$ is permissible, then a current-carrying configuration becomes unstable when both the conducting walls (or the axis) are more than something like 25% of the current-layer thickness "a" away from the current layer. On the other hand, if k^2 is restricted so that $(ka)^2 > 1$, the configuration is stable even without conducting walls. Such a restriction on k can come about in cylindrical geometry, by virtue of the periodicity condition along z. When $B_{\theta o}/B_{zo}$ is large, k^2 must become small. This relationship, already indicated by Furth et al., has now been analyzed more precisely. One concludes that the field configurations in the levitron have generally been stable against the "tearing" mode. It is possible, however, to violate the theoretical stability conditions in the levitron by taking $B_{\theta o}/B_{zo}$ intentionally small, and this regime will be investigated experimentally.

For purposes of obtaining necessary stability conditions, we have derived a useful variational principle, analogous to the usual energy principle, and this approach is being developed.

---

[2] H. P. Furth, Phys. Fluids 3, 977 (1960).

IV. BERKELEY PLASMA RESEARCH

1. ROTATING-PLASMA RESEARCH

A. Homopolar V

Klaus Halbach, Robert W. Layman, and G. Donald Paxson

Most of our effort during the report period was directed toward development of better techniques to diagnose the plasma produced by the Homopolar V device; unfortunately, our efforts have been without too much success so far. The neutral gas injection at the outer electrode by means of a fast-acting valve, intended to produce detectable fast charge-exchange neutrals after breakdown, gave negative results. Since this was most likely due to the slow (thermal) speed with which the gas entered the apparatus, we built a device that allowed us to drive an aluminum or titanium rod into the plasma with a speed of approximately 4×10^{-2} mm/μsec. We hope that under the ion bombardment enough occluded gas is released to give detectable charge-exchange neutrals; experiments, however, are not yet conclusive either way. Fast-neutron-detection experiments, with the use of a Stilbene crystal and a pulse-shape discriminator,[1] give some neutron pulses as late as 200 μsec after breakdown. This, however, is not conclusive, since the pulse-shape discriminator circuit can produce "false-neutron" pulses due to a γ pulse pile-up or highly energetic γ rays. We intend to develop another circuit that does not have this drawback.

Due to the completion of the first quarter of the 1-MJ electrolytic bank, we were able to increase the E/B somewhat, which resulted in an increase of the total neutron production by about a factor 10 to 10^6 per discharge. Since at higher E/B the breakdown occurs faster, we are now using spark gaps in series with the fast banks. This allows us to introduce a delay between the valve opening and the breakdown that is long enough to ensure that the plenum is practically empty at breakdown time. A short time before the end of the report period, the second quarter of the megajoule bank was completed.

We wish to express our thanks to Frank Jorgensen, who, under the direction of Quentin A. Kerns, built the pulse-shape discriminator.

B. Homopolar Gun I

Kenneth W. Ehler and Klaus Halbach

Since only minor modifications of the Homopolar V device are necessary to obtain an apparatus that should have very desirable gun properties,[2] we built the Homopolar Gun I, schematically represented in Fig. IV-1. At the end of 1962, Homopolar Gun I was assembled. After two days of pumping, the pressure was down to 5×10^{-8} and we expect to do the first experiments early in 1963.

---

[1] W. Daehnick and R. Sherr, Rev. Sci. Instr. 32, 666 (1961).

[2] K. Halbach and W. R. Baker, Plasma Gun Aspects of an E × B System, UCRL-10206, January 1963.

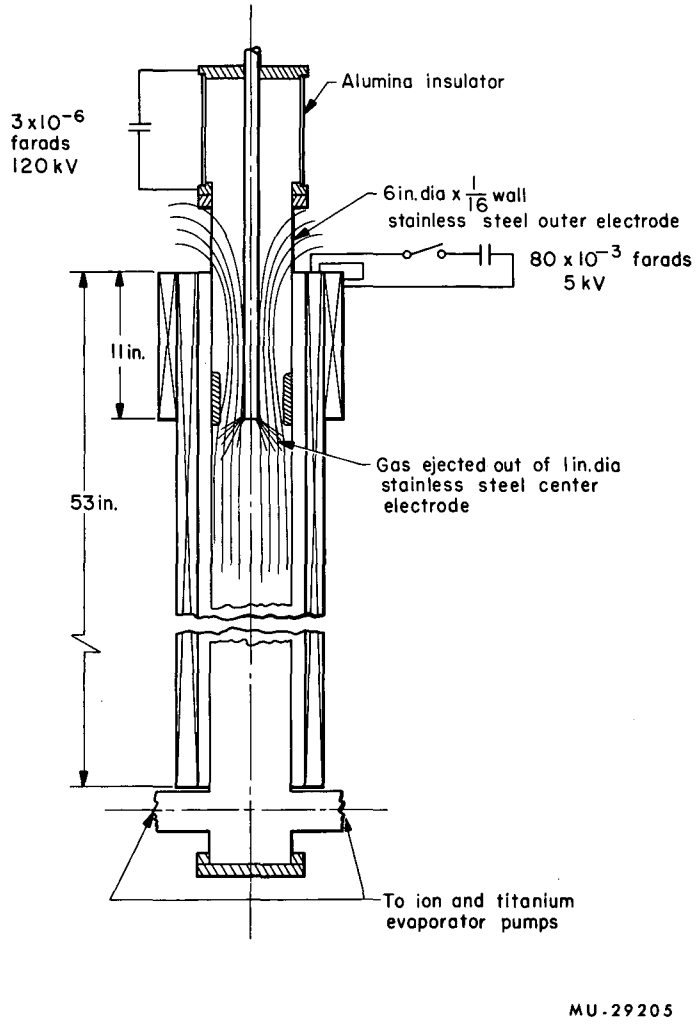

Fig. IV-1. Schematic representation of Homopolar Gun I.

2. BOUNDARY EFFECTS AND INSTABILITIES IN ROTATING-PLASMA EXPERIMENTS

Wulf B. Kunkel

The conditions at the electrodes and the stability of the circular flow in rotating-plasma experiments have been investigated theoretically by using a simple macroscopic approach. The study was prompted by our desire to publish some of the observations made several years ago in Homopolar III.[1] The results and a brief description of the Homopolar III experiment are summarized in a separate report.[2] The principal conclusions were as follows:

The radial current crossing the magnetic field, which is necessary to establish and maintain the rotation, tends to be carried by the ions of the plasma. This is certainly true during the acceleration phase, and will also hold true in steady-state rotation if the resistivity is not excessive and if azimuthal symmetry is assumed so that no Hall field can develop. On the other hand, since metallic surfaces in general do not emit ions, current continuity requires that near the anode the current be carried by electrons. It is therefore desirable that some magnetic flux surfaces thread the anode to allow the required electron flow. If not enough electrons are able to drain off along field lines toward the anode, a large negative space charge is left behind, creating a sheath in the immediate neighborhood of the anode. The existence of such a sheath would seriously limit the rotational energy that could be imparted to dense plasmas of axial symmetry.[3]

Fortunately, there is good reason to believe that dense space-charge sheaths in crossed electric and magnetic fields are unstable.[4] In fact, in connection with the development of certain electron tubes many years ago, several authors have investigated the nature of what is frequently called the "slipping stream" instability of electrons in crossed fields.[5-7] There is general agreement that space-charge waves grow rapidly so that electrons are transported readily across the magnetic field whenever the sheath plasma frequency equals the electron gyrofrequency. We therefore conclude that current continuity is ensured under all conditions and if axial symmetry is preserved an actual evacuation of the anode region is effected by the current crossing the magnetic field.

---

[1] A. Bratenahl, W. R. Baker, A. W. DeSilva, W. B. Kunkel, and K. Halbach, in Controlled Thermonuclear Research Quarterly Report, UCRL-8682, March 11, 1959, pp. 51 to 53.

[2] Wulf B. Kunkel, William R. Baker, Alexander Bratenahl, and Klaus Halbach, "Boundary Effects in Viscous Rotating Plasmas," UCRL-10399 Revised, January 1963.

[3] Conrad L. Longmire, Plasma Physics (to be published), Chapter III; available from author.

[4] M. E. Ebel and S. B. Treiman, Los Alamos Scientific Laboratory Report LA-2408 (1959), p. 16.

[5] O. Buneman, Nature 165, 474 (1950).

[6] G. G. MacFarland and M. G. Hay, Proc. Phys. Soc. (London) 63B, 409 (1950).

[7] C. W. Hartman and D. H. Sloan, Turbulence in Crossed-Field Electron Streams (University of California, Electronics Research Laboratory, Berkeley, unpublished).

The second question to be asked is whether axially symmetric flow is indeed likely to exist in these experiments. In the case of Homopolar III, as well as in the Ixion device,[8] various types of probes placed close to or directly into the surface of the outer electrode invariably registered fluctuating signals. During the nearly steady-state phases of the Homopolar discharges it had been noticed in particular that the current entered the outer electrode (anode) in approximately twelve fairly regularly spaced narrow bands which were lined up with the magnetic field and moved more or less with the rotating plasma speed.[1] Moreover, in all rotating plasma experiments it is found that the friction which must be overcome to maintain the state of motion is much too high to be explained by a normal viscosity if the flow is assumed to be laminar and axially symmetric. Unfortunately, a thorough analysis of the stability of plasmas that are rapidly rotating between coaxial electrodes proved to be very difficult. On the other hand, a considerable amount of work on the stability of certain types of revolving incompressible hydromagnetic flows can be found in the literature[9] and it is felt that some of the conclusions arrived at there may be applicable to our problem.

The cases studied in the past were limited to pressure-driven circular flows between rotating or stationary coaxial cylinders and to viscous and inviscid flows between rotating cylinders without radial current and without azimuthal pressure gradients in the unperturbed state (Couette flow). The first of these, which is called Poiseuille flow, corresponds most closely to our viscous rotating plasmas, although in our experiments the pressure gradient is replaced by a $j \times B$ body force. In general, it is found that in weak axial magnetic fields, or in poorly conducting fluids, all circular flows are primarily susceptible to the axisymmetric ($m = 0$) well-known Taylor instability.

Now it is intuitively obvious that an axial magnetic field should produce a stabilizing effect on the $m = 0$ instability in rotating conducting fluids. Indeed, Chandrasekhar finds for pressure-driven viscous flow circulating in a narrow gap between coaxial conducting cylinders in the presence of a strong axial magnetic field that the axisymmetric instability appears only if[10]

$$R_e^2 \, D/R \gtrsim 200 \, R_H^2, \tag{1}$$

where

D = width of the gap,
R = radius of the inner cylinder,
$R_e = \rho \bar{v} D/\mu$ = Reynolds number,
$R_H = BD\sqrt{\sigma/\mu}$ = Hartmann number,
σ = conductivity,

and

μ = viscosity coefficient.

---

[8] D. A. Baker, J. E. Hammel, and F. L. Ribe, Phys. Fluids 4, 1534 (1961); D. A. Baker and J. E. Hammel, Phys. Fluids 4, 1549 (1961).

[9] S. Chandrasekhar, Hydrodynamic and Hydromagnetic Stability (Clarendon Press, Oxford, 1961), Chap. IX.

[10] S. Chandrasekhar, ibid, paragraph 88.

The magnetic field B is considered to be strong in this context when $R_H > 50$. Unless some small-scale fluctuations produce an enhanced anomalous viscosity of the plasma, most rotating-plasma experiments operate with Hartmann numbers well above this value. Since the Reynolds numbers are rarely much larger than R_H in these experiments, the $m = 0$ instability is hardly ever expected to appear.

It is instructive to express Eq. (1) in terms of more familiar quantities in plasma physics. Introducing the Alfvén speed $V_a = B/\sqrt{4\pi\rho}$ and the magnetic Reynolds number $R_M = 4\pi\sigma\bar{v}D$, we can write

$$\bar{v}^2/V_a^2 \gtrsim 200\, R_M R/R_e D = 800\, \pi\sigma\mu R/\rho D. \tag{2}$$

If we now substitute the conventional expressions for σ and for $\mu \approx p_i \tau_{ii}/(1 + 4\omega_i^2 \tau_{ii}^2)$, Eq. (2) reads

$$\frac{\bar{v}^2}{V_a^2} \gtrsim \frac{1.5\times10^{14}\, T_e^{3/2} T_i^{5/2} R}{(1 + 4\omega_i^2 \tau_{ii}^2) n A^{1/2} D}. \tag{3}$$

Here, p_i is the ion pressure, ω_i is the ion gyrofrequency, τ_{ii} is the ion-ion collision time, T_e and T_i are the electron and ion temperatures expressed in volts, A is the ion mass in atomic units, and n is the number of ions per cm^3. This relationship becomes particularly simple when $4\omega_i^2\tau_{ii}^2 \gg 1$, because in that case condition (3) becomes independent of both the magnetic field and the number density, and we have

$$\bar{v} \gtrsim 10^8 \left(\frac{T_e^3 R^2}{A T_i D^2}\right)^{1/4} \text{cm/sec}, \tag{4}$$

or, introducing the ion thermal speed $v_{th} = (3kT_i/m_i)^{1/2}$,

$$\bar{v}/v_{th} \gtrsim 70\, A^{1/4} (R/D)^{1/2} (T_e/T_i)^{3/4}. \tag{5}$$

Actually, the extension of Eq. (3) to large values of $\omega_i \tau_{ii}$ may not be permissible because in the analysis the Hall effect was ignored and a simple scalar viscosity was assumed. Nevertheless, it is felt that these expressions can be used to demonstrate that none of the dense rotating plasmas, in which T_e/T_i cannot possibly be very small, are likely to be unstable in an axisymmetric mode. Only very tenuous plasmas in an azimuthally symmetric $E \times B$ configuration, such as those used in injection schemes like the Ion Magnetrons,[11]

[11] J. M. Wilcox, Revs. Mod. Phys. 31, 1045 (1959).

are in danger of satisfying the criterion (5) and hence possibly subject to this instability, because in that case the initial ratios of transverse energies are apt to be equal to the ratio of the masses.

On the other hand, the stability of rotating conducting fluids with regard to disturbances which are in phase along the magnetic lines of force has only been analyzed for inviscid plasmas with free surfaces,[12] but not for our case of viscous friction at a rigid boundary. At first glance, one might expect that the magnetic field would have no effect whatsoever if the lines of force are straight since in that case only simple interchanges are involved. Unfortunately, this mode has been investigated for ordinary hydrodynamic stability only in perfectly straight channels because very little curvature causes the Taylor instability to predominate.[13] The latter is driven basically by centrifugal effects, whereas the former is presumably due to the shear itself. Theoretically and experimentally it is found that the hydrodynamic rectilinear Poiseuille flow is unstable if the Reynolds number exceeds a certain value.[14] A similar situation must exist in the rotating-plasma experiments. It is also reasonable to expect that the curvature can only lower the critical Reynolds number, if it has any effect at all. Moreover, we expect that at its onset, the instability in our case results in a two-dimensional secondary flow with cells of roughly square cross sections (see Fig. IV-2) rather than in the general turbulence which appears in the absence of a magnetic field. At least we propose that such a cellular flow pattern, representing a type of "roller bearing" action, may be responsible for the regularly spaced current spokes observed on the anode of Homopolar III.

---

[12] Norman Rostoker and Alan C. Kolb, Phys. Rev. 124, 965 (1961).

[13] S. Chandrasekhar, Hydrodynamic and Hydromagnetic Stability (Clarendon Press, Oxford, 1961), p. 350.

[14] C. C. Lin, The Theory of Hydrodynamic Stability (Cambridge University Press, 1955) Chap. 3.

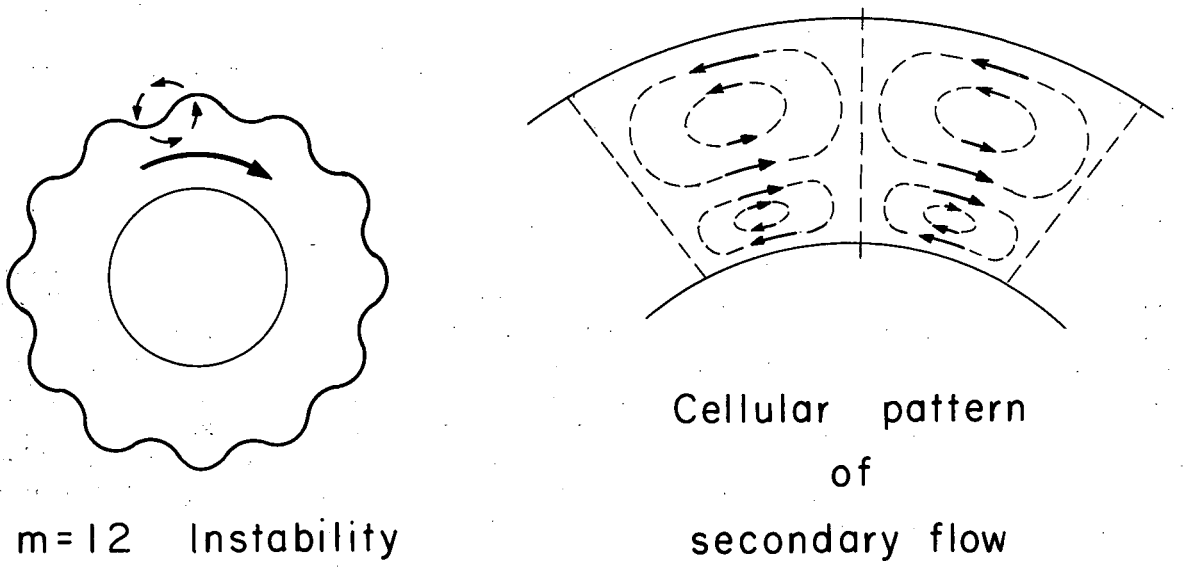

MU-28609

Fig. IV-2. Suggested m = 12 instability and cellular-flow pattern in the Homopolar III experiment.

3. HYDROMAGNETIC WAVES AND CYCLOTRON HEATING

A. Ion Cyclotron Resonance Experiment

Gordon W. Hamilton, Forrest I. Boley, and John M. Wilcox

The principal effort during this period has been to develop several diagnostic techniques by which plasma conditions in the ion cyclotron resonance experiment can be measured. Our objective is to determine what happens to the cyclotron wave energy following resonant absorption, which was previously reported.[1] Measurements have been made of the thermal pressure, ultraviolet radiation, electron temperatures, and impurity temperatures. In addition to these diagnostic measurements, improvements have made in the oscillator protective device which permits reliable operation at the full power of about one MW.

Diamagnetic Measurements

A probe designed to measure the diamagnetic effect of the heated plasma provides the clearest information available about plasma conditions in this experiment. The probe consists of a coil of 1200 turns wound upon a longitudinal axis and located within an axial glass tube of 8-mm outside diameter. A simple theory can be constructed for this probe either by equating the change in thermal pressure to the change in magnetic pressure during the heating pulse or by considering the plasma as a diamagnetic medium. The magnetic flux is confined within the copper vacuum shell during the application of wave power. The result of this theory can be stated as follows:

$$\text{Integrated Diamagnetic Signal} = \Delta H = \overline{(nkT_i + nkT_e)_\perp}/B_0,$$

where $\overline{(nkT_i + nkT_e)_\perp}$ is the average kinetic-energy density (equal to the thermal pressure) resulting from the motion of the ions and electrons in the direction perpendicular to the external field, B_0 (these quantities are averaged over the cross section of the chamber).

It was ascertained that the observed signal conforms to expectations in the following respects:

(a) ΔH is in the same direction as B_0, with either polarity of B_0. This is expected because the probe is actually measuring the induced currents in the copper shell, which are confining the flux within the shell.

(b) ΔH is proportional to the oscillator power.

(c) A typical signal (Fig. IV-3) indicates that the plasma is warming up during the first 300 μsec of the oscillator pulse, after which the signal remains constant or slowly decreases. The integrated signal returns to zero after the oscillator crowbar.

---

[1] Forrest I. Boley, Alan W. DeSilva, Peter R. Forman, and Gordon W. Hamilton, in Controlled Thermonuclear Research Semiannual Report, UCRL-10294, July 20, 1962, p. 45.

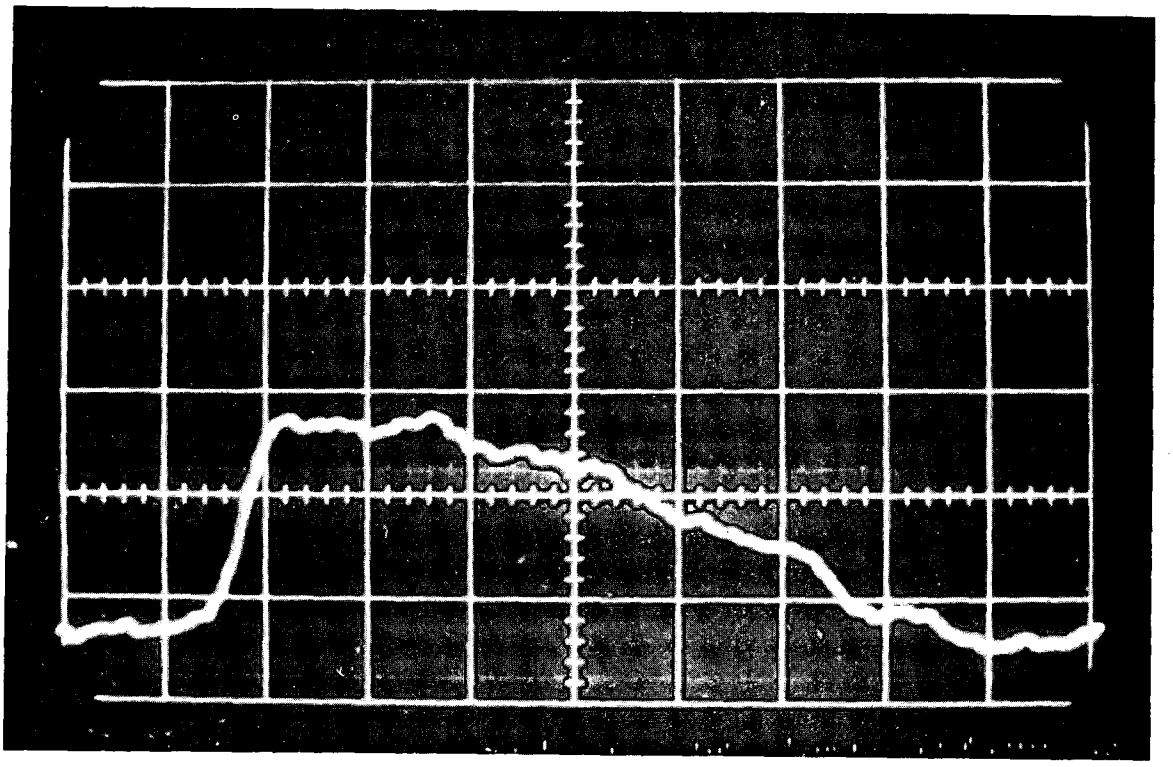

ZN-3551

Fig. IV-3. Diamagnetic signal as a function of time (typical).
Horizontal scale: 50 μsec per division.
Vertical scale: 2 G per division. Oscillator pulse extends from t = 60 μsec to t = 400 μsec.

(d) ΔH is dependent upon the magnetic field, having its maximum value at the axial position where the plasma is being heated by absorption of the ion cyclotron wave (see Fig. IV-4). This figure may be compared to Fig. IV-5 of the previous semiannual report,[2] which indicates absorption of the wave at the same axial position.

(e) When the probe is located at the midplane of the chamber and the magnetic field at this point is varied, a distinct resonance is observed (see Fig. IV-5). The maximum signal is obtained with a magnetic field about 8% higher than the field for single-particle resonance.

(f) When impurities are allowed to accumulate in the gas between pulses, the diamagnetic signal decreases.

The signal reaches its maximum of 2.4G when $B_0 = 11.5$ kG and when oscillator loading and plasma purity are optimized. This signal indicates a thermal pressure of 2.2×10^{-3} atm. The best estimate of ion density (obtained from the phase velocity of the cyclotron waves) is 6×10^{12} cm^{-3}, which yields a computed ion temperature of about 200 eV. By another method (to be described in the following section on Electron Temperatures) it is found that the electrons are cooler than the ions by an order of magnitude.

The data in Fig. IV-4 can be integrated over the volume of the chamber which results in a total energy content of about 4 joules. The downward slope of the diamagnetic signal immediately after oscillator crowbar indicates the energy loss rate to be about 300 kW, which is about equal to the steady-state cyclotron wave power under these conditions.

Vacuum Ultraviolet Radiation

The ultraviolet radiation intensity at wavelengths less than 1000 Å is measured by use of a simple tungsten photocathode together with instrumentation for measuring the photoelectron current. Because of inadequate data on quantum efficiencies for tungsten at wavelengths shorter than 400 Å, the result of this measurement can be interpreted only as an approximate limit of 30 kW for the energy loss rate due to far-vacuum ultraviolet-impurity radiation. This 30 kW is to be compared to a wave power at 300 kW, although it is believed that the actual energy loss due to ultraviolet impurity radiation considerably exceeds 30 kW.

Electron Temperatures

Electron temperatures have been measured by the relative intensities of the D_β spectral line and the continuum light. This measurement yields an average electron temperature, weighted by a function of the density of the emitting region. Electron temperatures of 20 eV are measured along a diameter at the center of the chamber. Electron temperatures are increased by 50% by adding liquid nitrogen to a trap to remove condensible impurities.

---

[2] Ibid, p. 49.

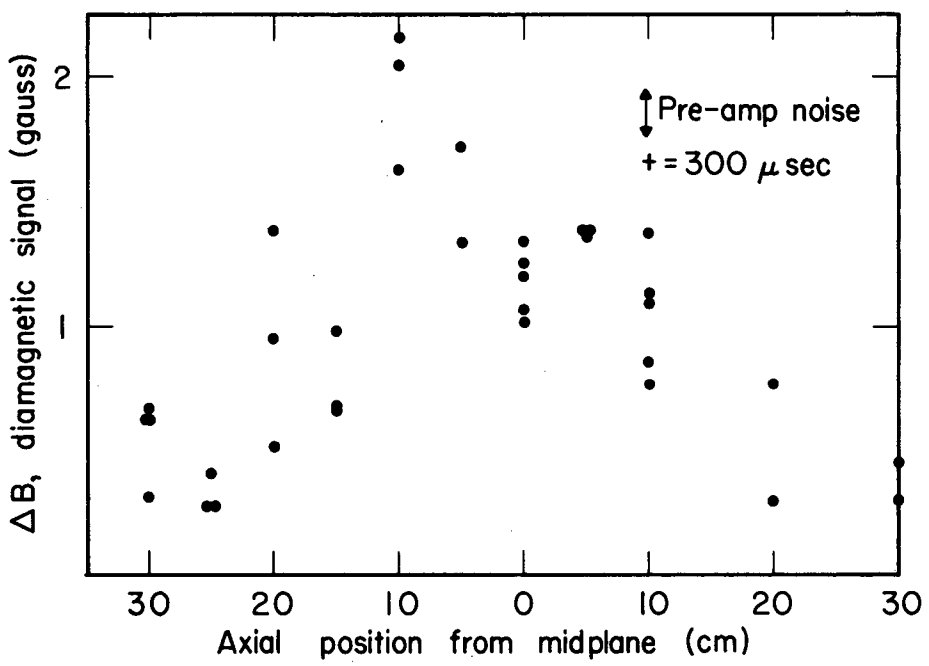

MU-29203

Fig. IV-4. Diamagnetic signal as a function of axial probe position.

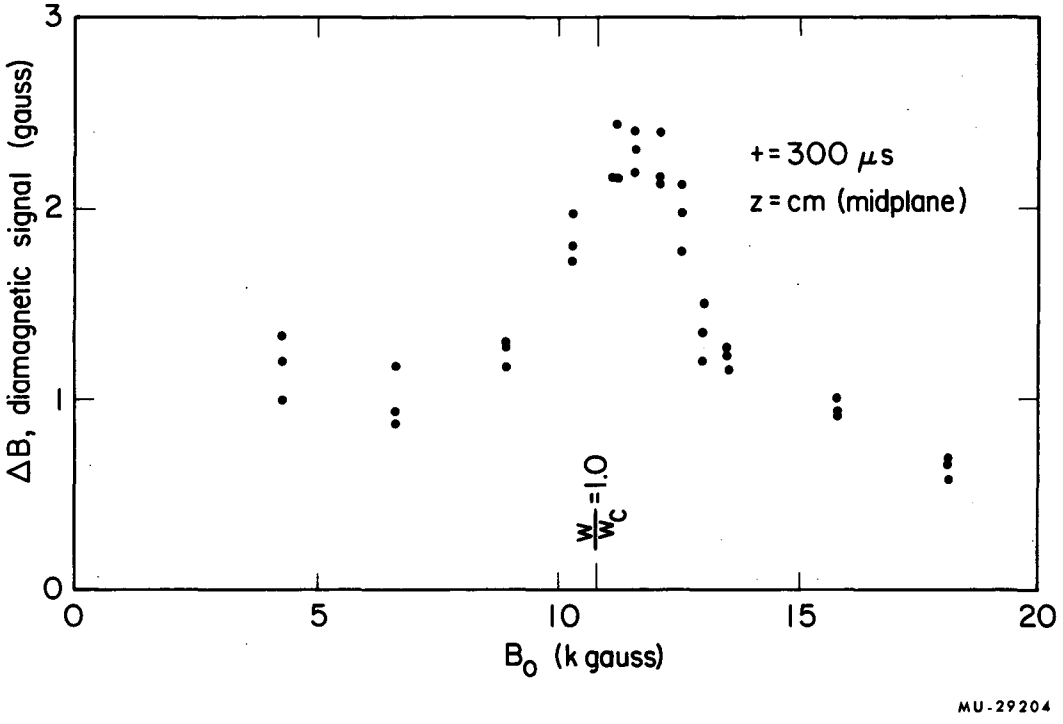

Fig. IV-5. Diagmagnetic signal as a function of magnetic field with a fixed probe position.

Doppler Broadening

There is little Doppler broadening of spectral lines in the deuterium Balmer series because the hot ions do not radiate Balmer light. A search was made for spectral lines from excited impurities, which might indicate emperatures in the hot portion of the chamber. The highest temperature observed by Doppler broadening was indicated by the 4089 Å line of silicon IV (ionization potential = 33.3 eV), which had a width corresponding to 46 eV.

B. Spectroscope Observation of a Decaying Hydrogen Plasma in the Hothouse I Experiment

William S. Cooper III, Forrest I. Boley, and John M. Wilcox

Most of the effort during the past six months has been spent in perfection of techniques for measuring ion density and electron temperature simultaneously, the goal being time- and space-resolved measurements of these quantities in a decaying hydrogen plasma. We have measured the ion density in the Hothouse I plasma in two independent ways: by observing the Stark broadening of the H_β line profile, using the polychromator described in the last semiannual report,[3] and by making absolute intensity measurements of the continuum radiation in the visible region of the spectrum. The measurements generally agree within the experimental errors, which are estimated to be about 20%, and indicate a high degree of ionization. Simultaneous electron-temperature measurements are made by measuring the ratio of the H_β line intensity to the intensity of the same continuum radiation. This method of measuring electron temperatures was suggested by Hans Griem.[4] His calculations have been checked and extended to higher temperatures.

Figures IV-6 and IV-7 show the time dependence of the ion density (a weighted average of the two independent measurements) and electron temperature, respectively, during a single shot. These data were taken looking at a narrow column of plasma parallel to the axis of the tube and midway between the axis and the tube wall.

Preliminary ion density and electron-temperature spatial profiles have been obtained by looking parallel to the axis at different radii on successive shots. These results indicate a peak in both ion density and electron temperature about halfway to the wall, and a drop in both density and temperature at the wall and also in the shadow of the electrode. There is no evidence of loss of plasma across the magnetic field by diffusion. The plasma appears

[3] George R. Spillman, Gordon W. Hamilton, William S. Cooper III, and Forrest I. Boley, ibid, p. 51.

[4] H. R. Griem, in Proceedings of the Fifth International Conference on Ionization Phenomena in Gases, North-Holland Publishing Company, Amsterdam (1962), II, p. 1872.

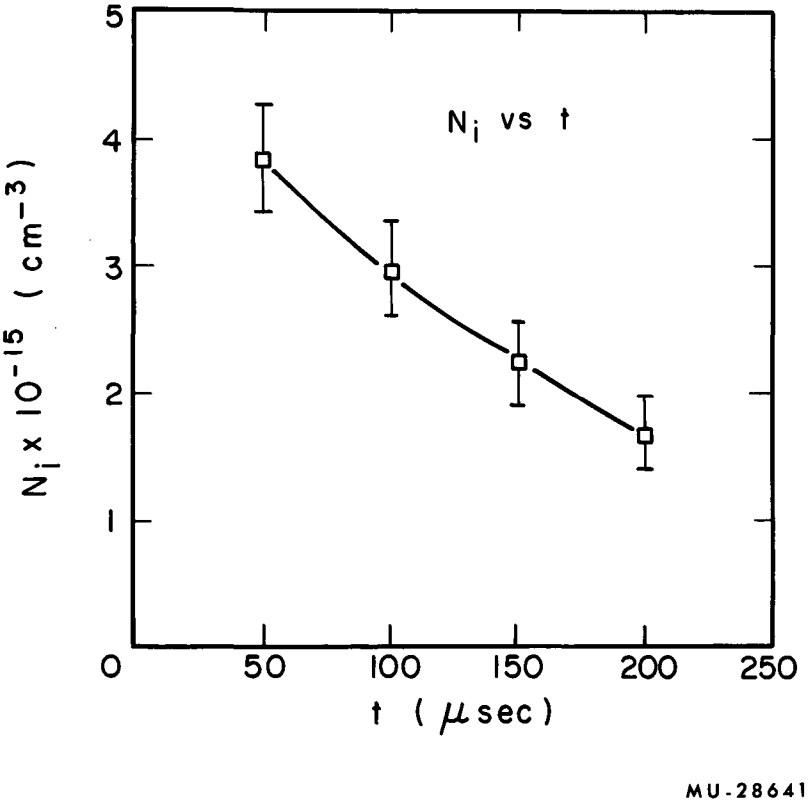

Fig. IV-6. Ion density as a function of time.

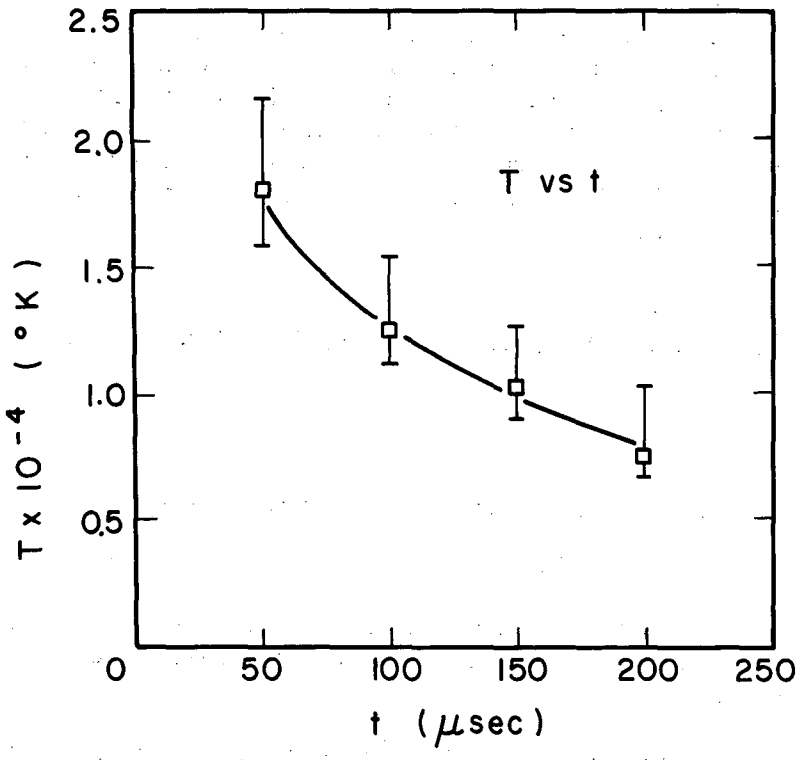

MU-28640

Fig. IV-7. Electron temperature as a function of time.

to decay by volume recombination. Recombination rates derived from the data shown in Figs. IV-6 and IV-7 agree with those calculated by Bates, Kingston, and McWhirter.[5]

Regions of luminosity in the plasma as observed by framing camera pictures looking into the end of the discharge are qualitatively explainable in terms of the measured ion density and electron-temperature profiles.

With late crowbar there are some discrepancies. Early in the decay period the line-profile measurements yield ion densities about 70% higher than the continuum measurements indicate. Temperatures also seem unreasonably high. A possible explanation for both observations would be partial reabsorption of the H_β line. This possibility is being investigated experimentally. We are also planning to repeat these measurements looking in the side of the tube to check for possible longitudinal variations in ion density and electron temperature.

---

[5] D. R. Bates, A. E. Kingston, and R. W. P. McWhirter, Proc. Roy. Soc. (London) 267A, 297 (1962).

4. HYDROMAGNETIC IONIZING FRONTS

Arthur R. Sherwood and Wulf B. Kunkel

Final assembly of the experiment for the investigation of hydromagnetic ionizing fronts has been completed, and the apparatus is now operational. In particular:

(a) The quasi-static magnetic field measurements have been made. The magnitude of the field is constant within 3% in the experimental region except for a 6% dip with 2% azimuthal asymmetry in the region where the two halves of the coil are joined.

(b) The vacuum system has been assembled within the magnetic field coils and has been found to be unaffected by the pulsing of the coils.

(c) The driving-current source has been connected to the driving electrodes, and the associated firing circuits have been connected and debugged.

(d) Preliminary results have been obtained but have not yet been evaluated.

5. SHEET PINCH STUDIES

Oscar A. Anderson

6 × 10 Triax

Flare effects,[1] which have previously hindered optical and spectroscopic measurements, have been essentially eliminated. Even at power levels sufficient to produce neutrons, the plasma configuration can now be deduced almost up to peak current. Plasma density and temperature have been measured spectroscopically at times up to the third bounce.

The decisive step in preventing flares was revision of the cathode shape. Formerly, particles which crumbled from the insulator wall accumulated on the lower electrode(cathode). These were vaporized by the discharge and produced the sudden intense flares previously reported. The new cathode consists of radial fins which carry the current but which are shaped so that insulator dust cannot collect on them. This cathode configuration is similar to that developed by C. W. Hartman in the Livermore cusp-pinch experiment.[2] It was used as early as 1948 by W. R. Baker in a high-current thyratron. Besides solving the dust-flare problem, the new cathode promotes a uniform discharge at gas pressures too low for breakdown with the old flat cathode.

When the intense cathode flares were eliminated, weaker flare effects were noted at the anode region. These occurred later in time. One type was caused by sparking and was stopped by installing bridges across the viewing slit. The only remaining effect is a diffuse glow which starts at 2 μsec and seems to exist between the slit and the covering window. So far this effect has only been partially reduced.

An idea of the plasma behavior can now be obtained almost up to peak current (3 μsec) if one utilizes all three stereoscopic streak views. Between 2 and 3 μsec there seems to be a gradual expansion toward the walls and decrease in light intensity. Nothing is observed optically that would explain the sudden voltage bump and neutron burst which occur at 2.75 μsec.

A Jarrel-Asch monochromator has been used to study the D_β line and the adjacent continuum at times up to 2 μsec. Ion density was estimated from the shape of the D_β profile, and electron temperature from the ratio of line and continuum intensities. The latter work was aided by W. S. Cooper who has extended the calculations of H. R. Griem up to temperatures of interest in the sheet-pinch program. The density and temperature obtained

---

[1] Oscar A. Anderson, in Controlled Thermonuclear Research Semiannual Report, UCRL-9969, Jan. 19, 1962, p. 62.

[2] C. W. Hartman, in Controlled Thermonuclear Research Semiannual Report, UCRL-10294, July 20, 1962, p. 33.

spectroscopically show interesting features such as rapid transfer of energy to the electrons at the first bounce, and cooling during the subsequent expansion. The numerical values obtained at these and at later times are in order-of-magnitude agreement with estimates based on a simple dynamic model.

6. EXPERIMENTS ON LORENTZ DISSOCIATION AND PARTIALLY IONIZED PLASMA

Klaus H. Berkner, Vincent J. Honey, Robert V. Pyle, Henry F. Rugge and J. Warren Stearns have contributed to the following experiments. In addition, John R. Hiskes, Selig N. Kaplan and George A. Paulikas have assisted with the dissociation experiments.

A. Lorentz and Gas Collisional Breakup of D^-, H^0, and H_2^+

Experiments on the Lorentz ionization of neutral hydrogen atoms[1-4] are continuing. The measurements are concerned with principal quantum numbers and values of $\vec{v} \times \vec{B}$ appropriate to reasonable parameters for injection into a fusion reactor, but the experiments are actually done at higher energy (10 MeV/nucleon) and lower magnetic fields (2 to 20 kG) than would be used in a reactor. The high energy has an advantage for the study of the excitation distributions from various H^0 production mechanism because neutral formation by charge exchange is negligibly small.

B. ac-Positive Column

More details of the instability investigation (described in Ref. 5) have been obtained and compared with analyses based on the Kadomtsev model. Quantitative to semi-quantitative agreement is obtained in all cases. However, this agreement may be in part fortuitous because Ecker[6] has shown that the numerical results of the analysis depend critically on the boundary conditions and the assumed form of the initial perturbation.

---

[1] In Controlled Thermonuclear Research Semiannual Report, UCRL-10294, July 20, 1962, p. 68.

[2] Robert V. Pyle, Selig N. Kaplan, and George A. Paulikas, 4th Annual Meeting of the APS Division of Plasma Physics, Nov. 28 through Dec. 21, 1962, I6 (UCRL-10501 Abstract).

[3] Selig N. Kaplan, George A. Paulikas, and Robert V. Pyle, Phys. Rev. Letters 9, 347 (1962).

[4] Robert V. Pyle, Selig N. Kaplan, and George A. Paulikas, Bull. Am. Phys. Soc., Ser. II 7, 487 (1962).

[5] In Controlled Thermonuclear Research Semiannual Report, UCRL-10294, July 20, 1962, p. 69.

[6] G. Ecker, private communication.

C. Hollow-Cathode Discharge

A detailed mapping of low frequency oscillations (0 to 400 kc) as functions of space, frequency, gas, pressure, discharge current, and electrode configuration is now in progress. The discharge can now be operated with gas input through a hollow anode as well as a hollow cathode.

7. ON THE MHD HELMHOLTZ INSTABILITY

Alan Macmahon

The Helmholtz instability of two compressible fluids of equal density and infinite conductivity permeated by a uniform magnetic field parallel to the fluid velocity has been investigated by use of a normal mode analysis. The configuration was found to be stable against perturbations uniform in the direction parallel to the fluid-fluid interface and perpendicular to the fluid velocity if

$$s^2/a^2 < [1 - (v^2/a^2 - 1)^2]/[1 + (v^2/a^2 - 1)^2],$$

where the fluid velocities are $\pm v$, s is the Alfvén speed, and a is the sound speed. In the limit of infinite sound speed, this reduces to the result given by Chandrasekhar[1] for the incompressible case. The configuration is less stable against more general perturbations but a general stability condition has not been obtained.

Northrop's[2] analysis of the Helmholtz instability of a plasma-vacuum interface when the plasma flows across a magnetic field has been reviewed and an inconsistency in his perturbation amplitudes is resolved. His vacuum electric-field amplitudes were found to be missing terms corresponding to the displacement of the unperturbed surface charge from its equilibrium position.

---

[1] S. Chandrasekhar, Hydrodynamic and Hydromagnetic Stability (Clarendon Press, Oxford, 1961), p. 508.

[2] T. G. Northrop, Phys. Rev. 103, 1150 (1956).

V. THEORETICAL AND BASIC EXPERIMENTAL PLASMA PHYSICS

1. A SELF-CONSISTENT DISTRIBUTION OF ELECTRONS IN THE ASTRON E LAYER

Warren Heckrotte and V. Kelvin Neil

A self-consistent distributions of electrons in the Astron E layer has been reported previously.[1,2] In Ref. 2 it was shown that the layer provided a surface current density in the azimuthal direction given by

$$j(z) = j_0 \cos \pi z/\ell, \tag{1}$$

in which ℓ is the length of the layer. The principle condition for validity of the solution was that ℓ be much greater than the radius, R, of the layer. With no additional approximation, it is possible to find a self-consistent distribution that provides a current density given by

$$j(z) < j_0 \begin{cases} \cos \pi \dfrac{(z + \frac{\delta}{2})}{(\ell - \delta)} & \text{at } -\ell/2 < z < -\delta/2 \\ 1 & \text{at } -\delta/2 < z < \delta/2 \\ \cos \pi \dfrac{(z - \frac{\delta}{2})}{(\ell - \delta)} & \text{at } \delta/2 < z < \ell/2. \end{cases} \tag{2}$$

Thus we may add a central region of length δ where the current (and number) density is uniform. The axial magnetic field is also uniform in this region. The condition for validity is that $\ell - \delta$ be much greater than R. There is no restriction on the length, δ, of the central region except as noted below.

The stability of the previous model against axial bunching and the B_θ instability was predicted in Ref. 2. These conclusions remain valid for the extended layer provided the central region is not too long. In the Astron device it may be desirable to have $\delta \leqslant \ell/2$, which is not a sufficient increase to allow either instability.

---

[1] Warren Heckrotte and V. Kelvin Neil, in Controlled Thermonuclear Research Semi-annual Report, UCRL-10294, June 1962, p. 72.

[2] Warren Heckrotte and V. Kelvin Neil, A Self-Consistent Distribution of Electrons in the Astron E Layer, UCRL-6942, June 1962.

2. THE EFFECT OF FINITE LARMOR RADIUS ON THE INTERCHANGE INSTABILITY

William A. Newcomb

The stabilizing effect of finite Larmor radius was first studied by Rosenbluth et al., and reported on at the Salzburg meeting in 1961.[1] One of the cases they treated was the interchange instability in a mirror machine, but they did not use the actual geometry. They took the magnetic lines of force to be parallel straight lines of infinite length and reproduced the effects of the curvature (which provides the driving force of the instability) by an effective gravitational field in the radial direction. They found that the finite Larmor-radius effects, under the appropriate conditions, would stabilize all the unstable modes except the lowest $m < 1$ mode, and they suggested that a conducting wall might stabilize that one too. It was not possible, though, to give a definite stability condition for the actual mirror machine with curved field lines, since the effective gravitational field was defined only in order of magnitude; it was to be proportional to the "average" curvature of the field lines, but there was no definite prescription for evaluating the average.

I have developed a new method for the treatment of finite-Larmor-radius effects, one which is simple enough to apply to the mirror machine with its actual geometry. The result is that the machine is always stable if the distance between mirrors is greater than a certain critical length, provided that there is a conducting wall to stabilize the lowest mode. In a typical case the following sufficient condition for stability was found:

$$\frac{L^2 a^2}{r^4} > \alpha_P + \alpha_F \frac{B^2}{4\pi\rho c^2},$$

where

L = distance between mirrors,
a = rms ion Larmor radius,
r = radius of the outermost field line evaluated at the median plane,
B = magnetic-field strength,
ρ = mass density of the plasma,

with a^2, B, and ρ evaluated at the center of the machine, and with numerical coefficients α_P and α_F depending as follows on the mirror ratio M:

$$\alpha_P = \begin{cases} 1.611\,(M-1) & \text{if } M \cong 1 \\ 1.732 & \text{if } M = 2 \\ 2.100\,M & \text{if } M \gg 1, \end{cases}$$

$$\alpha_F = \begin{cases} 3.795\,(M-1) & \text{if } M \cong 1 \\ 5.95 & \text{if } M = 2 \\ 5.60\,M^{3/2} & \text{if } M \gg 1. \end{cases}$$

[1] M. N. Rosenbluth, N. A. Krall, and N. Rostoker, Nuclear Fusion, 1962 Supplement, Part 1, p. 143.

Rough numerical estimates indicate that the existing machines, Toy Top and Table Top, are more or less marginal with respect to this criterion. Note also that the plasma may go unstable if its density is lowered (since the critical length increases). This is just the opposite of what one usually expects, but it seems to be verified by experiment.[2]

It should be emphasized that the present work considers only the interchange instability and not the universal instability. Stability against the latter, since it is primarily a long-wave instability, requires L to be less than a certain critical length,[3] but fortunately it is possible to arrange things so that the critical length is greater than the critical length for the interchange instability.

The work summarized here is presented in greater detail elsewhere.[4]

---

[2] R. F. Post, The Effect of Plasma Density and Composition on Finite-Orbit Stabilization, this report, Sec. I. 1.

[3] M. N. Rosenbluth, Recent Work on Universal Instabilities, invited paper Plasma Physics Division Meeting of the A. P. S. Atlantic City, N. J., Nov. 28 through Dec. 1, 1962.

[4] W. A. Newcomb, Lecture Notes on the Interchange Instability, to be published in Physics of Fluids.

3. PLASMA POTENTIAL AND ELECTRON ENERGY DISTRIBUTIONS IN THE ALICE EXPERIMENT

John Killeen[†], Archer H. Futch, Jr., and Robert V. Wagoner[‡]

The plasma potential problem which was initiated[1] in June 1962 has been essentially completed. A new code was written for solving the Fokker-Planck equation for the electron-velocity distribution as a function of time. Cold electrons and hot ions are injected according to the Alice buildup calculations.[2] At each time step of the calculation, the plasma potential and electron temperature are calculated with the condition that ion and electron densities are equal.

[†] Presently on assignment with United Kingdom Atomic Energy Authority, Culham Laboratory, Culham, Abingdon, Berkshire, England.

[‡] Graduate Student, Nuclear Engineering Department, Stanford University, Palo Alto, California.

[1] Archer H. Futch, Jr., and John Killeen, in Controlled Thermonuclear Research Semi-annual Report, UCRL-10294, June 1962, p. 74.

[2] A. H. Futch, Jr., W. Heckrotte, C. C. Damm, J. Killeen and L. E. Mish, Phys. Fluids 5, 1277 (1960).

The ions are deuterons at 20 keV; the electrons are initially at 10 eV. Calculations have been made for various ion-density buildups.[2] For a case with a neutral injection current of 4.9×10^{16} atoms/cm^2, the electrons reach 1 keV when the ion density becomes 10^{12}/cm^3. During the course of the calculation, the electron distribution remains quite close to the appropriate Maxwellian. Modifications have been made to previous analytic estimates[2] of the electron temperature and plasma potential.

4. LONGITUDINAL OSCILLATIONS IN MULTI-COMPONENT PLASMA WITH ANISOTROPIC VELOCITY DISTRIBUTIONS

Terry Kammash† and Warren Heckrotte

It has been demonstrated by Harris[1] that anisotropy in the velocity distribution of a two component (electrons and ions) iniform plasma causes instability in longitudinal plasma oscillations having frequencies approximately equal to integral multiples of the ion-cyclotron frequency. More specifically, if $T_\perp$ is the ion temperature perpendicular to the uniform magnetic field and $T_\parallel$ is the temperature parallel to it, Harris found that for $\frac{T_\perp}{T_\parallel}$ equal to infinity waves propagating parallel to ($k_\perp = 0$) or perpendicular to ($k_\parallel = 0$) the fields are stable; and that they are unstable when neither $k_\perp$ or $k_\parallel$ is zero. A sufficient criterion for the instability is found to be $\omega_{pe} > \omega_{ci}$, where ω_{pe} is the electron-plasma frequency and ω_{ci} is the ion-cyclotron frequency. For a purely electronic plasma, this condition reduces to $\omega_{pe} > \omega_{ce}$ where ω_{ce} is the electron-cyclotron frequency. Recently, Ozawa et al.,[2] have shown that in an anisotropic electron plasma, instabilities will occur for $\frac{T_\perp}{T_\parallel} > 2$.

In the present investigation we consider a three component (one electron and two ion species) infinite plasma in a uniform magnetic field. We assume a system which departs slightly from an equilibrium configuration in which there is no electric field and in which each component has an anisotropic Maxwellian velocity distribution. The second ion species (included at the suggestion of R. F. Post) is so introduced as to satisfy the charge neutrality condition. Perturbations of the form $\exp(i\underline{k} \cdot \underline{r} + i\omega t)$ are inserted in the

---

† Department of Nuclear Engineering, University of Michigan, Ann Arbor, Michigan.

[1] E. G. Harris, Plasma Instabilities Associated with Anisotropic Velocity Distributions, J. Nucl. Energy: Part C, January 1961.

[2] Y. Ozawa, I, Kaji, and M. Kito, Stability Criterion for Longitudinal Plasma Waves in a Magnetic Field, J. Nucl. Energy: Part C, to be published.

linearized Vlasov equation, yield the following dispersion relation:

$$1=\frac{2}{\gamma_1^2 t_1^2}\frac{\omega_{pi}^2}{\omega_{ci}^2}\left\{-(1+R)t_1^2\frac{T_{\perp 1}}{T_e}\left(1+i\sqrt{\pi}\frac{\omega_1}{\gamma_1 n_z}\sqrt{\frac{M_e}{M_1}}\sqrt{\frac{T_{\perp 1}}{T_e}}-2+t_1^2-\int_0^\infty\left[\left(i\omega_1+\frac{\gamma_1^2 t_1^2 n_z^2}{2}x\right)(t_1^2-1)+i\omega_1\right]\right.\right.$$

$$\times\exp\left[-i\omega_1 x-\frac{\gamma_1^2 t_1^2 n_z^2}{4}x^2-\gamma_1^2 n_\perp^2\sin^2\left(\frac{x}{2}\right)\right]dx$$

$$+R\frac{M_1}{M_2}\left(\frac{t_1^2}{\Gamma_\perp^2}-\frac{2}{\Gamma_z^2}\right)-R\int_0^\infty\left[\left(\frac{1}{2}\gamma_1^2 t_1^2 n_z^2\frac{M_2}{M_1}\Gamma_z^2 x+i\omega_1\right)\left(\frac{t_1^2}{\Gamma_\perp^2}-\frac{1}{\Gamma_z^2}\right)+i\frac{\omega_1}{\Gamma_z^2}\right]$$

$$\left.\times\exp\left[-i\omega_1\frac{M_2}{M_1}x-\frac{1}{4}\gamma_1^2 t_1^2 n_z^2\left(\frac{M_2}{M_1}\right)^2\Gamma_z^2 x^2-\gamma_2^2 n_\perp^2\sin^2\left(\frac{x}{2}\right)\right]dx\right\}.$$

In the above equation the electrons are assumed to be isotropic and the magnetic field is taken along the z direction. The subscripts e, 1, and 2 refer first to electrons, and second to ion species, respectively, and R is the ratio of n_2 to n_1 where n_1 is the particle density M is the particle mass. With α denoting the thermal velocity, ρ the radius of gyration, and k the wave number, the remaining terms in the equation are given by

$$t^2=\frac{\alpha_z^2}{\alpha_\perp^2}=\frac{T_z}{T_\perp},\quad \gamma=k\rho,\quad \Gamma_\perp=\frac{\alpha_{\perp 2}}{\alpha_{\perp 1}},\quad \Gamma_z=\frac{\alpha_{z2}}{\alpha_{z1}}\quad n_z=\frac{k_z}{k},\quad n_\perp=\frac{k_\perp}{k},\quad \omega_1=\frac{\omega}{\omega_{c1}}.$$

The dispersion equation is being solved numerically for different values of these parameters and the results will soon be available. Instabilities in a plasma with only one ion species can easily be deduced by letting R = 0.

5. ION DENSITY VERSUS TIME IN NEUTRAL INJECTION SYSTEMS

John R. Hiskes and C. Bruce Tarter†

Some solutions of the ion density versus time have been calculated for the case of neutral injection into the Alice and Phoenix mirror machines. The solutions have been given for a wide range of parameters: base pressures covering the range from 10^{-8} to 10^{-11} mm Hg, plasma containment volumes whose longitudinal dimensions range from the injection-beam width to the mirror-to-mirror distance, and for neutral beam currents which are integral multiples of 50 mA. The contribution of Lorentz ionization to the ion density is compared with the ion density due to gas collisions. On the basis of these solutions it is clear that if the effects of Lorentz ionization are fully utilized, the requirements on base pressure and beam current necessary to achieve significant ion densities are considerably relaxed.

Of particular interest is the growth of an inverted cascade of the initial excited-state population distribution for ion densities of order 10^{10} ions/cm^3 or more. The successive collisional excitation of the excited-state distribution of an energetic neutral beam can result in the almost complete Lorentz ionization of the excited states. The development of the cascade may permit an exponential growth of the ion density in contemporary neutral-injection experiments for base pressures an order of magnitude higher than required for exponentiation by collisional ionization. Also, the growth of the cascade may place less emphasis on the initial rate of Lorentz ionization and allow for greater flexibility in the choice of magnetic-field profiles.

This work is discussed in more detail in previous reports.[1,2]

---

† Physics Department, Cornell University, Ithaca, New York.

[1] John R. Hiskes and C. Bruce Tarter, Ion Density Versus Time in the Alice and Phoenix Experiments, UCRL-7033, September 1962.

[2] John R. Hiskes, Inverted Cascades in Neutral Injection Systems, UCRL-7115, November 1962.

6. LOW-β PLASMA STABILITY IN THE ASTRON

Cornelius H. Woods

The development of a self-consistent distribution of electrons in the Astron E layer[1,2] has made possible the investigation of low-β plasma stability. Since plasma is to be generated somewhat slowly by the energetic electrons, the plasma must pass slowly through the low-β stage before reaching the ultimate pressure, and stability is essential throughout the whole pressure range.

---

[1] Warren Heckrotte and V. Kelvin Neil, A Self-Consistent Distribution of Electrons in the Astron E Layer, UCRL-6942, June 1962.

[2] Warren Heckrotte and V. Kelvin Neil, in Controlled Thermonuclear Research Semi-annual Report, UCRL-10294, p. 72, July 1962.

The interchange instability has been investigated in the limiting case where magnetohydrodynamic theory is applicable. A pressure distribution has been found which is stable according to this theory. This distribution involves the maximum pressure gradients allowed if the plasma is to be stable.

7. BUMPY TORUS

Gordon Gibson,† Willard C. Jordan,‡ and Eugene J. Lauer

The mechanical assembly of the electron gun and injection section[1] has been completed. The magnetic field resulting from the injection coils and iron pole tips has been measured and the shape of the field agrees with the theoretical predictions. Design of the remainder of the torus is nearly completed.

A preliminary design of iron pole arrays (called stabilizers) for the purpose of introducing shear into the electron-model Bumpy Torus has been carried out. These stabilizers consist of poles arranged alternately N and S inside a ring-shaped flux leader. The number of poles and the orientation of the poles will be variable. Stabilizers can be installed outside of the vacuum chamber in approximately half of the planes located midway between adjacent coils of the torus. Numerical calculations of the resulting field have been carried out for various arrangements of six-pole stabilizers under the assumption the iron poles may be approximated by monopoles. "Magnetic surfaces" have been found, and the existence of shear has been demonstrated.

The calculations that were to determine the limitations on the application of the longitudinal invariant, J, to the Bumpy Torus, as described in the last progress report,[2] have been carried out. Trajectories of guiding centers obtained from the integration of the drift equations show that J is conserved if the ratio of the particle-orbit radius to coil radius is not too large (greater than approx 0.1) except for the special case where the particle tends to "balance" near the plane of a coil. In this instance the guiding center may drift across "invariant surfaces". The extent of this effect has been determined for various initial conditions.

---

† Westinghouse Electric Corporation, Atomic Power Dept., Pittsburgh, Pa.

‡ The Bendix Corporation, Reserach Laboratories Division, Southfield, Mich.

[1] Gordon Gibson, Willard C. Jordan, and Eugene J. Lauer, in Controlled Thermonuclear Research Semiannual Report, UCRL-9969, January 19, 1962, p. 166.

[2] Gordon Gibson, Willard C. Jordan, and Eugene J. Lauer, in Controlled Thermonuclear Research Semiannual Report, UCRL-10294, July 20, 1962, p. 83.

8. ATOMIC SCATTERING AND CROSS-SECTION MEASUREMENTS

Forrest S. Baker, Gilbert O. Brink,† Edmund S. Chambers, Robert H. McFarland, and Edward A. Soltysik‡

Hydrogen-Ion Cross Sections

Work leading to cross sections of the following reactions is being continued:

Dissociative recombination..... $H_2^+ + e^- \rightarrow 2H$

Dissociation (breakup)..... $H_2^+ \rightarrow H^+ + H^0$ (typical)

Charge exchange..... (neutral production) on molecules... $H^+ + H_2 \rightarrow H^0 + H_2^+$

Charge exchange on atoms..... $H^+ + H \rightarrow H^0 + H^+$

The emphasis in this work so far has been to measure the fast-reaction products. Recent work, in which fast neutrals and ions were compared calorimetrically, however has disclosed a possible 30% error associated with the fast-ion measurements. This problem will be discussed further below.

Dissociative Recombination

Cross sections for the reaction $H_2^+ + e^- \rightarrow (H_2) \rightarrow 2H$ have been calculated in the low-energy range by Bauer and Wu.[1] Below 1.2 eV, σ is of the order of 10^{-15} cm^2. As far as we know there is no experimental data available. Barnett, Fite, and Branscomb were all having trouble (in June 1961) with beam experiments in which ions such as H^+, H_2^+ and C^- were crossed with electrons. There were modulation effects on the ion beam and some of the cross sections had uncertainties of many magnitudes.

To avoid such difficulties, R. H. McFarland conceived the idea of passing H_2^+ ions axially through a magnetic mirror in which electrons were liberated from a heated oxide cathode. The electrons should be confined and provide a target for the ions.

Such an electron target was fabricated and during the third quarter was tried out. The ion beam was focused and directed until about 0.5 μA of 5 keV H_2^+ ions were focused through the 1/8-in. diam hole of the target.

---

† Presently on leave of absence since September 1 at the University of Pittsburgh.

‡ Presently employed at the University of Massachusetts.

[1] E. Bauer and T. Wu, Dissociative Recombination Research Report NYU-RR-CX-21, 1955.

After thorough outgassing, neutral production from charge exchange in the target became negligible. However the cathode heater was burned out before adequate emission could be attained.

A more effective cathode is planned. In addition, the electron-confining mirror coils will be pulsed. Then, by using a frequency and phase-sensitive detector, the background neutrals from charge exchange can be discriminated against.

Dissociation (Breakup) of H_2^+ or H_3^+ on H_2 Gas

The reaction $H_2^+ \rightarrow H^+ + H^0$ has been studied by passing a beam of H_2^+ ions of energy E through H_2 gas. By setting the magnetic analyzer for H^+ ions of energy E/2, this current may be compared with the current of H_2^+ ions of energy E. The cross section is thus obtained assuming the broken-off ions follow identical paths as the parent ions (at the two appropriate analyzer settings). During the second quarter of 1962, such measurements were made between 5 keV and 58 keV to complement the work of Sweetman[2] between 100 keV and 250 keV. Before publication, it is planned to repeat this work to ensure that space-charge blowup is not affecting the results. Also, the current work on measuring an ion beam may affect the result. This work will be discussed in the next section.

Charge Exchange of Hydrogen Ions on H_2 Molecules

To calibrate a fast neutral detection method involving secondary-electron emission, charge exchange of H^+, H_2^+ and H_3^+ with the H_2 molecule was measured between 1.2 keV and 57.5 keV. These results were compared with previous experiments,[3, 4, 5] in which charge exchange was obtained from the slow-ion production. Because of the discrepancies found, the method of detecting fast neutrals and ions has been studied in greater detail.

As a first step, the number of secondary electrons per incident particle was measured. Simultaneously, the beam power was measured calorimetrically. This gave a direct basis to compare the neutrals with the ions. Between 3 keV and 34 keV the neutrals apparently produced 1.15 more secondaries than the same number of ions did. There was a larger spread in the experimental points than expected and the ratio differed by 15% or more depending on whether the ion beam passed through the 58-cm drift region at a pressure of 8×10^{-7}-mm Hg or at 8×10^{-5}-mm Hg. The 8% neutrals in the second case do not account for the discrepancy. The ion beam is more compact at the lower pressure and it was first thought that the target surface was inhomogenous. A second, more carefully made electropolished target showed the same effect.

---

[2] D. R. Sweetman, Proc. Roy. Soc. (London), Ser. A, 256, 416 (1960).

[3] F. Schwirzke, Dissertation, Technischen Hochshule, Karlsruhe (1959).

[4] P. M. Stier and C. F. Barnett, Phys. Rev. 103, 896 (1956).

[5] R. Curran, T. M. Donahue, and W. H. Kasner, Phys. Rev. 114, 490 (1959).

Numerous experiments made in the past few weeks have not yet exposed the difficulty. A repulsion analysis of the secondaries produced showed that about 12% were positive. However the upper energy limit of both plus or minus species was only about 25 eV. Increasing the positive collector voltage had only a slight effect.

A high-energy ion beam can be considered a rigid matrix of positive points which could form a conducting channel for electrons. Consider 0.5 μA of 10 keV H_2^+ ions having a cross section of 0.13 cm^2. The ion density will be $2.5 \times 10^5/cm^3$. A rough calculation shows the work function of such a beam would only be 10^{-4} V; thus, only electrons with energies less than this would be contained. Such a weak plasma would not provide any significant shielding from the collection field. Further work may solve this problem which may unknowingly have affected other experiments.

Charge Exchange on H Atoms

Both Gerjuoy[6] and Fite[7] have emphasized the need for further experimental work on the reaction $H^+ + H \rightarrow H^0 + H^+$ around 40 keV. A crossed-beam apparatus, capable of studying this and other hydrogen ion and neutral reactions, is nearing completion and will be assembled in the new building. Ion energy extends to 60 keV and a Paul spectrometer is included to analyze the slow ions formed.

Before publication, the swarm experiments discussed in preceding sections will be checked, where possible, by a corresponding crossed-beam experiment.

Electron Inelastic Scattering

Both the crossed-beam and atomic-excitation experiments using electron beams have undergone modifications during this period.

Work with the crossed-beam machine has been toward improving and stabilizing the electron-gun system. Interactions between the electron-focusing magnetic field, the accelerating and ion extraction voltages, and surface charging has been severe enough to warrant time spent on their reduction if not elimination. Results obtained presently are promising.

Modifications in the atomic-excitation experimental system were indicated as necessary by the results previously reported for hydrogen. At energies as low as 10 eV, insufficient intensity and energy resolution were to be had. A barium-impregnated tungsten cathode has been obtained to replace the previously used triple carbonate cathode. It is hoped that this will help reduce surface impurity charging. In any event, an improved optical path should provide sufficient intensity that retarding potential difference measurements can be used to obtain effective energy resolution.

---

[6] E. Gerjuoy, Natl. Acad. Sciences, Natl. Res. Council Publ. 752 (1958).

[7] W. L. Fite, R. F. Stebbings, D. G. Hummer, and R. T. Brackmann, Phys. Rev. 119, 663 (1960).

Two UCRL Reports[8, 9] describe electron cross-section work completed during this period.

[8] Robert H. McFarland and Edward A. Soltysik, An Alternate Method of Measurement of the Polarization of Light Emitted by Helium Atoms Excited by Energetic Electrons, UCRL-7037, August 22, 1962.

[9] Forrest S. Baker and Gilbert O. Brink, On the Ionization of Alkali Atoms by Electron Bombardment, (to be published as UCRL-7087).

VI. ENGINEERING AND TECHNOLOGICAL DEVELOPMENT

1. ULTRAHIGH-VACUUM DEVELOPMENT

Norman Milleron

Two UCRL reports[1, 2] issued during this period cover most of the work done.

In addition to the above, the self-scattering of oil in diffusion-pump jets was examined. This work was done at three locations: our Livermore Vacuum Laboratory, at the Berkeley Hilac Accelerator, and in Cory Hall on the Berkeley Campus. Once again, our objective is to reduce the self-scattering in high-mass-flow oil jets and at the same time to increase the entrainment efficiency of the jets for helium and hydrogen gases. Our progress towards solutions of these questions was not great.

In Livermore, we worked with a single horizontal jet of OS 124 oil traveling 6 in. from nozzle to condensing chamber. We tested a series of water-cooled skimmers as collimators for this jet and are as yet unable to reduce to an acceptable level the oil scattering at right angles to the direction of the flow of the jet. It is hoped that successful results in the future will make details of this sort of experiment worth reporting.

The work at the Hilac in Berkeley was on a 12.25-in.-diam experimental pump for He gas. Similar work was done in Cory Hall on a 7-in. pump. Both of these pumps were powered by ribbon heaters operating on OS 124 pump oil. So far, oil backstreaming from the top jets of each of these pumps is about 1 order of magnitude greater than we have achieved in the past. From this experience it seems doubtful that we can improve the entrainment efficiency of the top jet for helium gas and still reduce the oil backstreaming to a level permitting us to eliminate a conventional baffle.

Tests of the radial stainless to stainless bladder seal were successful as follows: by using differential pumping of approximately 0.01 liter/sec, total leakage through the seal was reduced to about 1×10^{-10}-mm liters of helium per second. This leakage rate was measured after about 17 h of baking at 200°C plus 6 h of baking at 380°C. The leakage measurements were taken while the seal was still hot. When depressurized, this seal released perfectly.

---

[1] Norman Milleron and Finn S. Reinath, Performance of a Six-Inch Triode P.I.G. Pump Compared to a "Perfect" Pump, UCRL-6958-T, August 23, 1962.

[2] Norman Milleron and Leonard L. Levenson, Progress on Optimization of Oil-Diffusion Pump Systems for Ultrahigh Vacuum IV, UCRL-6963-T, August 27, 1962.

2. MECHANICAL ENGINEERING DEVELOPMENT

Thomas H. Batzer

A. 2X Multistage Compression Facility

John R. Benapfl, Edward G. Scarlett, James F. Ryan, and James N. Doggett

Construction of the timber support structure is completed and assembly of the machine has begun. All of the 5-ft.-diam aluminum vacuum tanks have been delivered. Two of these aluminum sections have been set up on the rails of the support structure and vacuum checked. The tanks will be used in the near future for source testing.

Seventeen of the twenty-five 6-ft. -i. d. -dc magnet coils have been delivered. Twelve of these coils were set up on the machine support rails and were checked electrically and for water flow.

Two of the ten vacuum pumping systems have been assembled for test. Each vacuum pumping package consists of a 10-in. diam stainless steel mercury diffusion pump, a 1/2 hp refrigerator, a liquid-nitrogen-cooled chevron trap and a 10-in. Temescal gate valve. The refrigerator is used to cool the upper half of the diffusion-pump barrel. The base pressure of these systems is about 1.8×10^{-7}-mm Hg. With the valve removed and the cover plate directly over the trap, the base pressure is about 7×10^{-8}-mm Hg. Speed runs have not been taken as yet.

Two 310 Kinney pumps and one 130 Kinney pump have been set up on the concrete pad outside of Bldg. 180 (Livermore). The 6-in. diam aluminum holding and roughing lines are also complete except for the line traps.

B. Low-Energy Neutral-Beam Experiment

William S. Neef, Jr., James F. Ryan, and James N. Doggett

Two operational problems were encountered on the Alice machine. The first requires that great care be taken while cooling the magnets to prevent liquid nitrogen from contacting the joints between the pump boxes and the reaction chamber. If a large amount of liquid is allowed to flow from the exhaust side of the magnets, small leaks tend to appear in these joints. However, with proper cooling procedures this situation is acceptable. A new seal has been devised using aluminum foil and will be installed during the next major shutdown. It is hoped it will reduce sensitivity of this joint.

The second problem involved a coil failure. This section was replaced and subsequent operation has been satisfactory. The possible reasons for the failure have been outlined in Engineering Note ENA-156 by A. Harvey of the Sherwood Coil Shop.

A number of new parts to be installed in the beam tube during the next shutdown have been designed and fabricated. Included are two adjustable beam trimmers, an additional molybdenum pump, a short neutralizer, and a new exit frustrum.

The beam tube employing liquid-nitrogen-cooled zeolite-filled cartridges was assembled and tests completed. It demonstrated that the base pressure in the 10^{-10} Torr range can be obtained, but it showed negligible pumping speed on hydrogen.

A vaned drum rotating at 7000 rpm has been designed to reduce the streaming of water and hydrogen from the neutralizer down the beam tube. About 98% of the streaming particles will be struck by the vane giving them velocities transverse to the beam tube thereby allowing them to be pumped away by several stages of downstream pumping. This device will be used to replace the "water vapor curtain" if the latter cannot show improved efficiency.

Also near completion is the design of the Fast Atom Counting Tube (FACT) that uses a phototube to sense fast neutrals and incorporates shutters and diaphragms for investigation of ultraviolet radiation effects.

The 60 kV beam source (to supplement Alice's 20 kV beam) is near completion. Tests may be started on the first unit in the 100 kV. Injector Facility by late February.

A new magnetically shielded, adjustable mount for the partial pressure analyzer and ion gages has been designed and fabricated. It was designed for installation at the end of the existing reaction-chamber pressure-probe tube.

C. Astron

Charles A. Hurley and James F. Ryan

Gun and Accelerator

Operation of the 720 kV Electron Gun begun in December. Mechanical problems were encountered with the Freon gas system. Freon gas is circulated at about 2 atm through the gun for cooling purposes. The problems included overloading the blower motor, failure of the oil seals in the blower, insufficient mechanical strength of the heat exchanger, and excessive vibration in the supporting structure.

A larger motor and a new heat exchanger have been installed. Rubber mounts, bellows, and a stiffer support structure have helped considerably to isolate the vibration. The oil-seal problem has not yet been solved. Another blower has been purchased. The manufacturer claims the seal has been improved. Also, a different type of seal is being designed and fabricated by LRL to replace the manufacturer's seal if necessary.

Because of the failure of the heat exchanger and oil seals, water and oil were deposited throughout the gun assembly. To minimize this in future failures, a contaminant knockout pot has been installed in the system.

Assembly of the spare gun is waiting on delivery of another ceramic accelerating column. The spare column which was to be used in this assembly developed a leak.

Six accelerator units have been assembled and installed. One additional accelerator unit is completed and available as a spare. Parts are on hand for an eighth unit. Focussing magnets have been installed. Continuing work is being done on diagnostic gear including analyzing magnets, variable diaphragms, Faraday cups and "Fly's Eye" type targets.

Beam Research Facility

All major parts are on hand. Assembly of the Transition Section is started and a new 87° turning magnet and two 2-1/8-in. bore quadrapole focussing magnets have been designed and built. A beam shutter to reduce the flow from the gas target through the pressure transition section is being designed.

90-Ft Trapping Chamber

All major parts are on hand. Installation of the field coils is 50 percent complete and assembly of the cantilever sections has begun. Half of the trapping resistors have been delivered and a modular frame to hold thirty resistors in a 2-ft. length has been designed.

D. Bumpy Torus

Eugene T. Bradley and Manuel O. Calderon

The weld test of a section of the Bumpy Torus was completed and no insurmountable problems were encountered. Some redesign of the welding jigs will be required. By using extreme care in the welding procedure, it is possible to keep the distortion of the coils and other components within tolerable limits. The apparatus for the beam injection studies was assembled. The split injection coils shorted to their vacuum cases and required repair, but have been tested and were found to meet physics requirements. Magnetic fields have been plotted and agree with calculated field configurations.

The 150 kV electron gun has been completed and testing is in progress.

Components necessary to build one quadrant of the main torus are on order.

E. Cryogenic Project

Clyde E. Taylor, Robert L. Nelson, and David C. Holten

The 8-in. i. d. sodium coil was operated several times at increasing current levels. The blowdown refrigeration system operated satisfactorily. At 8300 A, and 16.5 kG (approx 10°K), coil resistance measurements ranged from 2.5 to 3.7 $\mu\Omega$. This agrees with predicted resistance values within experimental error. After five tests, in which a maximum field of 21 kG was reached, the coil developed an open circuit because of a broken joint in the crossover connection between two layers. While preparing to reweld the joint, the coil was accidentally damaged beyond repair and therefore, tests at high-current levels were not made.

Development work is now in progress which will lead to a new test coil of better mechanical design.

F. Component Development

Thomas H. Batzer and James F. Ryan

The 6-in. Hg ultra-high vacuum system is undergoing bakeout tests. This system uses synthetic zeolite and copper wool as a forevacuum pump and will be used to explore the ability of an oil-free system to recover from up-to-air accidents.

One-sixth scale models of the 4-ft major by 1-ft minor diam torus are being made by hydraulic pressing and welding. The 1/6th scale models are being pressed from 8-mil and 10-mil 304 stainless steel sheets. They will be subjected to external hydraulic pressure to determine the minimum wall thickness that can be used in fabricating a full scale torus capable of holding external atmospheric pressure.

A coil of Nylon tubing has been tested as a nonconducting substrate for molybdenum evaporation. Results were unsatisfactory. Even at liquid nitrogen temperature the material was too gassy. Further trials will be made with Teflon tubing.

Continuing investigations are being made concerning the use of aluminum in ultra-high vacuum systems at elevated temperatures. A new 70-liter vessel has been made of 5456 aluminum alloy. It has aluminum foil gaskets and will be baked to 300° C. A 3-in. bakeable "Conoseal" valve ahead of the aluminum vessel allows rate-of-rise tests to determine surface outgassing rate. A mass spectrometer is mounted on the vessel to identify residual gases. The largest flange is about 22 in. in diameter and the three smaller flanges mount the spectrometer, the nude ion gage, and a bakeable roughing valve. The vessel bolts on the "Conoseal" valve by means of an aluminum foil gasket.

The vessel is pumped through a new 4-in. vertical liquid nitrogen trap and a PMC 720 pump. The system is backed by a zeolite-copper wool, pump-trap cooled in liquid nitrogen. This pump combination operates in the low 10^{-10}-mm Hg range with no pressure bursts. A recorder placed on this system after bakeout, prior to the mounting of the aluminum vessel, held 3.6^{-10}-mm Hg for four days with no variations greater than about 0.5×10^{-10}-mm Hg. We attribute this behavior to the isolation from forepump oil contamination that the zeolite pump trap provides.

Additional bakeout tests will be made on the aluminum vessel using a molybdenum evaporator with a liquid nitrogen cooled liner. This will be placed between the trap and the valve. The molybdenum evaporator is expected to stop recontamination of the baked aluminum surface by cracked gases from the diffusion pump.

Aluminum foil gaskets are being used routinely in the component development laboratory. Reliability is excellent and the cost of replacement gaskets is negligible.

3. ELECTRICAL ENGINEERING DEVELOPMENT

Hugh W. Van Ness

A. Pyrotron

David R. Branum and Gordon G. North

2X

The past six months have been spent in constructing the energy storage capacitor banks and controls in Building 180(Livermore).

The five 232,000J, semifast-capacitor banks in the North Bay of Building 180 are 90% complete. The bank charging circuits and controls are now under construction.

The four 32,000J fast-capacitor banks are 75% complete. The output transmission lines, pulse transformer trigger lines, charging circuits and controls are now under construction.

The 1,000,000 Joule, semifast capacitor bank is 40% complete. All ignitron hardware is now on hand. The ignitron assembly and transmission line assembly will be started early in January. This capacitor bank will utilize capacitors from banks 3C and 4 of the Toy Top III experiment which will be deactivated.

The transmission line support structure for the four $2.5 \times 10^{+6}$ J, mediumfast capacitor banks in Building 156 is now under construction.

The ignitron switch hardware for one bank section has been designed and is in the process of going to outside fabrication.

The main control center in Building 180 is 30% complete. The main control trunks to the North Bay capacitor banks have all been installed. The power-supply control and pulse-chassis control trunks are now under construction. All the control panels have been fabricated.

The output cable runs for the eight 300-kW, dc magnet supplies have been run from Building 156 to Building 180. The runs have been connected to the 2X machine terminal boxes only. The supply ends will be connected when Toy Top III is deactivated.

The dc cable runs for three additional 300-kW dc-magnet supplies are now under construction.

Alice

The Alice machine facility has been in an operational state during most of this period. There has been one mirror-field modular-coil failure caused by the opening of one small pancake-coil-to-pancake-coil connector block with subsequent destructive local arcing. A careful study of this failure showed it to be due to poor soldering technique employed by an outside fabricator.

The P-3 occluded-gas ion source has been satisfactorily operated into the Alice machine confinement chamber. Two auxillary 200 μsec pulse-forming network sections have been built for this source permitting a total discharge pulse length of up to 600 μsec at 10 kV and 5,000 A.

To precisely time modulate the ion beam, the positive gate output from a Tektronix oscilloscope is used to modulate the reference input to the Alice ion source high-voltage regulator system. The off and on response time is limited to about 150 μsec by the present regulator system.

The 20-cps ripple filter consisting of a 330,000 uF electrolytic capacitor bank and a 3-mH 9-in. i. d. modular magnet coil was built and connected to the output of the MG set energizing the ion-source field coils. This filter reduced the previous 0.5% 20-cps field ripple by a factor of 20. There has been no conclusive evidence, however, that this has improved the ion-source current output significantly.

Planning and construction of the new Piggy-Back Ion-Source Facility is continuing. An elevated platform with equipment racks and a high voltage enclosure has been built to contain the electrical system. This new ion source will be initially operated in the 100-kV Injector Facility in Building 180 to debug and assess the merit of the design and more closely determine the various power-supply requirements.

Cryogenics-Coil Experiment

All electrical and electronic systems for the cryogenics-coil experiment have been completed. In tests, the sodium coil has repeatedly been cooled to 10°K, and operated with currents to 8,000 A and fields to 20,000 G.

During a recent test the coil failed while the circuit was open. The failure occurred in the sodium interconnection between coil sections. Testing, therefore, will not be resumed until a redesigned coil is completed.

B. Pinch Program

Gordon G. North

Levitron Experiment

During the past six months, the Levitron has been operating on a routine basis. Except for occasional component failures, operation of both the high voltage and electrolytic capacitor banks has been satisfactory. The 10-kc 30-kW motor generator used for induction heating of the stainless steel vacuum liner has also given satisfactory operation.

Recent additions to the experiment include an expanded screen room to accomodate more diagnostic oscilloscopes. Also, a 4-mm microwave diagnostics system has been added to measure transmission and reflection properties of the plasma. Operation with this new equipment will begin when a vacuum leak in the split copper shell is corrected.

Energy Storage System Investigation

Limited effort is still being supplied to the homopolar generator. Investigation of machine characteristics using field pulsing techniques is presently underway.

In tests to date, pulse currents of 200,000 A into a 90 μΩ load have been reached. This current level was attained in 0.2 sec after initiation of the field pulse. The total stored energy released in these pulses was 1.5 MJ. It is hoped current pulses approaching one million amperes can be obtained.

Beta Pinch Capacitor Bank

Because of other project commitments, only limited effort has been supplied to the new 150 kJ capacitor bank for the Beta Pinch experimental area. As a result, it was decided to have the bank construction done by an outside contractor. At present, plans have specifications for an outside contract are being readied.

C. Switch Development

David B. Cummings

Ignitron Development

The WX 4973 is a more easily produced version of the WX 4564 which is a short, low-inductance, stabilized ignitron. Ten were ordered of which six have been received. Two have been tested as a single crowbar tube on Table Top bank No. 1. They operated well as high as 12 kV with currents up to 3,000 A. The decay-time constant was over 0.050 sec, so the charge passed was at least 150 C. The ignitor resistance remained high during the test. When cut open, there was no evidence of arc transfer to the wall which it was designed to prevent. The voltage limitation appeared to be the clearance between the glass pantleg and the anode stem. The tenth tube will have an increased clearance. The next test will be with two tubes in series to determine whether the limitation is on voltage or charge.

Tests of the WX 4973 on two sections of the Squash Court bank at up to 3,000 A with an R-C decay time constant of 600 μsec were successful. The tube reached its minimum arc drop in about 50 μsec as against 100 μsec for the WX 4681. In addition, the minimum drop was about 30% lower. Both effects were expected and desired.

The WX 4839 was an attempt to develop an ignitor which will not wet in a tube with a metal anode. It now appears that the test was not valid because the ignitor resistance was not high enough to begin with. Westinghouse is repeating the test at a reduced price with a higher initial impedance.

D. Microwave Diagnostic Development

Joseph E. Katz and Ronald S. Hawke

Astron Electron Beam Experiment

Transmission measurements at wavelengths of 3 mm, 8 mm, and 3 cm were performed on the small discharge experiment. In all three cases, careful alignment of the radiating horns and a reflectionless coating on the walls of the vacuum chamber produced clean traces. The time at which the microwave energy is no longer cut off is taken as the time the plasma frequency has decayed to below that of the microwave frequency.

Attempts to measure the electron temperature by microwave radiometry were unsuccessful. No matter how the discharge parameters were varied, no obviously "thermal" radiation could be seen at the time the plasma was just coming out of cutoff. From these measurements at 8-mm and 4-mm wavelengths, an electron temperature of less than a few eV is concluded.

Toy Top

Four millimeter microwave slot radiators for radiation and transmission measurements have been developed and fabricated. These, plus a low-loss transmission-line system will permit microwave measurements far up inside the machine.

Levitron

An 8-mm interferometer and transmission experiment has been assembled and used in the Levitron experiment. The transmission path through the experiment is novel in that the microwave energy is reflected off the hard core.

P-4

Transmission cutoff measurements were made at 4 mm and 8 mm as described above.

E. Astron System Engineering

Dean O. Kippenhan

The Astron Facility

Magnet power supplies. The specification for the main-field power supplies has been modified. The regulation response-time requirements have been greatly reduced. This was based on the cost of power supplies which could respond to line transients and the ability of manufacturers to design stable power supplies. To remove the line transients, a large motor-alternator from A-48's power supply No. 1 will be used.

A scheme of utilizing large, unregulated, nonadjustable power supplies and obtaining fast response, regulation, filtering, and multiple outputs

by transistor pulse-width modulation is being investigated.

Accelerator Construction

All procurements, chassis, cables, connectors, etc., for the accelerator construction have been received except for 100 compensator chassis for the seventh section and a spare chassis. Construction is complete except for installation of miscellaneous signal cable runs, interlock chains, small focusing-magnet supplies, and about one half of the seventh section load cables.

Additional items are becoming operationally necessary. These include monitoring systems for (a) the core voltage, (b) detection of prefires of the thyratron switch chassis, and (c) timing of the switch chassis. The core monitor-prefire detector system is designed and construction of the chassis has started. The timing monitor system has been designed, procured and tested, and is in the process of being installed. Some degree of automatic control, or at least a faster correction means, may be necessary to decrease startup and setup time.

Accelerator Operation

The Gun Section and Accelerator Sections No. 1 and 2 have been operated up to 31 kV on the pulse-forming networks (PFN) at 5 pulse/sec repetition rate. When the sections are turned on, minor problems are sometimes experienced because of the usual human errors in construction. There have been basic design problems in the charging system power supplies and some of these are associated with tying the power supply to the pulse forming networks. There are also problems in obtaining the required regulation in this supply. These problems are now under investigation and solutions are actively being sought.

The design-maximum rating of the accelerator section is 60 pulse/sec repetition rate with 32-kV charge on the PFN's. Operation to date has shown that two fundamental limitations must be overcome before the design goal can be achieved with reasonable reliability. These limitations are the component's statistical failure rate and the thyratron prefire rate.

A maintenance-record system is being set up to collect information for statistical studies of component failures. The accelerator has approximately 10^5 electronic components, some of the more important of which have shown low mean time between failure rates. The statistical studies will enable the scheduling of preventive maintenance, and aid in the redesign of marginal components.

The thyratron prefire problem requires a fundamental understanding of the mechanism involved in the tubes. Otherwise, a method for rapid detection, removal, and replacement of thyratrons with excessive prefire rates will be required. The replacement of such defective thyratrons would have to be accomplished without interrupting the operation of the remainder of the accelerator system.

F. Bumpy Torus Experiment

Gordon G. North

All major design and planning on this experiment is now complete. The control racks and 80% of the required electrical equipment are in place and electrical installation of this equipment is now underway.

Preliminary tests of both the injection-coil power supply and the electron-gun high-voltage supply have been completed. Operation of both units appear satisfactory. No further tests are anticipated until electrical installation of the total injection system is completed.

G. Advanced Applications Development

Kristian Aaland

This engineering group was formed to serve the advanced development needs of the entire Sherwood program. The group has a background of specialized design experience in high-power hard-tube modulators, high-power pulse transformers, pulse behavior of magnetic materials, precise regulated power supplies, and digital-timing systems.

An intensive investigation of the pulse capabilities of silicon controlled rectifiers has been made. Initial tests indicated that all units from the smallest to the largest fail at a few hundred amperes on short pulses. Further investigation showed that preventing current buildup for several microseconds after application of the gating pulse corrected the situation. Under such conditions, pulse currents up to 20,000 A have been switched in single units.

At the present time, silicon controlled rectifiers are being utilized in the core reset pulsers for the Astron experiment. If the thyratron prefire problem for the main core pulsing cannot be adequately improved, it now appears possible to develop units utilizing silicon controlled rectifiers.

At present, work is in progress on a 20-kV, 2-A precision regulator for the Alice program. A 30-kV pulse generator for an electron gun for the Table Top experiment has been completed. A probe sweep generator has been developed for use in the Levitron experiment.

VII. TALKS AND PUBLICATIONS

1962 Cryogenic Engineering Conference, Los Angeles, California, August 14-16, 1962.

Angus L. Hunt, Charles C. Damm, and Earl C. Popp, Gettering of Residual Gases and the Adsorption Rate of Hydrogen on Evaporated Molybdenum Films at Liquid Nitrogen Temperatures (UCRL-6652 Rev. July 31, 1962).

APS 1962 Summer Meeting in the West, University of Washington, Seattle, Washington, August 27 to 29, 1962.

Henry F. Rugge and Robert V. Pyle, Instability of the Positive Column of an Alternating-Current Discharge in a Magnetic Field, Bull. Am. Phys. Soc. Ser. II, 7, 442 (1962) (UCRL-10303 Abst., June 1962).

Edward A. Soltysik and Robert H. McFarland, Polarization of the $\lambda = 5876$ Å and $\lambda = 6679$ Å Lines in Helium Excited by Electrons, Bull. Am. Phys. Soc. Ser. II, 7, 457 (1962) (UCRL-6929-T Abst., June 7, 1962).

Robert H. McFarland and Edward A. Soltysik, Magnetic-Field Dependence of Polarized Helium Light Excited by Electrons, Bull. Am. Phys. Soc. Ser. II, 7, 457 (1962) (UCRL-6949-T Abst., June 6, 1962).

Laurence S. Hall, The Extremization of Entropy Production Rates, Bull. Am. Phys. Soc. Ser. II, 7, 465 (1962) (UCRL-6959-T Abst., June 14, 1962).

Daryl D. Reagan, Plasma-Traveling Wave Interaction, Bull. Am. Phys. Soc. Ser. II, 7, 480 (1962) (UCRL-6947-T Abst., June 5, 1962).

John R. Hiskes, The Formation of Excited Hydrogen Atoms in the Collisional Dissociation of H_2^+ Ions, Bull. Am. Phys. Soc. Ser. II, 7, 486 (1962) (UCRL-6960-T Abst., June 14, 1962).

Robert V. Pyle, Selig N. Kaplan, and George A. Paulikas, Electron Detachment from D^- Ions by the Lorentz Force of a Magnetic Field, Bull. Am. Phys. Soc. Ser. II, 7, 487 (1962) (UCRL-10302 Abst., June 1962).

Archer H. Futch, Jr., and Charles C. Damm, Charge-Transfer and Ionizing Collisions of Hydrogen Beams with Water Vapor, Bull. Am. Phys. Soc. Ser. II, 7, 487 (1962) (UCRL-6956-T Abst., June 12, 1962).

F. S. Baker and G. O. Brink, Production of Protons from Water by Electron Bombardment, Bull. Am. Phys. Soc. Ser. II, 7, 487 (1962) (UCRL-6967-T Abst., June 15, 1962).

G. O. Brink, Ionization of Arsenic by Electron Impact, Bull. Am. Phys. Soc. Ser. II, 7, 487 (1962) (UCRL-6966-T Abst., June 15, 1962).

International Symposium on Plasma Coaxial Guns, Case Institute of Technology, Cleveland, Ohio, September 6-7, 1962.

Klaus Halbach, Plasma Gun Aspects of an E x B System, (UCRL-10206 Abst., May 7, 1962).

Fifteenth Annual Gaseous Electronics Conference, Sponsored Jointly by the University of Colorado and the National Bureau of Standards, Boulder, Colorado, October 10-12, 1962.

R. H. McFarland and E. A. Soltysik, An Alternate Method of Measurement of the Polarization of Light Emitted by Helium Atoms Excited by Energetic Electrons (UCRL-7037-T Abst., August 22, 1962).

Melvin J. Bernstein, Wulf B. Kunkel, and Gary A. Pearson, Crossed-Field Breakdown in Hydrogen (UCRL-10412 Abst., August 10, 1962).

Ninth National Symposium on Vacuum Technology, Los Angeles, California, October 31 - November 3, 1962.

Norman Milleron and Finn S. Reinath, Performance of a Six-Inch Triode PIG Pump Compared to a "Perfect" Pump (UCRL-6958-T Abst., June 14, 1962).

Norman Milleron and Leonard L. Levenson, Progress on Optimization of Oil Diffusion Pump Systems for Ultrahigh Vacuum IV (UCRL-6963-T Abst., June 15, 1962).

Kenneth W. Ehlers, Color Production from Energetic Ions Impinging on Metals, (UCRL-9845 Abst., May 1, 1962).

APS Division of Plasma Physics, Fourth Annual Meeting, Atlantic City, New Jersey, November 28 to December 1, 1962.

C. C. Damm, Formation and Containment of a 20-keV Hydrogen Plasma in the Alice Mirror Experiment, invited paper, I2.

W. A. Newcomb, The Interchange Instability, invited paper, M4.

J. M. Wilcox, A Plasma Gun Experiment and Alfvén's Theory of the Origin of the Solar System, invited paper, T5.

Dale H. Birdsall, Stirling A. Colgate, and Harold P. Furth, Toroidal Hard-Core Pinch Operation in the Levitron, B1 (UCRL-7108-T Abst., October 17, 1962).

Stirling A. Colgate, Dale H. Birdsall, and Harold P. Furth, Low-Density Plasma Confinement in the Levitron, B2 (UCRL-7109-T Abst., October 17, 1962).

Charles E. Kuivinen, Experimental Study of a Resistive Instability in the Reverse-Field Sheet Pinch, C8 (UCRL-7077-T Abst., October 17, 1962).

Wulf B. Kunkel, William R. Baker, Alexander Bratenahl, and Klaus Halbach, Flow Pattern in Rotating-Plasma Experiments, C11 (UCRL-10489 Abst., October 5, 1962).

G. Gibson, W. C. Jordan, E. J. Lauer, and C. H. Woods, Guiding-Center Motion in the Bumpy Torus, G9 (UCRL-7092-T Abst., October 15, 1962).

W. C. Jordan, G. Gibson, E. J. Lauer, and C. H. Wood, Plasma Equilibrium and Stability in the Bumpy Torus, G10 (UCRL-7100-T Abst., October 15, 1962).

Frank J. Gordon and Charles C. Damm, A High Intensity Source of 20-keV Hydrogen Atoms, I3 (UCRL-7095-T Abst., October 15, 1962).

C. Bruce Tartar and John R. Hiskes, Radiative Lifetimes for the Hydrogen Atom, I4 (UCRL-7088-T Abst., October 10, 1962).

John R. Hiskes, Inverted Cascades in Neutral Injection Systems, I5 (UCRL-7115-T Abst., October 16, 1962).

Robert V. Pyle, Selig N. Kaplan, and George A. Paulikas, Lorentz Dissociation of Neutrals from H_2^+, H_3^+, and D^- Collisions, I6 (UCRL-10501 Abst., October 9, 1962).

Archer H. Futch, Jr., and Charles C. Damm, Lorentz Ionization of Excited Hydrogen Atoms Produced by Charge-Exchange Collisions, I7 (UCRL-7105-T Abst., October 16, 1962).

Angus L. Hunt and Charles C. Damm, Gas Evolution from Metallic Surfaces Bombarded with 10 - 15 keV Deuterons, I8 (UCRL-7096-T Abst., October 15, 1962).

William S. Cooper III, Ion Density and Electron-Temperature Measurements in a Decaying Hydrogen Plasma, L8 (UCRL-10511 Abst., October 15, 1962).

Harold P. Furth, Stability Conditions for Long-Wave Finite-Resistivity Modes, M7 (UCRL-7110-T Abst., October 17, 1962).

Richard F. Post, The Effect of Plasma Density and Composition on Finite-Orbit Stabilization, M10 (UCRL-7106-T Abst., October 16, 1962).

Andrew L. Gardner and William L. Barr, Pulsed Compression Studies on a Segment of the P-4 Steady-State Plasma Column, N7 (UCRL-7113-T Abst., October 17, 1962).

Walton A. Perkins, Instability Studies with a Mirror Machine Using Different Compression Times, Q5 (UCRL-7098-T Abst., October 15, 1962).

Richard F. Post and Walton A. Perkins, Analysis of a Rotating Plasma Instability by Means of an Electrostatic Pickup, Q6 (UCRL-7099-T Abst., October 17, 1962).

F. H. Coensgen, W. F. Cummins, W. E. Nexsen, Jr., and A. E. Sherman, Plasma Containment in a Low Gradient Magnetic Mirror Systems, Q7 (UCRL-7102-T Abst., October 16, 1962).

W. F. Cummins, F. H. Coensgen, W. E. Nexsen, Jr., and A. E. Sherman, Large Low Inductance Pulsed Magnets for Symmetric Fields, Q8 (UCRL-7101-T Abst., October 15, 1962).

R. E. Ellis, Computer-Calculated Currents in Coupled Pyrotron Pulsed Coils, Q9 (UCRL-7103-T Abst., October 16, 1962).

E. S. Chambers, Fast Neutral Detection for Hot Plasma Experiments, R1 (UCRL-7093-T Abst., October 15, 1962).

James F. Steinhaus, Norman L. Oleson, and W. L. Barr, Investigation of a Plasma from an Occluded Gas, Cold Plasma Source, T3 (UCRL-7097-T Abst., October 15, 1962).

Seventh Lockheed Symposium on Magnetohydrodynamics, Palo Alto, California, December 14-15, 1962.

Harold P. Furth, Hydromagnetic Instabilities Due to Finite Resistivity, (UCRL-7107-T Abst., October 16, 1962).

APS 1962 Winter Meeting in the West, Stanford University, Stanford, California, December 27-29, 1962.

F. S. Baker and G. O. Brink, On the Ionization of Alkali Atoms by Electron Bombardment, Postdeadline paper (UCRL-7087-T Abst., October 17, 1962).

Publications

Journal of Applied Physics

John M. Wilcox, William S. Cooper III, Alan W. DeSilva, George R. Spillman, and Forrest I. Boley, Swirls Produced in a "Crowbarred" Rotating Plasma, 33, 2714 (1962) (UCRL-10010, January 12, 1962).

Journal of Nuclear Energy, Part C

J. M. Wilcox, W. R. Baker, F. I. Boley, W. S. Cooper III, A. W. DeSilva, and G. R. Spillman, Devices for Generating Highly-Ionized Hydrogen Plasma, 4, 337 (1962) (UCRL-10121, May 7, 1962).

Journal of Chemical Physics

Forrest S. Baker and Gilbert O. Brink, Adsorption of Potassium Beams on Surfaces, 37, 1012 (1962) (UCRL-6796, March 16, 1962).

Proceedings of the Physical Society (London)

Laurence S. Hall, On the Harrison-Thompson Generalization of Bohm's Sheath Condition, 80, 309 (1962) (UCRL-6868, April 16, 1962).

The Physical Review

Melvin J. Bernstein, Electron Drift and Diffusion Measurements in H_2 and D_2 with Crossed Electric and Strong Magnetic Fields, 127, 335 (1962) (UCRL-10016, January 20, 1962).

Melvin J. Bernstein, Townsend Ionization Coefficient for Hydrogen in a Transverse Strong Magnetic Field, 127, 342 (1962) (UCRL-10017, January 20, 1962).

Gilbert O. Brink, Ionization of Alkali Atoms by Electron Bombardment, 127, 1204 (1962) (UCRL-6806, March 9, 1962).

Robert H. McFarland and Edward A. Soltysik, On the Polarization of Light Resulting from the Excitation of Helium by Electrons, 127, 2090 (1962) (UCRL-6749, January 13, 1962).

The Physics of Fluids

Laurence S. Hall and Andrew L. Gardner, Highly Ionized, Steady-State Plasma System, 5, 788 (1962) (UCRL-6561, September 27, 1961).

Andrew L. Gardner, William L. Barr, Raymond L. Kelly, and Norman L. Oleson, Diagnostic Measurements on a Highly Ionized, Steady-State Plasma, 5, 794 (1962) (UCRL-6562, October 24, 1961).

Wulf B. Kunkel, Remarks on Magnetoacoustic Waves, 5, 867 (RN) (1962) (UCRL-10161, April 9, 1962).

A. H. Futch, W. Heckrotte, C. C. Damm, J. Killeen, and L. E. Mish, Plasma Production by Neutral Atomic Injection: Equations and Numerical Solutions, 5, 1277 (1962) (UCRL-6728, January 22, 1962).

Klaus Halbach, William R. Baker, and Robert W. Layman, Production of a Hot Rotating Plasma, 5, 1482 (RN) (1962) (UCRL-10269, May 29, 1962).

Science

Forrest I. Boley and John M. Wilcox, Alfvén Waves, 137, 511 (1962) (UCRL-10114, March 14, 1962).

This report was prepared as an account of Government sponsored work. Neither the United States, nor the Commission, nor any person acting on behalf of the Commission:

A. Makes any warranty or representation, expressed or implied, with respect to the accuracy, completeness, or usefulness of the information contained in this report, or that the use of any information, apparatus, method, or process disclosed in this report may not infringe privately owned rights; or

B. Assumes any liabilities with respect to the use of, or for damages resulting from the use of any information, apparatus, method, or process disclosed in this report.

As used in the above, "person acting on behalf of the Commission" includes any employee or contractor of the Commission, or employee of such contractor, to the extent that such employee or contractor of the Commission, or employee of such contractor prepares, disseminates, or provides access to, any information pursuant to his employment or contract with the Commission, or his employment with such contractor.

[redacted]